INVESTIGATION OF LIME MORTAR CHARACTERISTICS FOR THE CONSERVATION OF THE OTTOMAN BATHS IN SEFERİHİSAR-URLA REGION

Özlem ÇİZER

July, 2004

Investigation of Lime Mortar Characteristics for the Conservation of the Ottoman Baths in Seferihisar-Urla Region

By

Özlem ÇİZER

A Dissertation Submitted to the
Graduate School in Partial Fulfillment of the
Requirements for the Degree of

MASTER OF SCIENCE

Department: Architectural Restoration
Major: Architectural Restoration

İzmir Institute of Technology
İzmir, Turkey

July, 2004

We approve the thesis of **Özlem ÇİZER**

--   **19.07.2004**
Assoc. Prof. Dr. Başak İPEKOĞLU
Department of Architectural Restoration
Advisor

--   **19.07.2004**
Assoc. Prof. Dr. Hasan BÖKE
Department of Architectural Restoration
Co- Advisor

--   **19.07.2004**
Assist. Prof. Dr. S. Sarp TUNÇOKU
Department of Architectural Restoration

--   **19.07.2004**
Prof. Dr. Ömür BAKIRER
METU, Faculty of Architecture
Department of Architecture

--   **19.07.2004**
Assoc. Prof. Dr. Neriman ŞAHİN GÜÇHAN
METU, Faculty of Architecture
Department of Architecture

--   **19.07.2004**
Assoc. Prof. Dr. Başak İPEKOĞLU
Head of Department of Architectural Restoration

ACKNOWLEDGEMENTS

ABSTRACT

Lime mortars are among the binding agents used in binding masonry units such as brick and stone in many historic buildings. Their physical, mechanical strength and durability properties, raw material compositions can play significant roles in structural behaviour of historic buildings. Their production technologies may be also different according to their specific use in the structural layout. Therefore, the characteristics of lime mortars are of particular interest in the evaluation of structural characteristics of the historic buildings. Besides, determination of characteristics of the lime mortars is also important for the production of intervention mortars to be used in the restoration of historic buildings.

In this study, lime mortars used in the walls and domes of some historic Ottoman baths in Seferihisar-Urla region near İzmir were analyzed in order to understand their characteristics for the purpose of conservation of these buildings. It is also aimed to investigate characteristics of the lime mortars in relation to their specific use in the structural elements of the walls and domes. Therefore, several laboratory studies were carried out on the collected mortar samples. Their basic physical and mechanical properties, raw material compositions, pozzolanic activity of aggregates used in the mortars, soluble salts in the mortars, their mineralogical and chemical compositions, and microstructural and hydraulic properties were determined. In addition, basic physical properties and pozzolanic activity of bricks used in the construction of domes were also determined in order to evaluate their contribution to the structural stability of the domes.

Stone masonry mortars used in the walls and brick masonry mortars used in the domes of the Ottoman baths are lime mortars. Lime ratios of the stone masonry mortars are relatively higher than those of the brick masonry mortars. Some differences have been identified in the aggregates used in the mortars. Particle size distributions of the aggregates used in each mortar are almost the same. Fine aggregates used in each mortar have similar mineralogical and chemical compositions with their coarse aggregates. However, the fine aggregates have higher pozzolanic activity than their coarse aggregates due to high contents of amorphous materials, silicon dioxide and aluminium oxide in their compositions. Either of high-calcium lime and lime containing silica at high ratios was used as binding material in the stone and brick masonry

mortars. All brick masonry mortars and some of the stone masonry mortars have hydraulic properties owing to the use of pozzolanic aggregates and lime containing silica at high ratios. These pozzolanic aggregates have good adhesion with the lime used in these mortars. Hydraulic lime mortars used in all domes have higher mechanical strength properties than non-hydraulic lime mortars used in the walls built of stone. Such differences in the stone and brick masonry mortars have been explained with a mortar technology developed consciously in relation to the difference in structural behaviour of the wall and dome. Even though the bricks used in the domes have poor pozzolanicity, they are tightly adhered to the lime mortar. This contributes to the structural strength of the domes.

All these results indicate a lime mortar technology developed according to the use of the lime mortars in structural layout and its traditional character peculiar to the Ottoman baths in Seferihisar-Urla region.

The first part of the study defines its subject and aim, limits and method. The second part deals with the subject of lime mortars in respect to their general characteristics and production process. In the third part, method of the study composed of sampling and experimental study is presented. In the fourth part, the results of the experimental studies are evaluated and discussed in respect to results of the related studies in the literature. The fifth part is devoted to the conclusions of the study.

ÖZ

Kireç harçları, tarihi yapılarda taş, tuğla gibi yapı malzemelerini bir arada tutan bağlayıcı malzemelerdendir. Harçların fiziksel ve mekanik özellikleri ile ham madde kompozisyonları yapıların strüktürel davranışlarında etkilidir. Kireç harçlarının ham madde özellikleri ve üretim teknolojileri, yapılarda kullanıldıkları strüktürel elemanlara göre farklı özellikler gösterebilir. Bundan dolayı bu harçlar, tarihi yapıların strüktürel özelliklerinin değerlendirilmesinde önemli bir yere sahiptir. Ayrıca, kireç harçlarının özelliklerinin belirlenmesi, tarihi yapıların korunması çalışmalarında kullanılacak olan onarım harçlarının hazırlanması açısından son derece önemlidir.

Bu çalışmada, İzmir'e yakın yerleşmelerde bulunan Seferihisar-Urla bölgesindeki bazı Osmanlı dönemi hamamlarının kubbe ve duvarlarında kullanılan kireç harçlarının özellikleri, bu tarihi yapıların korunması amacına yönelik olarak incelenmiştir. Harçların özelliklerinin, kullanıldıkları duvar ve kubbelerin strüktürel özellikleri ile ilişkisini ele alan bir yaklaşım ile incelenmesi amaçlanmıştır. Bu kapsamda, yapılardan toplanan harç örnekleri laboratuvar çalışmaları kapsamında incelenmiştir. Harçların temel fiziksel ve mekanik özellikleri, ham madde kompozisyonları, harçlarda kullanılan agregaların puzolanik aktiviteleri, harçlardaki çözünen tuzlar, harçların mineralojik ve kimyasal özellikleri, mikroyapıları ve hidrolik özellikleri belirlenmiştir. Ayrıca, kubbelerde kullanılan tuğlaların temel fiziksel ve puzolanik aktiviteleri, kubbelerin strüktürel dayanımlarının sağlanmasındaki etkisini değerlendirmek amacı ile belirlenmiştir.

Hamamların duvar ve kubbelerinde kullanılan harçlar, kireç harçlarıdır. Duvar harçlarındaki kireç oranları, kubbe harçlarındaki kireç oranlarından biraz yüksektir. Harçlarda kullanılan agregaların farklı özellikler gösterdiği tespit edilmiştir. Her bir harç örneğinde kullanılan agregalar, benzer tane büyüklüğü dağılımı göstermektedirler. Harçlardaki ince taneli agregalar, iri taneli agregalar ile benzer mineralojik ve kimyasal kompozisyona sahiptirler. Buna karşılık, ince taneli agregalar, yüksek oranlarda amorf malzeme, silisyum dioksit ve alüminyum oksit içerdikleri için iri taneli agregalardan daha yüksek puzolanik özelliğe sahiptirler. Harçlarda bağlayıcı malzeme olarak saf kireç ve yüksek oranlarda silisyum içeren kireç kullanılmıştır. Puzolanik agrega ve yüksek oranlarda silisyum içeren kireç kullanımından dolayı kubbelerde kullanılan kireç harçlarının tümü ve duvarlarda kullanılan kireç harçlarının bazıları hidrolik kireç

harçlarıdır. Bu harçlardaki puzolanik agregalar ile kirecin birbirleri ile iyi bir şekilde bağlandığı tespit edilmiştir. Kubbelerde kullanılan hidrolik kireç harçları, duvarlarda kullanılan hidrolik olmayan kireç harçlarından daha yüksek mekanik özelliklere sahiptirler. Kubbe ve duvar harçlarında gözlenen bu farklılık, alt ve üst yapı elemanlarının farklı strüktürel davranışına bağlı olarak bilinçli bir şekilde üretilen harç yapım tekniği ile açıklanabilir. Kubbelerde kullanılan tuğlalar düşük puzolanik özelliğe sahip olmalarına rağmen kireç harçları ile iyi bir şekilde bağlanmaktadır. Bu durum, kubbelerin strüktürel dayanımlarının sağlanmasında etkilidir.

Bu sonuçlar, hamamlardaki kireç harçlarının kullanıldıkları yapı elemanlarının özelliklerine göre bilinçli bir şekilde üretildiği ve bunun Seferihisar-Urla bölgesinde yer alan hamam yapılarına özgü geleneksel bir harç yapım tekniği olduğunu göstermektedir.

Birinci bölümde çalışmanın konusu, amacı, kapsamı ve metodu belirtilmiştir. İkinci bölümde, kireç harçlarının genel özellikleri ve üretim aşamaları verilmiştir. Üçüncü bölümde, harç örneklerinin yapılardan toplanması ve deneysel çalışmalardan oluşan çalışma metodu tanımlanmıştır. Dördüncü bölümde, deneysel çalışmaların sonuçları değerlendirilmiş ve bunlar literatürde yer alan benzer çalışmaların sonuçları kapsamında tartışılmıştır. Beşinci bölümde, çalışmadan elde edilen başlıca sonuçlara yer verilmiştir.

TABLE OF CONTENTS

LIST OF FIGURES

LIST OF TABLES

Chapter 1

INTRODUCTION

1.1. Subject and Aim

In conservation studies of historic buildings, interventions should be carried out with the aim of safeguarding their authentic values such as aesthetic, historical, social and cultural values[1]. These values include not only their architectural characteristics such as form, design, function and location characteristics, but also their structure and material characteristics. Characteristics of the building materials are of particular importance in conservation studies since they provide information on traditional material characteristics and evaluation of structural behaviour of the historic buildings. Therefore, material conservation plays the fundamental role in conservation studies of the historic buildings. This requires an interdisciplinary collaboration that deals with the types and characteristics of original building materials, their conservation problems and determination of compatible intervention materials that would be used in restoration studies.

Conservation of original building materials with minimum intervention in the restoration studies of historic buildings was defined by international charters and documents as one of the basic principles of contemporary conservation approaches. Among them, the Venice and Burra Charters are the most important ones that point out the importance of conservation of the original materials. The Venice Charter exposed the fact that historic monuments should be safeguarded for future generations in their full authenticity as works of art and historical evidence[2]. The 9th article of this charter has a remarkable importance in emphasizing the conservation of the original materials together with aesthetic and historic values of monuments. In the 10th article, special emphasis is given to the use of traditional techniques and materials in conservation studies. It is also pointed out that modern techniques and materials may be used in some circumstances as long as their efficacy is proved by scientific data and experience.

---

[1] The Nara Document on Authenticity, http://www.international.icomos.org/naradoc_eng.htm
[2] The Venice Charter, http://www.international.icomos.org/e_venice.htm

Likewise, the Burra Charter contributed to the development of the scope of the material conservation principles defined by the Venice Charter[3].

Even though the aforementioned charters were accepted in Turkey, restoration studies have been carried out without regarding the material conservation principles defined in these charters. Original building materials are generally renewed without understanding their material characteristics and identification of their deterioration problems, and modern building materials are frequently used without testing their compatibility with the original materials. Among them, cement-based mortars are the ones used most frequently in many restoration studies of historic buildings in Turkey. However, their use in restoration studies is completely in disagreement with the material conservation principles recommended by the Venice and Burra Charters.

Use of cement-based mortars in restoration studies is not advisable since they are different from historic lime mortars in terms of physical and mechanical properties, and chemical and raw material compositions. Since cement mortars are rigid materials having a high compressive strength, they can create high local stresses that can lead to serious damage in adjacent original building materials such as brick, stone and mortar. Furthermore, thermal expansion of the cement-based mortars is higher than that of lime mortars (Schaffer 1972). This accelerates deterioration of the lime mortars. In addition, the cement-based mortars have high contents of soluble salts. Therefore, they can lead to serious problems caused by re-crystallization of soluble salts (Schaffer 1972). Moreover, since such mortars are less permeable than lime mortars, they retain moisture and can not provide the evaporation of masonry. Therefore, evaporation takes place through the porous original building materials. This causes crystallization of soluble salts in the original building materials, which induces severe deterioration problems (Schaffer 1972, Peroni et al. 1981, Kent 1995, Steward et al. 1994, Hughes et al. 1998, Holmes and Wingate 1997). For such reasons, the cement-based mortars are not suitable intervention mortars to be used in the restoration of historic buildings and their use should be strongly avoided. Therefore, determination of appropriate intervention mortars that would be used in the restoration of the historic buildings gains special importance.

Within this context, the problem in this study is defined as the use of incompatible mortars in restoration of historic buildings in Turkey. Therefore, the subject of this

---

[3] The Burra Charter, http://www.icomos.org/australia/burra.html

study is the determination of the characteristics of lime mortars used in walls and domes of some historic Ottoman baths in Seferihisar-Urla region near İzmir. Aim of this study is to provide basic data about the lime mortar characteristics for the purpose of conservation of these historic buildings. It is also aimed to investigate the characteristics of the lime mortars in relation to their specific use in the structural elements of the walls and domes. Special emphasis is given to the investigation of basic physical, mechanical, microstructural and hydraulic properties of the mortars, their raw material compositions, mineralogical and chemical compositions of the raw materials for the purpose of the production of new intervention mortars compatible with the original ones.

Determination of lime mortar characteristics for the conservation of historic buildings became an important subject in the second half of the 20th century due to extensive damage of cement-based mortars in the historic buildings. Therefore, several scientific researches have been carried out on characterization of historic lime mortars and determination of intervention mortars compatible with them. These researches were compiled by Hansen et al. in a bibliography which provides an extensive source regarding lime mortars (Hansen et al. 2003). However, researches carried out about the related subject in Turkey are very scarce. These are the ones carried out by Akman et al., Aktaş, Tunçoku, Güleç, Satongar, Güleç and Tulun, İpekoğlu et al. and Böke et al. (Akman et al. 1986, Aktaş 1988, Tunçoku 1993, Güleç 1992, Satongar 1994, Güleç and Tulun 1996, Tunçoku 2001, İpekoğlu et al. 2003, Böke et al. 2004a, Böke et al. 2004b). Therefore, this thesis gains special importance for its contribution to the present researches related with investigation of lime mortar characteristics for the purpose of conservation of historic buildings in Turkey.

1.2. Limits of the Study

Historic buildings whose mortars were examined in this study were selected according to a series of criteria such as same function, similar construction period and location, and their authentic values. Therefore, the historic buildings were limited with the five Ottoman baths in Seferihisar-Urla region near İzmir. These baths, dated back to the 15th and 16th centuries, are Düzce Bath, Seferihisar Bath and Ulamış Bath in Seferihisar, and Hersekzade Bath and Kamanlı Bath in Urla. These Ottoman baths are important historic buildings of their periods and in their locations since they have been

mostly preserved with all their authentic values without any extensive interventions. Thus, their original building materials have been mostly preserved. Moreover, these baths show almost similar characteristics with respect to their traditional construction techniques and building materials. However, these historic baths are in danger of becoming demolished since any studies have not been conducted yet for their conservation. Therefore, these historic Ottoman baths were studied in two concurrent master theses for the purpose of their conservation. While this Master's thesis investigates the characteristics of the lime mortars used in these baths, their construction techniques and materials were examined in another Master's thesis (Reyhan 2004).

In the construction of the Ottoman baths, mortars were used in stone masonry walls and brick masonry superstructures of domes and vaults. Therefore, the mortars collected have been defined according to their specific use in the structural layout as stone masonry mortars collected from the walls and brick masonry mortars collected from the domes. This criterion has provided the examination of their material characteristics in relation to the structural characteristics of the walls and domes where the mortars were used.

1.3. Method of the Study

Method of the study is composed of sampling and experimental study. Sampling covers the collection of mortar samples from the walls and domes of the selected baths in order to carry out laboratory studies for the determination of their material characteristics. Experimental study covers a series of laboratory studies in order to determine basic physical and mechanical properties of mortars, their raw material compositions, pozzolanic activity of aggregates used in the mortars, soluble salts in mortars, their mineralogical and chemical compositions, microstructural and hydraulic properties. Moreover, determination of basic physical and pozzolanic activity properties of bricks used in the construction of domes and microstructural examination of mortar-brick interfaces were also included. Results of these laboratory studies were then evaluated, discussed and compared with the results of analyses of other lime mortars used in some historic buildings of the Byzantine, Seljuk and Ottoman periods.

Chapter 2

LIME MORTARS

Mortar is a composite building material which consists of binder and filling material. It is used as a bonding agent for bedding and jointing masonry units, and rendering masonry surfaces (Cowper 2000, Davey 1961).

Several kinds of mortars were used in construction of historic structures. Mud is known to have been the oldest mortar which was used for laying sun-dried bricks. It consisted of sand, silt and clay particles as the binder and was used usually with chopped straw or reeds (Davey 1961). Gypsum mortar was used for bedding stonework in ancient Egypt. It acted as not only a bonding material, but also a lubricating film that allowed large stone blocks to set in their right positions by sliding them (Davey 1961). Asphaltic mortars had been used for bedding fired bricks. By the time, their use was replaced by hydrated lime mortars sometimes containing clay, bitumen, ashes, or other materials (Davey 1961).

Among the historic mortars, lime mortar is the most widely used historic building material which is primarily composed of lime as the binder and aggregates as the filling material. The earliest documented use of lime in buildings dated back to 4000 B.C. by the use of plastering in pyramids in Egypt (Boynton 1966, Cowper 2000). By the remains of a limekiln, it was approved that lime burning had been practiced in Mesopotamia in 2450 B.C. (Davey 1961). Romans were the ones who had successfully improved the use of lime mortars in masonry structures. They had discovered that when lime was mixed with pozzolanas (reactive aggregates), it hardened under water. This had led to the development of a durable and a strong material called Roman concrete which allowed the construction of magnificent structures with great interior spans (Cowan 1997, Davey 1961).

The present chapter deals with lime mortars in respect to their production process. First, functions and properties of mortar in masonry are described. Then, characteristics of lime used as a binding material are given. Finally, process of lime production and preparation of lime mortars are mentioned in detail including respectively types of limestone used for production of lime, calcination of limestone, hydration (slaking) of

quicklime, characteristics of aggregates used in lime mortars, preparation of lime mortars and hardening of lime mortars.

2.1. Functions and Properties of Mortar in Masonry

Mortar has certain functions as a bonding agent in masonry. First of all, the mortar in a structural element should provide a uniform bedding surface for masonry units so that load is spread evenly over them. Secondly, the most important function of the mortar is that it should bind the masonry units into a monolithic mass and help them to resist forces occurred in masonry. Therefore, it should have sufficient strength to hold the masonry units together and to spread loads evenly together with the masonry units (Davison 1976, Allen et al. 2003). Furthermore, the mortar should seal the joints against rain penetration (Allen et al. 2003). Besides, it should ensure adequate durability to resist severe damages of atmospheric conditions such as frost action and wetting-drying cycles due to changes in temperature, humidity and wind (Davison 1976). Last of all, the mortar should be capable of drawing moisture out of a wall and providing a good surface for evaporation. Therefore, the mortars are preferred to be more porous and permeable than the masonry units (Holmes and Wingate 1997).

Mortar mixture should have some certain properties prior to its hardening in order to achieve its aforementioned functions in masonry. The primary ones are plasticity, workability and water retentivity properties. The plasticity of the mortar can be defined as the property which enables the mortar to have a satisfactory workability and contributes to water retentivity (Cowper 2000). Workability is the ability of the mortar to be smooth and mouldable. Good workability provides good workmanship that enables the mortar to be spread over the masonry units easily under the influence of a trowel, to flow into all crevices of the masonry units, and to correct any dimensional irregularities of the masonry units to form an even bed. However, poor workability makes the mortar become stiff and useless as the water evaporates. The workability is in fact the combination of several factors including plasticity, consistency and cohesion (Davison 1976, Holmes and Wingate 1997).

Water retentivity is the ability of the mortar to retain its water against the absorption of masonry units so that the mortar retains its workability. When mortar is spread over the masonry units, it starts to lose water through the absorption of the

masonry units and by evaporation to the air from the surface of the joints. The former improves the bonds between the masonry units and the mortar. However, if water in the mortar is lost quickly, the mortar becomes less workable and poor quality. For this reason, it is important that sufficient amount of water be retained in the mortar to ensure good workability and a good bond with the masonry units (Davison 1976, Holmes and Wingate 1997).

It is of particular importance that hardened mortar should not be stronger than masonry units to be bounded and should be sufficiently resilient to accommodate small structural movements, shrinkage and expansion of masonry (Davison 1976, Allen et al. 2003). This is owing to the fact that soft mortars are capable of tolerating small deformations occurred in the masonry. For instance, stresses and strains developed in the masonry can be relieved by many fine cracks occurred within lime mortars. These fine cracks are then sealed by a successive mechanism where free lime is converted into calcium carbonate by rain water permeating the masonry (Davison 1976, Holmes and Wingate 1997). Thus, the lime mortars have a distinct property of self-healing which contributes to the survival of masonry throughout years. Unlike lime mortars, cement-based mortars used in contemporary masonry are not capable of absorbing stresses in this manner. Therefore, large cracks occur and provide open paths for rain penetration (Davison 1976, Holmes and Wingate 1997). This can lead to serious problems caused by re-crystallization of soluble salts (Schaffer 1972).

2.2. Characteristics of Lime as a Binding Material

Lime used as a binding material for building purposes has certain characteristics that can be presented as follows (Holmes and Wingate 1997):

- Lime is a sticky material that provides good adhesion to masonry surfaces.
- Lime acquires good workability to lime-based building materials. It imparts plasticity and increases the water carrying capability of the lime-based building materials.
- Lime has self-healing ability which is the property of developing fine cracks rather than individual large cracks when buildings are subjected to small movements. This property depends on the plasticity characteristic of the lime.

- Lime-based building materials have the ability of breathability which is the property of handling moisture movements through masonry. Therefore, lime-based materials can enable the masonry to dry out easily. This protects building materials from condensation problems that can give rise to salt crystallization.

- Lime-based building materials improve comfort conditions due to the property of low thermal conductivity which enables surface temperatures within buildings to remain warmer in cool climates and cooler in warm climates.

- Lime is a durable material that enables the structure to survive for longer years.

- Lime provides soft texture that acquires comfortable feeling and good appearance to lime surfaces.

Due to its favourable characteristics, lime has been used as a binding material in building materials for thousands of years. It has a wide variety of uses in the structural elements such as foundations, walls, floors, vaults and domes, and in many finishes including paints, plasters, renders and decorative work such as cornices and hand-modelled stucco.

2.3. Production of Lime and Preparation of Lime Mortars

Lime is produced through chemical reactions of calcination of limestone and slaking of quicklime. When limestone is heated, calcium carbonate is converted into calcium oxide known as quicklime. Then, the quicklime is slaked with water for the formation of lime (Cowper 2000, Boynton 1966) (Figure 2.1).

Lime mortar is composed of lime and aggregates. Such mortar can harden either by carbonation reaction or hydraulic set. In the carbonation reaction, the lime mortar hardens by a slow reaction of lime with carbon dioxide gas in the atmosphere. Hydraulic set takes place when lime is combined with silicates and aluminates in the presence of water (Cowper 2000, Boynton 1966) (Figure 2.1).
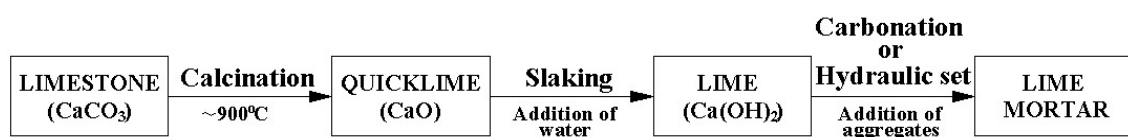
Figure 2.1 Schematic overview of the lime production and lime mortar preparation.

2.3.1. Types of Limestone Used for the Production of Lime

Limestone that provides the raw material of lime is a sedimentary rock whose principal constituent is calcium carbonate ($CaCO_3$). Since pure limestone is rarely found in nature, limestone always contains some impurities in small or large quantities such as magnesium oxide (MgO), silicon dioxide (SiO_2), aluminium oxide (Al_2O_3), iron oxide (Fe_2O_3), sulphur and alkalies (Eckel 1928, Davey 1961). Therefore, limestones are generally classified according to the contents of the calcium carbonate and the impurities as high-calcium limestones, magnesium limestones and dolomitic limestones. Limestones containing 90 % and more of calcium carbonate are called high-calcium limestones, the ones containing 10 % and more of magnesium carbonate are magnesium limestones and those containing magnesium carbonate over 25 % are called dolomitic limestones (Gay and Parker 1932, Holmes and Wingate 1997).

There are certain types of limestones used for the production of lime. These are oolitic limestones, dolomitic and magnesian limestones, clayey (argillaceous) limestones, calcareous tufa and travertine, some carboniferous (mountain) limestones, and some metamorphic limestones (Eckel 1928, Davey 1961, Holmes and Wingate 1997). Although marble is a type of limestone composed of calcium carbonate, it is not a suitable material for producing lime since it has large grains that can not slake easily (Torraca 1988).

2.3.2. Calcination of Limestone

When limestone is heated at around 900°C in a 100 % CO_2 atmosphere at 760 mmHg pressure, calcium carbonate ($CaCO_3$) is dissociated through the release of carbon dioxide gas (CO_2) and the formation of calcium oxide (CaO) which is a white solid material known as "quicklime", "lump lime" or "unslaked lime" (Eckel 1928, Boynton 1966, Holmes and Wingate 1997). This process is called calcination of limestone and its overall reaction is as follows:

$$CaCO_3 \xrightarrow{\;900°C\;} CaO \;+\; CO_2$$

| Calcium carbonate | Calcium oxide | Carbon dioxide |
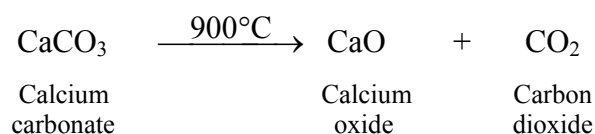
Calcination temperature depends on chemical composition of limestone. While the calcination temperature of high-calcium limestone is at around 900°C, the one of magnesium limestone is at around 600-700°C (Eckel 1928). During the calcination process, limestone loses 44 % of its weight due to the release of carbon dioxide gas. This causes quicklime to have a porous microstructure. Quicklime with very small particle sizes and high specific surface areas is the most desirable end product in order to have a high reactivity (rate of slaking) with water in the following slaking process (Potgieter et. al. 2002). After the calcination process is over, quicklime should not be exposed to air since it has a tendency to react with moisture present in the atmosphere and subsequently to reconvert back into calcium carbonate through the reaction with carbon dioxide gas in the atmosphere (Boynton 1966, Holmes and Wingate 1997, Potgieter et. al. 2002).

Calcination of limestone takes place in limekilns. They were often built inside a hill from which limestones were quarried so that limestone could be fed into the limekilns with minimum labour (Davey 1961). This also provided easily charging of the limekiln with limestones, to supply fuel and to draw out quicklime (Eckel 1928). Wood and charcoal were the fuels used in ancient times (Davey 1961). Lime burners were highly skilled people who worked unusual hours. In Roman period, inmates and criminals were often sent to work at limekilns (Krumnacher 2001).

Flare (intermittent) kiln and continuous (running) kiln were the two basic types of traditional limekilns used for calcination of limestone. In flare kilns, where intermittent burning took place, quicklime did not come into direct contact with fuel, but with only heat and flames (Figure 2.2). In order to load the kiln, a rough arch of limestone lumps was built over a framework or hearth of iron bars and further limestones were added to fill the kiln completely (Davey 1961). After the limestone was burnt for 1.5 or 2 days and cooled for an equal length of time, quicklime was removed from the bottom of the kiln prior to the addition of new limestones (McKee 1971).

In running kilns where loading and burning were continuous, limestones and fuel were charged into the kiln in alternate layers (Figure 2.3). These alternate layers of limestone and fuel (coal) were piled up to the top of the kiln and fire was started at the bottom. As the lower layers of limestone became calcined, quicklime was drawn out from the bottom of the kiln. Meanwhile, further layers of fuel and limestone were deposited in the top of the kiln in order to fill the limekiln successively. It took about a week for a limestone layer to pass from the top to the bottom of the kiln. The quicklime

produced was not as pure, as white and as evenly burnt as the one burnt in a flare kiln since ashes of the fuel could not be removed from the quicklime. This prevented the even burning and reduced the quality of the quicklime (Davey 1961).
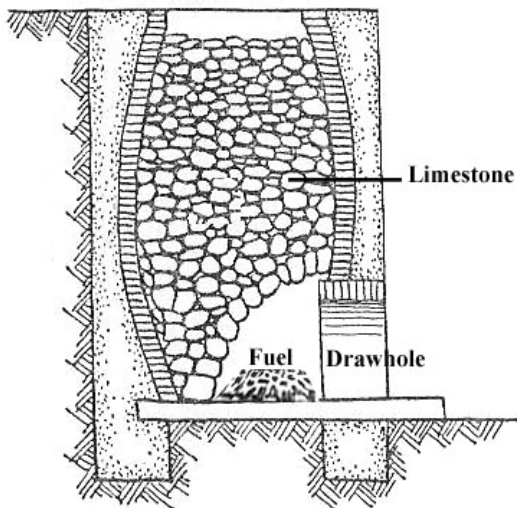
Figure 2.2 Drawing illustrating a flare kiln (Source: Davey 1961).
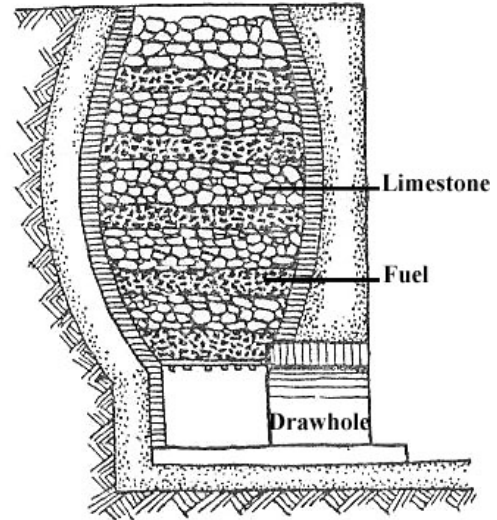
Figure 2.3 Drawing illustrating a continuous kiln (Source: Davey 1961).

Ring (chamber) kiln and Rotary kiln are the modern types of kilns used for both lime and Portland cement burning. In these kilns, oil and gas are used as fuel and calcination of limestone takes place at high temperatures. Therefore, there is the disadvantage of quicklime to become over-burnt (Ashurst and Dimes 1990).

2.3.2.1. Factors Influencing the Characteristics of Quicklime

Major factors that influence the characteristics of quicklime are chemical composition of limestone, physical characteristics of limestone (surface area, pore size distribution, crystallite size, etc.) and calcination conditions (calcination temperature, retention time, rate of calcination, pressure acquired in limekilns, carbon dioxide concentration in limekilns, fuel quality).

Chemical composition of limestones: Chemical composition of limestone directly influences the characteristics of quicklime produced. When pure limestone is heated, quicklime with high percent of calcium oxide is produced. However, calcination of a magnesian limestone produces quicklime consisting partially of calcium oxide and

11

magnesia (Eckel 1928, Holmes and Wingate 1997). Moreover, argillaceous limestones, which naturally contain active clays such as silica, alumina and ferric oxide, can produce quicklime containing active compounds of calcium-aluminates-silicates. These compounds are the ones that will further acquire lime to have a hydraulic property (Cowper 2000, Eckel 1928, Davey 1961).

Physical characteristics of limestones: Physical characteristics of limestone influence the physical characteristics of quicklime. When porous limestone is heated, the produced quicklime mostly has high values of porosity, total cumulative volume and specific surface area. On the other hand, when a dense limestone with less porosity is heated, the produced quicklime has a dense structure, low values of porosity and specific surface area, and high pore radius average (Moropoulou et al. 2001).

Sizes of limestones influence the calcination temperature and their retention time in a limekiln. Calcination develops from the outer surface towards the inside of the limestone particles. Therefore, heat penetration into the limestone particles varies according to their particle sizes. The calcination of small limestones proceeds rapidly since they provide a great surface area for heat transference. However, the calcination of larger ones proceeds slower and this process often requires high temperatures in order to provide the calcination of the interior of the large limestone particles (Boynton 1966, Hassibi 1999).

Calcination conditions: Calcination temperature plays a significant role in the characteristics of quicklime produced. This will in turn influence the properties of lime to be produced. The temperature of around 900°C is the most appropriate calcination temperature since quicklime produced at this temperature has the greatest surface area, highest porosity and highest reactivity (Cowper 2000, Davey 1961, Boynton 1966). However, calcination temperature lower than 900°C causes less reactive quicklime called under-burnt quicklime containing cores of uncalcined carbonate due to incomplete calcination. On the other hand, when a limestone is heated at a temperature higher than 900°C, quicklime occurred at the end of this process may become hard-burnt (Holmes and Wingate 1997). If the calcination is carried out at considerably high temperatures of around $1400^{\circ}C$, dead-burnt quicklime having a low porosity (8-12 %) is obtained (Swallow and Carrington 1995). This leads to densification, and a decrease in the surface area and chemical reactivity of the quicklime (Gillot 1967).

Retention time of quicklime in a limekiln is the other factor influencing the characteristics of quicklime. Long retention time in the limekiln can cause quicklime to become either hard-burnt or dead-burnt. On the other hand, short retention time in the limekiln can cause less reactive quicklime containing cores due to the incomplete calcination (Potgieter et. al. 2002).

Fuel used in limekilns influences the reactivity of quicklime. Traditional lime was high-quality since wood and charcoal, which acquired the temperature of about 900°C, was used as fuel in traditional limekilns (Davey 1961). Wood produces relatively low flame temperature, long flames and steam, which provides reactive quicklime (Cowper 2000). However, by the middle of the 19th century, use of oil, gas and carbon dust as fuel in limekilns caused the production of much heat. Therefore, calcination temperature increased and the quicklime became less reactive (Wingate 1985, Moropoulou et al. 2001).

2.3.3. Hydration (Slaking) of Quicklime

When quicklime (CaO) reacts with water, calcium hydroxide (Ca (OH)$_2$) known as lime is produced. This process is called hydration or slaking. The terms of hydration and slaking are technically synonyms. However, they are differentiated with the end products they produce. Hydration involves only required water and produces dry powder called "hydrated lime" whereas, slaking involves some excess water and yields wet hydrated lime in the form of plastic paste. Such lime is called "slaked lime", "lime putty" or "lime paste" (Elert et al. 2002). It contains about 30-40 % of free water surrounding the hydrated lime particles (Boynton 1966).

During the hydration of quicklime, water is absorbed by quicklime, a great deal of heat is evolved and lime paste expands in volume. This expansion results in breaking up the entire mass into a fine powder (Boynton 1966). Chemical reaction involved in the hydration of quicklime is as follows:

$$CaO \;\; + \;\; H_2O \;\; \rightarrow \;\; Ca(OH)_2 \;\; + \;\; heat\uparrow$$

Quicklime   Water   Lime
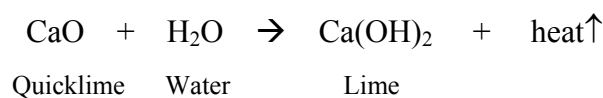
Hydration should be carried out very slowly and carefully since reaction between lime and water raises temperature of the water to almost boiling temperature. Therefore,

quicklime should be added by a shovel into a tank containing water. Enough water should be used to avoid coagulation of particles which considerably reduces the plasticity of the lime (Boynton 1966, Ashurst and Ashurst 1998).

During the hydration of quicklime, surface area and volume of lime increase (Eckel 1928, Boynton 1966). Expansion rate is influenced by the characteristics of the quicklime. High calcium quicklime expands 3.5 times in volume if slaked entirely. On the other hand, air-slaked quicklime expands only about 1.7 times of its original volume. Impure quicklimes present less expansion depending on the amount of impurities (Eckel 1928).

2.3.3.1. Factors Influencing the Characteristics of Lime

Characteristics of lime are influenced by various parameters such as characteristics of quicklime (surface area, porosity, pore size distribution, crystallite size, impurity, calcination conditions), water quality, water/lime ratio, slaking temperature, slaking time, agitation rate and aging of lime putty.

Characteristics of quicklime: Characteristics of quicklime produced in the previous calcination process are the most important factors influencing the characteristics of lime. Pure quicklime with high porosity slakes rapidly due to its high water permeability. The end product is a high calcium lime. However, quicklime containing calcium-aluminates-silicates produces hydraulic lime. Such quicklime slakes much slower than high calcium quicklime since the impurities may give rise to formation of slag (waste product) which fills the pores and makes the surface impervious to water (Eckel 1928, Davey 1961, Boynton 1966). Moreover, quicklime containing high amounts of magnesia slakes slowly with less evolution of heat and less expansion in volume (Eckel 1928). Furthermore, powdered quicklime slakes more rapidly than lumps and produces lime composed of fine particles (Boynton 1966). However, hard-burnt quicklime, and quicklime exposed to air-slaking and re-carbonation slake slowly (Holmes and Wingate 1997, Potgieter et. al. 2002).

Water quality: Water quality is an important factor influencing the characteristics of lime. Water of high purity is preferred in order to avoid soluble salts. Water

containing sulfates and sulfites can cover the surface of the lime particles and prevent water penetration into pores. This can lead to incomplete slaking. On the other hand, some chemicals such as chlorides and sugars have a favourable effect on the slaking process (Boynton 1966, Hassibi 1999, Holmes and Wingate 1997). However, chlorides cause serious deterioration problems in the long term due to dampness caused by hygroscopic salts and subsequent salt crystallization (Boynton 1966, Hassibi 1999, Holmes and Wingate 1997).

Lime/water ratio: The amount of water required for slaking process depends on the characteristics of quicklime. High calcium lime requires more water than the lime containing impurities (Eckel 1928). In the slaking process, ratios of calcium oxide and excess water generally range from 1:2.5 to 1:6 (Boynton 1966, Hassibi 1999). In order to produce dry hydrate, one part of quicklime by weight is mixed with about 0.5-0.75 part of water (Boynton 1966, Holmes and Wingate 1997). On the other hand, inadequate water content can lead to localized overheating (above 200°C), which causes the hydrated lime to become burnt and may even result in dehydration process (Boynton 1966).

Slaking temperature: During slaking of quicklime, heat is generated. Therefore, slaking temperature should be under control. This temperature depends on the characteristics of quicklime and lime to be produced. Hydration should be performed at boiling temperature or slightly less, and slaking at about 71-93°C (Boynton 1966). Excessively high temperatures reduce plasticity of lime since fine lime particles could coagulate (Cowper 2000).

Slaking time: High reactive lime hydrates completely in 2-3 minutes. Hydration of moderate reactive limes takes place in 5-10 minutes. Low reactive limes, hard-burnt limes and magnesium limes hydrate completely in 15-30 minutes (Boynton 1966, Hassibi 1999).

Agitation rate: Agitation during slaking has a favourable effect on the slaking rate. It prevents localized overheating, increases dispersion of lime particles and provides high temperature during slaking (Boynton 1966). It was also found that high stirring speed mostly results in a great deal of lime putty. On the other hand, little agitation

results in hot and cold spots due to uneven slaking temperature (over 100°C). This leads to a decrease in surface area of lime particles. Agglomeration of lime particles and cold spots can cause unhydrated calcium oxide particles (Boynton 1966, Hassibi 1999).

Aging of Lime Putty: Aging of lime putty by storage under water for a period of time as long as possible has been regarded as an important phase in improving the quality of lime since ancient times. Upon aging, portlandite (calcium hydroxide) crystal size reduces and platelike portalandite crystals occur due to dissolution of prism faces and secondary crystallization of sub-micrometer large portlandite crystals. This leads to an increase in surface area. As a result, more water can penetrate into newly formed large portlandite crystals. This gives rise to the evolution of lime putty with high workability, plasticity and water retention (Navarro et al. 1998, Cazalla et al. 2000).

Romans were aware of favourable effects of aged lime. Roman laws dictated that lime was not to be used until it had been slaked for three years (EHDBL 1997). Even presently in Denmark, local regulations state that lime which will be used for the repair of historic churches must be at least five years old (Holmes and Wingate 1997).

2.3.3.2. Classification of Limes

A formal classification of lime according to its ability to set under water was firstly introduced by Louis Vicat at the beginning of the 19th century (Vicat 2003, Eckel 1928, Cowper 2000). This classification was based on the proportions of the constituents of calcium oxide and impurities present within the limes, and the way the limes hardened. This classification is as follows:
- Non-hydraulic limes
  - o Fat limes
  - o Lean limes
  - o Magnesian limes
- Hydraulic limes
  - o Feebly hydraulic limes
  - o Moderately hydraulic limes
  - o Eminently hydraulic limes

Non-hydraulic limes contain calcium carbonate over 90 %. Such limes slake rapidly, evolve much heat during slaking and expand greatly in volume with a high degree of plasticity (Eckel 1928). They hold much water in their pastes and retain water against the absorption of masonry units. This derives from the property of these limes to be fatter than hydraulic limes, which provides good workability for lime mortars (Holmes and Wingate 1997). Non-hydraulic limes are classified according to impurities they contain. Fat limes (rich or high-calcium limes) contain calcium oxide over 95 %. The rest of 5 % is composed of impurities such as silica, alumina, and iron oxide. Lean limes known as poor limes contain impurities more than 5 % (Vicat 2003, Eckel 1928). Magnesian limes are produced from magnesian limestones having magnesium carbonate content over 30 %. Such limes are less plastic, slake very slowly, and develop little heat and less expansion in volume (Eckel 1928). They can give early set, provide good workability, are much stronger than high calcium limes and carry more aggregates (Eckel 1928, Boynton 1966, Holmes and Wingate 1997). However, late hydration of MgO can lead to poor soundness by pitting and popping (Ramachandran et al. 1964, Holmes and Wingate 1997).

Hydraulic limes are produced by either calcination of limestones naturally containing clay or of mixtures of clays and pure limestones. Such limes are classified according to the amount of active clay materials they contain. Feebly hydraulic limes contain active clay materials less than 12 %, moderately hydraulic limes contain 12-18 % and eminently hydraulic limes contain 18-25 %. Such limes slake more slowly and expand less in volume with a small increase in comparison to non-hydraulic limes (Vicat 2003, Cowper 2000).

Non-hydraulic and hydraulic limes can also be distinguished from each other by a value called hydraulic index (Eckel 1928, Cowper 2000). This is the ratio of percentages of silica and alumina to the percentages of lime and expressed as follows:

$$\text{Hydraulic Index} = \frac{\text{Silica}(\%) + \text{Alumina}(\%)}{\text{Lime}(\%)}$$

Fat limes present a hydraulic index less than 0.1, feebly hydraulic limes give a hydraulic index in the range of 0.1-0.2 and good hydraulic limes exhibit a hydraulic index between 0.2 and 0.4 (Cowper 2000).

2.3.4. Characteristics of Aggregates Used in Lime Mortars

Lime is never used alone as mortar since evaporation of water during its hardening causes contraction in volume. This contraction leads to deep cracks. Therefore, lime is mixed with aggregates in order to be used as mortar. The aggregates have an important role on the performance of mortars by acting as a filling material that prevents shrinkage and consequent cracking while drying (Eckel 1928, Davey 1961, Holmes and Wingate 1997). The addition of aggregates is also necessary to impart strength, hardness and a certain degree of porosity that will facilitate the carbonation process (SLCHS 1995). The aggregates also act as air antrainers, which enables the mortar to resist frost damage to some degree (SLCHS 1995).

Aggregates used in lime mortars can be either quarried aggregates or river and sea sand. The latter can be used as aggregates only if they are well washed in order to remove impurities (Davey 1961). Aggregates quarried should also be rinsed in order to remove salts, and clay or organic materials which can slow the hardening of mortar (Holmes and Wingate 1997).

Physical characteristics of aggregates directly influence the workability and performance of a mortar. For mortar with good strength, angular and sharp-edged aggregates are preferred to round ones since the former provides the highest specific surface area for the best adherence with lime (Davey 1961, Holmes and Wingate 1997). Range of particle sizes of the aggregates is another critical factor. The aggregates should be composed of a wide range of particle sizes which are equally and evenly distributed so that spaces between larger grains will be filled with smaller ones. If the aggregates are not well-graded, the mortar will be of low quality (Davey 1961, Holmes and Wingate 1997).

Mineralogical compositions of aggregates are also critical to the performance of mortar. Aggregates with high contents of quartz minerals might make little contribution to the early setting of mortar. Aggregates containing feldspars and schists may contribute to a degree of slightly pozzolanic reaction and to the future strength of the mortar. Some mortars contain carbonate aggregates such as crushed limestones and calcareous sand. These porous aggregates provide a porous structure which resists decay from frost and salt crystallization and improves the process of carbonation. These

carbonate aggregates are also capable of improving internal bonding of the mortar (Holmes and Wingate 1997, SLCHS 1995).

2.3.4.1. Classification of Aggregates

Aggregates used in lime mortars are classified as inert aggregates and pozzolanic aggregates. Inert aggregates are the ones that do not undergo any chemical reaction with lime. Unlike the inert aggregates, pozzolanic aggregates are active aggregates containing reactive silicates and aluminates that can readily react with lime in the presence of water (Davey 1961).

Pozzolanic aggregates are not cementitious by themselves but contain some compounds of silica and alumina. When such compounds react with lime, stable insoluble compounds of cementitious properties such as calcium-silicate-hydrates and calcium-aluminates-hydrates are produced. These compounds make up a network of fibrous crystals or gelatinous amorphous material (gel), which enables lime mortar to produce hydraulic set and to impart great strength (Cowper 2000, Lea 1940).

Pozzolanic aggregates are classified as natural and artificial pozzolanas (Cowper 2000, Lea 1940). Natural pozzolanas are generally of volcanic origin but also include some certain diatomaceous earths. Pozzolanas of volcanic origin are composed of reactive silicates, and contain glassy and crystalline particles. However, all volcanic ashes do not have pozzolanic property and some of them can be used as inert aggregates (Lea 1940). Diatomaceous earths are mainly comprised of opal which is an amorphous form of hydrous silica (Lea 1940). Reactivity of opal with lime is derived from its amorphous character and its structure which allows pores to absorb alkali solutions into all parts of the aggregate. Therefore, amorphous silica contributes to the hydraulic properties of lime mortars (Diamond 1976).

Artificial pozzolanas are mainly obtained by heat treatment of natural materials such as clays, certain siliceous rocks, and ground fuel ash (fly-ash) (Lea 1940). Burning of certain clays at temperatures between 600°C and 900°C destroys the crystallographic structure of clay minerals. This leads to an amorphous mixture of silica and alumina that can react with calcium hydrate. Reaction produces more or less hydraulic components depending on the amount of clays, their mineralogical compositions and burning temperatures (Davey 1961, Lea 1940, Baronio et al. 1997, Charola and Henriques

1999). Lightly-burnt (at ~600°C) and finely-ground clays contribute to the best reactivity (Holmes and Wingate 1997).

Traditional use of pozzolanas in lime mortars was in a relativley coarse state. Coarser particles acted as inert aggregates and only the finer ones act as active pozzolanas. Activity of all pozzolanas was increased by grinding them finely (Lea 1940).

Use of lime mortars containing pozzolanic aggregates developed dramatically during the Roman period and resulted in astonishing changes in construction techniques (Cowan 1977). In fact, the most important use of pozzolana with lime was in the form of a mixture of lime, pozzolana and broken bricks and tiles. This technology produced a strong and a durable material called "Roman Concrete" or "*opus caementitium*" (Cowan 1977). Roman concrete together with brickwork enabled the construction of strong vaults and domes with enormous spans providing excellent and magnificent structures such as Pantheon, Baths of Caracalla, and Basilica of Constantine (Davey 1961). In the dome of Pantheon, a rational concrete technology was developed. While the lowest parts of the dome were built in crushed-brick layer followed by the layer of brick and tuff, in the upper parts lightweight concrete, which was composed of lightweight aggregate of tuff and pumice, was used (Cowan 1977).

2.3.5. Lime Mortar Preparation

Lime-aggregate ratio is mainly composed of 1 part of lime paste to 2-4 parts of aggregates (Eckel 1928). In aged-lime mortars, low binder/aggregate ratio of 1:4 is preferred since higher ratios can induce cracks that can be due to high water retention of small plate-like portlandite crystals in aged lime putties. Unlike aged lime mortars, non-aged lime mortars require high binder/aggregate ratio of 1:3 and do not present this kind of crack development (Cazalla et al. 2000). Traditional lime-pozzolana mortar was composed of 1 volume of lime putty to 2 volumes of unground pozzolana, 3-4 volumes of aggregates (about 1:3.5:8-12 by weight) (Lea 1940).

Sand-carrying capacity of lime is very important. It depends on plasticity of lime, size of hydrated lime particles, amount of impurities in lime, and average size and particle size distribution of aggregates used. Shrinkage will be almost entirely prevented

when aggregate particles are in direct contact with one another. The spaces among the aggregates will then be filled with fine particles of lime (Cowper 2000).

There are certain mixing methods that enable lime and aggregates to mix firmly. Hot lime technology is a method in which aggregates are mixed with lime during slaking of lime. This method has a distinct advantage in that introduction of aggregates to the lime during the slaking process is believed to enhance the covering of all aggregates with lime in such a good way that this cannot be achieved by conventional mixing procedures (Holmes and Wingate 1997, Ashurst and Ashurst 1998). Besides, storage of the lime putty mixed with aggregates as wet coarse stuff is the other mixing procedure which provides the mixture to mature well. The coarse stuff is stored in plastic bins with air-tight lids as long as possible (Ashurst and Dimes 1990, EHDBL 1997).

Beating or ramming lime-aggregate mixture is required to ensure that aggregates and lime are thoroughly united by filling the voids between them. This technique also provides high plasticity, reduces the amount of water required for plasticity and workability, and drive off excessive moisture. High plasticity provides more workable lime mortar, better bond between the mortar and masonry unit, and great sand-carrying capacity. However, since hydraulic mortars set under water and acquire a rapid set, they should not be beaten or worked after the initial set occurred (Cowper 2000).

Some organic or synthetic additives were assumed to have been used in some historic lime mortars. Additives such as egg white, blood, fig juice, rye dough, hogs' lard, curdled milk, casein, fats, oils and etc. were predicted to have been used for improving workability, extending and retarding setting time, increasing cohesion and strength of mortars (Cowper 2000, Sickels 1981). Moreover, hair was added if the mortar was to be used for rendering walls and ceilings (Davey 1961).

2.3.6. Hardening of Lime Mortars

Lime mortars harden by two different reactions as carbonation and hydraulic set. Carbonation is the reaction in which non-hydraulic lime gains strength by slow combination with carbon dioxide gas in the atmosphere. Hydraulic set occurs when lime is combined with silicates and aluminates in the presence of water.

2.3.6.1. Hardening by Carbonation

Non-hydraulic lime mortars harden by carbonation reaction composed of conversion of lime into calcium carbonate by absorbing carbon dioxide gas in the atmosphere. This reaction proceeds in two phases formulated as follows (Moorehead 1986):

$$CO_2 + H_2O \rightarrow H_2CO_3 \qquad\qquad (1)$$

$$Ca (OH)_2 + H_2CO_3 \rightarrow CaCO_3 + 2H_2O + 74kj\uparrow (2)$$

Carbonation takes place after the fresh mortar has partially dried as a result of water loss through evaporation and absorption by porous masonry units (Cazalla et al. 2000). Subsequently, carbonation starts with the penetration of carbon dioxide gas in the atmosphere through large capillaries from the surface of the mortar. At first, carbon dioxide dissolves in the water within small capillaries and water becomes acidic with the formations of H^+, HCO_3^- and CO_3^{-2} ions (1). Subsequently, calcium hydroxide particles are dissolved in the acidified solution and Ca^{+2} ions are formed. Afterwards, reaction between the ions of Ca^{+2} and CO_3^{-2} forms calcium carbonate which precipitates and expands into larger pores (2). This carbonation reaction continues either until all calcium hydroxide is converted into calcium carbonate or until all water in the capillaries is evaporated by heat generated during the reaction (Moorehead 1986).

Carbonation is a slow process lasting for months or even many years. It takes place inside the pores of the mortar and causes an increase of 35 % in weight corresponding to an increase of 11.8 % in volume in comparison with lime (Moorehead 1986). Therefore, total pore volume decreases and the mortar tends to become less permeable to the carbon dioxide gas as the carbonation reaction proceeds (Moorehead 1986). Besides, carbon dioxide absorption takes place only through the surface of the masonry with a depth of 10-12 mm. inside the joint (Holmes and Wingate 1997). Therefore, lime mortar in the interior of the masonry may never harden completely (Eckel 1928).

2.3.6.1.1. Factors Influencing the Carbonation Reaction

Carbonation reaction is influenced by several factors such as moisture content, permeability of mortar, carbon dioxide gas concentration, thickness of the mortar, calcium hydroxide concentration, use of aged-lime putty and climatic factors (relative humidity, temperature, wind speed and rain water).

Moisture content: Moisture content is critical for carbonation reaction since it plays a significant role in the diffusion of carbon dioxide gas within lime mortar (Cazalla et al. 2000, Van Balen and Van Gemert 1994). A minimum amount of water in which the carbon dioxide gas will be dissolved is required for the carbonation reaction. The optimum water content is the one required for the maximum adsorption on the pore surface before extensive capillary condensation occurs (Van Balen and Van Gemert 1994). When 50 % of the pore volumes of mortar are filled with water, the reaction rate is assumed to be maximum (Moorehead 1986). At such moisture content, it is assumed that smaller capillaries rather than larger ones are filled with water so that the larger pores are able to diffuse carbon dioxide gas inside the mortar and water vapour to evaporate. On the other hand, carbonation is retarded when the mortar is entirely saturated with water since diffusion of carbon dioxide in water is much slower than in the air (Van Balen and Van Gemert 1994).

Carbon dioxide gas concentration: Increase in carbon dioxide gas concentration leads to a considerable increase in carbon dioxide concentration in the pore volumes where the carbonation reaction takes place. As a result, solution of the carbon dioxide gas in water is increased. Therefore, the reaction proceeds rapidly. However, rapid carbonation at 100 % carbon dioxide concentration may result in generation of excessive heat, which can lead to premature drying of the mortar. This can stop the carbonation reaction (Moorehead 1986).

Calcium hydroxide concentration: Carbonation reaction depends on the amount of lime that will react with carbon dioxide diffusion in the mortar (Van Balen and Van Gemert 1994). Higher proportions of calcium hydroxide reduce the carbonation rate

since lime mortars containing high calcium hydroxide concentration necessitate more time for complete carbonation (Moorehead 1986).

Permeability of the mortar: Decrease in permeability of mortar reduces the carbon dioxide gas content that will penetrate into the pores where the chemical reaction occurs. Thus, low permeability slows down the carbonation reaction. Addition of aggregates generally increases porosity of mortar and enhances the diffusion of carbon dioxide gas (Moorehead 1986).

Thickness of the mortar: Carbonation reaction proceeds from the outside towards the inside of the mortar. Therefore, diffusion of carbon dioxide and carbonation time depends considerably on the thickness of the mortar. Increase in thickness leads to an increase in the diffusion path of carbon dioxide gas. Thus, increasing the thickness reduces the carbonation rate. Carbonation proceeds longer if the thickness of porous mortars is more than 25 mm., and the one of dense and impermeable mortars is more than 5 mm. (Moorehead 1986).

Use of Aged-Lime Putty: Aged-lime putty contributes to rapid and extensive carbonation. This is attributed to small platelike calcium hydroxide crystals in aged lime putties which are very reactive due to their high surface areas. Therefore, lime mortars develop their structural function in a short period of time. Moreover, carbonation of small platelike portlandite crystals in aged lime putties lead to the formation of small and interlocked calcite crystals that provide a resistant mortar (Cazalla et al. 2000).

Climatic factors: Climatic factors such as relative humidity, temperature, wind speed and rain water influence the water content of lime mortar by wetting and drying. Increase in relative humidity has a favourable effect on the carbonation reaction (Cazalla et al. 2000). Higher temperatures generally increase the chemical reactions but reduce the solubility of carbon dioxide gas and hydrated lime. Therefore, optimum carbonation rate is found to be at about 20°C (Van Balen and Van Gemert 1994). Drying of the lime mortar is influenced by the wind speed influencing the mass transfer coefficient by temperature and relative humidity of the ambient air. The optimum drying of fresh mortar is favoured by low relative humidity, strong wind speed and high temperature (Van Balen and Van Gemert 1994).

2.3.6.2. Hardening by Hydraulic Set

Hydraulic lime mortars are produced either by using hydraulic lime or by intentional addition of pozzolanas (natural or artificial) to non-hydraulic lime (Lea 1940, Charola and Henriques 1999). In hydraulic lime mortars prepared with hydraulic lime, hydraulic compounds of calcium silicate hydrates and calcium aluminate hydrates are formed due to the reaction of calcium alumina silicates with water. In hydraulic lime mortars prepared using non-hydraulic lime together with pozzolanas, hydraulic compounds of calcium silicate hydrates and calcium aluminate hydrates are formed due to the pozzolanic reaction between lime and pozzolanas in the presence of water. These hydraulic compounds are stable, insoluble and of cementitious properties. They are the ones that provide a rapid hardening for the mortar and acquire great strength properties to it (Akman 1986, Davey 1961, Lea 1940).

Since hydraulic lime mortars could set under water in the absence of carbon dioxide, are waterproof and of high durability, they were of great importance in ancient times (Davey 1961, Cowan 1977). Such mortars were extensively used in foundations in waterlogged grounds, drainage systems, bridges, locks, as an external render in baths, water storage tanks and damp climates, and for sealing the spaces between roofing tiles to prevent the penetration of rain water (Davey 1961, Cowan 1977).

Chapter 3

EXPERIMENTAL METHODS

Mortars used in walls and domes of five historic Ottoman baths located in Seferihisar-Urla region near İzmir were analysed in order to determine their production technologies and to investigate the relation between their properties and structural characteristics of the structural elements where they were used.

3.1. Sampling

The Ottoman baths whose mortars used in their walls and domes would be analysed are Düzce Bath, Seferihisar Bath and Ulamış Bath located in Seferihisar, and Hersekzade Bath and Kamanlı Bath located in Urla. These baths, which dated back to the 15th and 16th century, show almost similar characteristics with respect to their construction techniques and building materials (Reyhan 2004). Walls are comprised of stone masonry containing mostly rubble stones. Domes and vaults were built in brickwork in which bricks were laid up on thick (3-6 cm.) mortar joints (Reyhan 2004).

Sampling was carried out from partially demolished parts of the walls and domes where mortar samples could be easily taken from exposed mortar joints by a chisel and hammer. Stone masonry mortar samples were collected from the external parts of the mortar joints of outdoor masonry since indoor masonry was plastered with lime plaster. The samples were taken from the parts of the walls, which were not subjected to deterioration problems. Brick masonry mortar samples were collected from the mortar joints at the upper parts of the domes built in brickwork. Each of the mortar samples was labelled according to the abbreviations starting with the name of town where the bath was located, and respectively following up with the bath name and the type of the mortar indicating its use in the masonry (Table 3.1).

Table 3.1 Definition of the collected mortar samples.

Sample	Definition
Se.s.	Stone masonry mortar from the north wall of the Seferihisar Bath
Se.Dü.s.	Stone masonry mortar from the southeast wall of the Düzce Bath
Se.Ul.s.	Stone masonry mortar from the southwest wall of the Ulamış Bath
Ur.He.s.	Stone masonry mortar from the southwest wall of the Hersekzade Bath
Ur.Ka.s.	Stone masonry mortar from the southeast wall of the Kamanlı Bath
Se.Dü.b.	Brick masonry mortar from the dressing-hall dome of the Düzce Bath
Se.Ul.b.	Brick masonry mortar from the caldarium dome of the Ulamış Bath
Ur.He.b.	Brick masonry mortar from the caldarium dome of the Hersekzade Bath
Ur.Ka.b.	Brick masonry mortar from the caldarium dome of the Kamanlı Bath

Se: Seferihisar Town   Ur: Urla Town

Dü: Düzce Bath   He: Hersekzade Bath   Ka: Kamanlı Bath
Se: Seferihisar Bath   Ul: Ulamış Bath

s: stone masonry mortar
b: brick masonry mortar

Seferihisar Bath, which is a 16th-century-Ottoman bath, is located at the centre of Seferihisar (Reyhan 2004). Stone masonry mortar samples (Se.s.) were collected from its 76-cm-thick north wall from a height of approximately 150 cm. (Figures 3.1 and 3.2). Brick masonry mortar samples could not be taken from the dome of this bath since it was plastered with Horasan plaster and cement-based mortar over it.
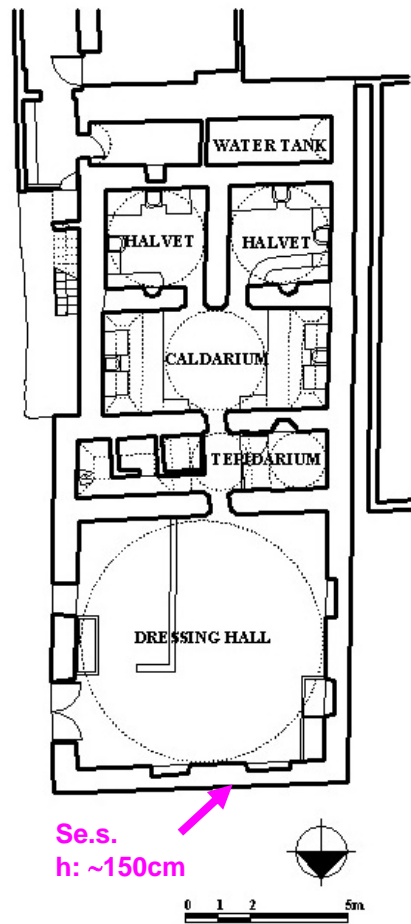
Figure 3.1 Plan of the Seferihisar Bath, showing where stone masonry mortar samples (Se.s.) were collected.

Figure 3.2 View from the east and north elevations of the Seferihisar Bath, showing where stone masonry mortar samples (Se.s.) were collected.

Düzce Bath located in Düzce Village in Seferihisar dated back to the 16th century (Reyhan 2004). Stone masonry mortar samples (Se.Dü.s.) were collected from the southeast exterior wall, approximately 75 cm. in thickness from 100 cm. above the existing ground (Figures 3.3, 3.4 and 3.5). Brick masonry mortar samples (Se.Dü.b.) were collected from the demolished parts of the dome of the dressing hall (Figures 3.4 and 3.6). This dome with its approximate span of 660 cm. and thickness of 35 cm. was built in 3.5-cm.-thick brick units and 5-cm.-thick mortar joints (Reyhan 2004).
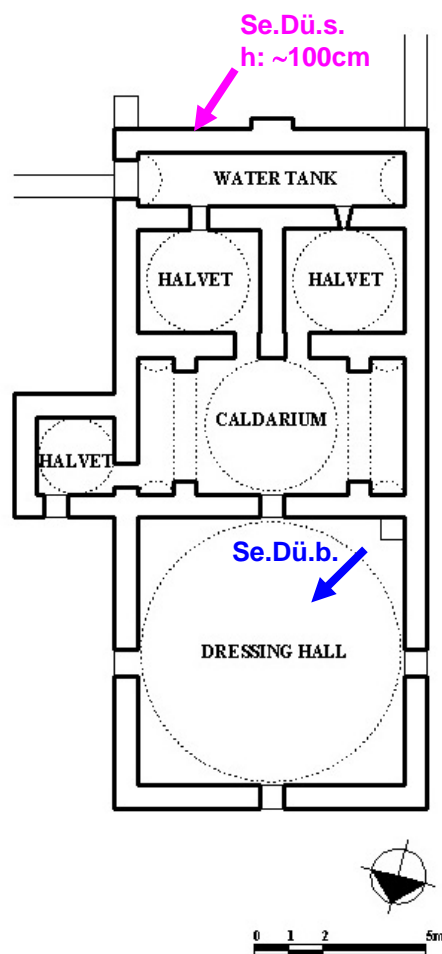
Figure 3.3 Plan of the Düzce Bath in Seferihisar (Reyhan 2004), showing where stone masonry mortar samples (Se.Dü.s.) and brick masonry mortar samples (Se.Dü.b.) were collected.

Figure 3.4 View from the southeast and southwest elevations of the Düzce Bath in Seferihisar, showing where stone masonry mortar samples (Se.Dü.s.) and brick masonry mortar samples (Se.Dü.b.) were collected.

Figure 3.5 Stone masonry mortar sample (Se.Dü.s.) taken from the Düzce Bath.

Figure 3.6 Brick masonry mortar sample (Se.Dü.b.) taken from the Düzce Bath.

Ulamış Bath, dated back to the 16th century, is located in Ulamış Village in Seferihisar (Reyhan 2004). Stone masonry mortar samples (Se.Ul.s.) were taken from its 70-cm.-thick southwest exterior wall from approximately 120 cm. above the existing ground (Figures 3.7, 3.8 and 3.10). Brick masonry mortar samples (Se.Ul.b.) were taken from the caldarium dome constructed with brick units being 4 cm. in thickness and mortar joints being 6 cm. in thickness (Figures 3.9. and 3.11). Span of this dome is 235 cm. and its thickness is 30 cm. approximately (Reyhan 2004).
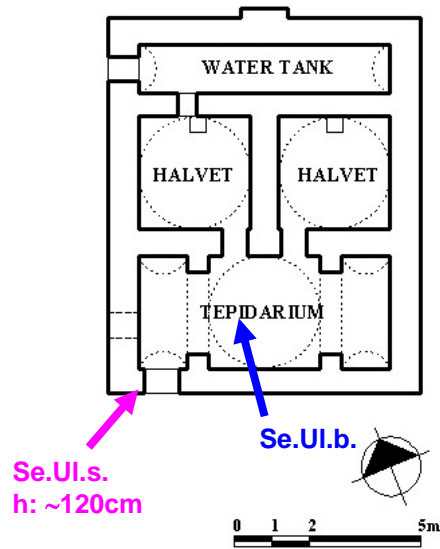
Figure 3.7 Plan of the Ulamış Bath in Seferihisar (Reyhan 2004), showing where stone masonry mortar samples (Se.Ul.s.) and brick masonry mortar samples (Se.Ul.b.) were collected.

Figure 3.8 View from the southwest elevation of the Ulamış Bath in Seferihisar, showing where stone masonry mortar samples (Se.Ul.s.) were collected.

Figure 3.9 View from the northwest elevation of the Ulamış Bath in Seferihisar, showing where brick masonry mortar samples (Se.Ul.b.) were collected.

Figure 3.10 Stone masonry mortar sample (Se.Ul.s.) taken from the Ulamış Bath.

Figure 3.11 Brick masonry mortar sample (Se.Ul.b.) taken from the Ulamış Bath.

Hersekzade Bath, which is a 15th-century- Ottoman bath, is located at the centre of Urla (Reyhan 2004). Stone masonry mortar samples (Ur.He.s.) were collected from the demolished upper parts of the southwest wall (Figures 3.12 and 3.13). Brick masonry mortar samples (Ur.He.b.) were collected from the demolished parts of the caldarium dome (Figure 3.14.). This dome, which was approximately 290 cm. in diameter and 42 cm. in thickness, was built in 3-cm.-thick brick units and 4-cm.-thick mortar joints (Reyhan 2004).
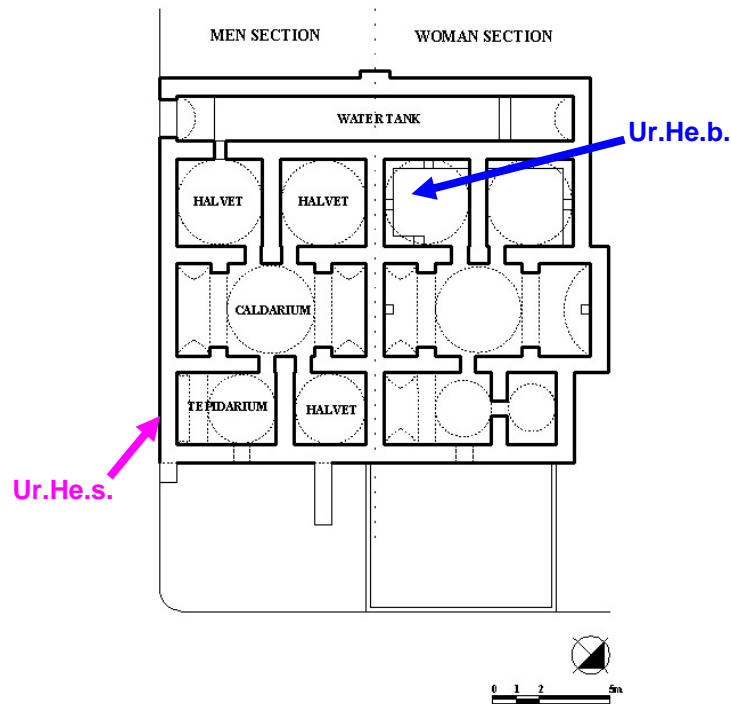
Figure 3.12 Plan of the Hersekzade Bath in Urla (Reyhan 2004), showing where stone masonry mortar samples (Ur.He.s.) and brick masonry mortar samples (Ur.He.b.) were collected.

Figure 3.13 View from the southeast elevation of the Hersekzade Bath in Urla, showing where stone masonry mortar samples (Ur.He.s.) were collected.

Figure 3.14 View from the southeast elevation of the Hersekzade Bath in Urla, showing where brick masonry mortar samples (Ur.He.b.) were collected.

Kamanlı Bath is located at the Kamanlı site of Urla. This bath dated back to the 15th century (Reyhan 2004). Stone masonry mortar samples (Ur.Ka.b.) were taken from its 80-cm-thick southeast wall from approximately 200 cm. above the existing ground (Figures 3.15 and 3.16). Brick masonry mortar samples (Ur.Ka.b.) were collected from the demolished parts of the tepidarium dome. This dome with its span of 295 cm. and thickness of 32 cm. was constructed with brick and mortar whose thicknesses are 3 cm. and 3.5 cm. respectively (Reyhan 2004).
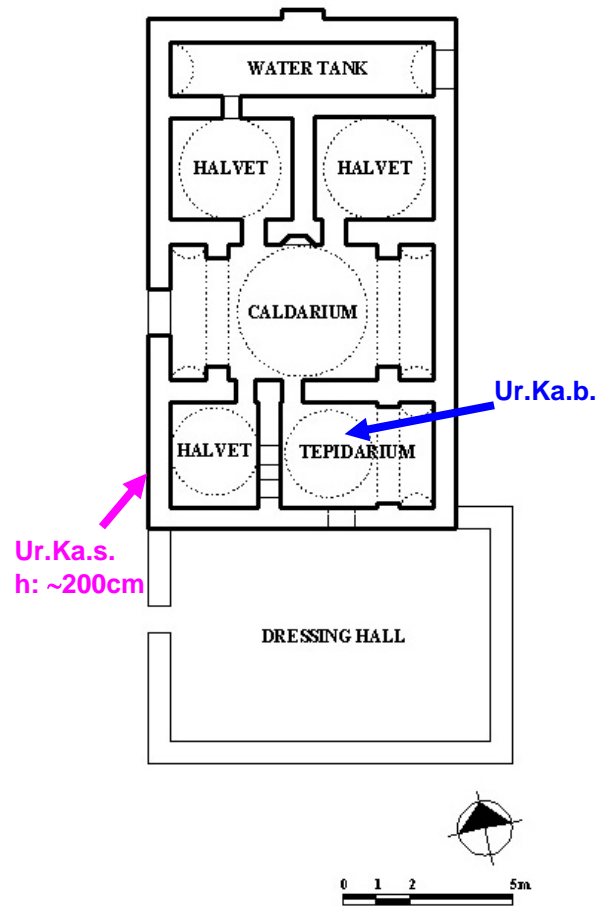
Figure 3.15 Plan of the Kamanlı Bath in Urla (Reyhan 2004), showing where stone masonry mortar samples (Ur.Ka.s) and brick masonry mortar samples (Ur.Ka.b.) were collected.

Figure 3.16 View from the northwest elevation of the Kamanlı Bath in Urla, showing where stone masonry mortar samples (Ur.Ka.s) were collected.

3.2. Experimental Study

Experimental study includes determination of the following properties of mortars and bricks, which were carried out by a series of laboratory tests presented in Appendix A:

- Basic Physical Properties of Mortars and Bricks
    - o Bulk density
    - o Porosity
- Basic Mechanical Properties of Mortars
    - o Uniaxial compressive strength
    - o Tensile strength
    - o Modulus of elasticity
- Analysis of Soluble Salts in Mortars
    - o Percent soluble salts in mortars
    - o Anion parts of soluble salts
- Raw Material Compositions of Mortars
    - o Lime-aggregate ratios of mortars
    - o Particle size distributions of aggregates
- Pozzolanic Activity of Aggregates and Bricks
- Mineralogical and Chemical Compositions and Microstructural Properties of Lime Binders, Aggregates and Mortar Matrices
- Hydraulicity of Mortars by TGA

3.2.1. Determination of Basic Physical Properties of Mortars and Bricks

Basic physical properties of bulk densities and porosities of mortars and brick masonry units used in domes were determined by using RILEM standard test methods (RILEM 1980). Bulk density is defined as the apparent density which is the ratio of the mass to its bulk volume. It is expressed in grams per cubic centimetres (g/cm^3). Porosity is the ratio of the pore volume to the bulk volume of the sample, and is usually expressed in per cent (%).

Measurement of bulk density and porosity was carried out on three samples of each mortar and on two samples of each brick. First of all, the samples were dried in an oven at 60°C at least for 24 hours in order to allow moisture to be released from the samples. Subsequently, they were weighed by a precision balance (AND HF-3000G) to determine their dry weights (M_{dry}). After the dry weights were recorded, the samples were left under distilled water in a vacuum oven (Lab-Line 3608-6CE Vacuum Oven) so that they were entirely saturated with water. Afterwards, their hydrostatic weighing was carried out separately in distilled water by using the precision balance and the measured weights were recorded as Archimedes weight (M_{arch}). Then, saturated weights (M_{sat}) were measured. As a result, bulk densities (D) and porosities (P) of the mortar and brick samples were calculated by using the following formulas:

D (gr/cm^3) = M_{dry} / (M_{sat} - M_{arch})

P (%)   = [(M_{sat} - M_{dry}) / (M_{sat} - M_{arch})] × 100

where;

M_{dry} : Dry weight (g)

M_{sat} : Saturated weight (g)

M_{arch} : Archimedes weight (g)

M_{sat} - M_{dry} : Pore volume (g)

M_{sat} - M_{arch} : Bulk volume (g)

3.2.2. Determination of Basic Mechanical Properties of Mortars

Determination of basic mechanical properties is generally evaluated by measuring uniaxial compressive strengths, tensile strengths and modulus of elasticity of mortars. These measurements provide the necessary information regarding strength and rigidity properties of the mortars.

3.2.2.1. Determination of Uniaxial Compressive Strength of Mortars

Uniaxial compressive strengths of mortars were measured by Shimadzu AG-I Mechanical Test Instrument which performed automatic compression testing (ISRM 1981, Ulusay et al. 2001). Uniaxial compressive strength test was carried out on at least three cubic specimens being relatively free from cracks (Figure 3.17). These cubic

specimens were prepared by using a cutting machine (Discoplan-TS 372). Subsequently, they were dried in an oven at 60°C for at least 24 hours. The cubic specimens with thicknesses varying between 20 cm. and 55 cm. could be prepared since narrow mortar joints only allowed collecting specimens of such sizes. Even though cylindrical specimens with minimum dimensions of 30×75 mm. were required to conduct the mechanical test, cubic specimens were used since it was very difficult and often impossible to obtain entirely cylindrical specimens from the mortars that were easily broken into pieces while drilling the specimens.
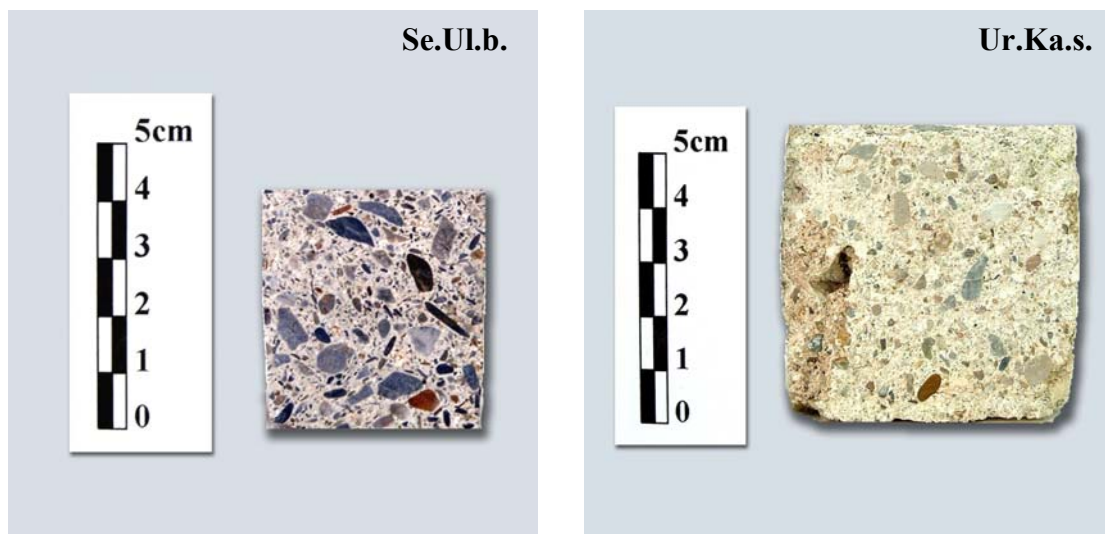
Figure 3.17 Cubic specimens of the mortar samples, which were used for the uniaxial compressive strength test.

Shimadzu AG-I Mechanical Test Instrument automatically computed, displayed and recorded test results using a software system. A test procedure including the setting of force magnitude, force unit and test speed was configured initially according to the hardness of the mortars. Maximum force magnitude was configured as 15 kN and test speed as 1 mm/min. This test speed provided a continuous compression loading that would be applied for a length of 1 mm. per one minute. After the configuration of the test procedure was done, cubic specimens were placed between two loading platens; one was fixed and the other was mobile to provide the compression loading (Figure 3.19). It was ensured that surfaces of the specimens which would be in direct contact with the loading platens were uniform in order to provide a uniform contact with the platens. The instrument recorded strokes under continuous compression loading, and presented the relationship between the strokes and load by a graph which was automatically displayed on the test condition monitor. This graph was composed of

a curve whose peak point gave the maximum force (F) under which the specimen failed (Figure 3.18). As a result, uniaxial compressive strengths represented by **"σ"** were calculated by using this graph with the following formula (ISRM 1981, Ulusay et al. 2001):

$\sigma = F / A$

where;

F   : Failure load (kN)

A   : Area onto which loading was applied (mm^2)
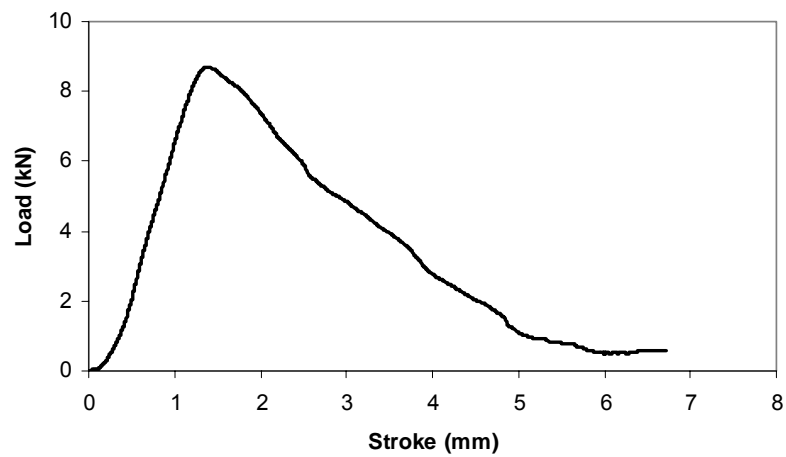
Figure 3.18 Load-stroke graph of the mortar sample of Ur.He.s., which was obtained after uniaxial compressive strength test was carried out.
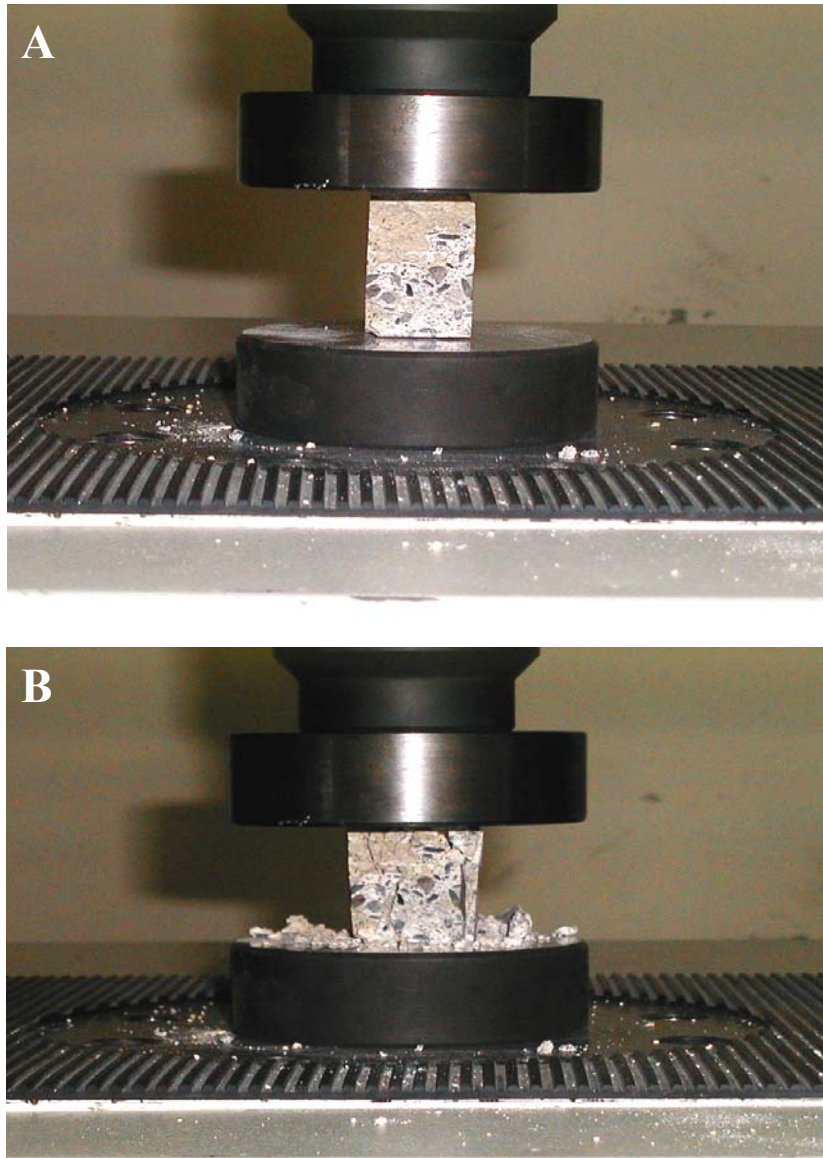
Figure 3.19 Images showing how uniaxial compressive strength test was carried out. Image A shows the situation in which the sample is placed between two compression platens prior to loading. Image B shows the situation in which the compression test is carried out.

3.2.2.2. Determination of Tensile Strength of Mortars

Tensile strengths of lime mortars were determined with Brazilian Test Method by using Shimadzu AG-I Mechanical Test Instrument. Brazilian Test Method is a type of testing which determines tensile strength indirectly under diametrical loading (ISRM 1981, Ulusay et al. 2001). Even though this method required cylindrical specimens of at least 54 mm. in diameter and 27 mm. in height, the cylindrical specimens of such

dimensions could not be obtained by an electrical core driller since these mortars were easily broken into pieces due to their composite nature. Therefore, only cylindrical specimens of 25 mm. in diameter and 1.25 mm. in thickness could be prepared (Figure 3.20).

Figure 3.20 Cylindrical specimen drilled from the mortar sample of Se.Dü.b.

Tensile strength test was carried out on at least two cylindrical specimens being relatively free from cracks. Similar to the uniaxial compressive strength test, a test procedure was configured initially, including the setting of force magnitude, force unit and test speed. Maximum force magnitude was configured as 2.5 kN and test speed as 0.1 mm/min. Cylindrical specimens were placed between two loading platens in such a way that their lateral surfaces were in contact with the platens (Figure 3.21). It was ensured that samples failed along the axis of their diameters during the loading (Figure 3.21). Strokes under continuous loading were automatically recorded and presented by a graph which was displayed on the test condition monitor (Figure 3.22). Peak point of the curve in this graph gave the maximum force (F) under which the specimens failed. As a result, tensile strengths represented by σ_t were calculated by using this graph with the following formula (ISRM 1981, Ulusay et al. 2001):

$\sigma_t = 0.636 \times F / D \times t$

where;

0.636 : Constant

F : Failure load (kN)

D : Diameter of the sample (mm)

t : Thickness of the sample (mm)
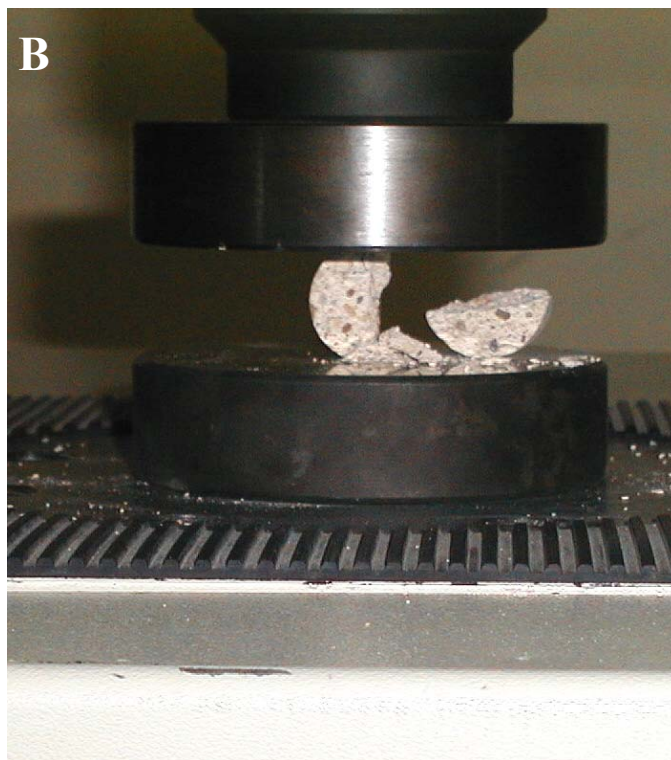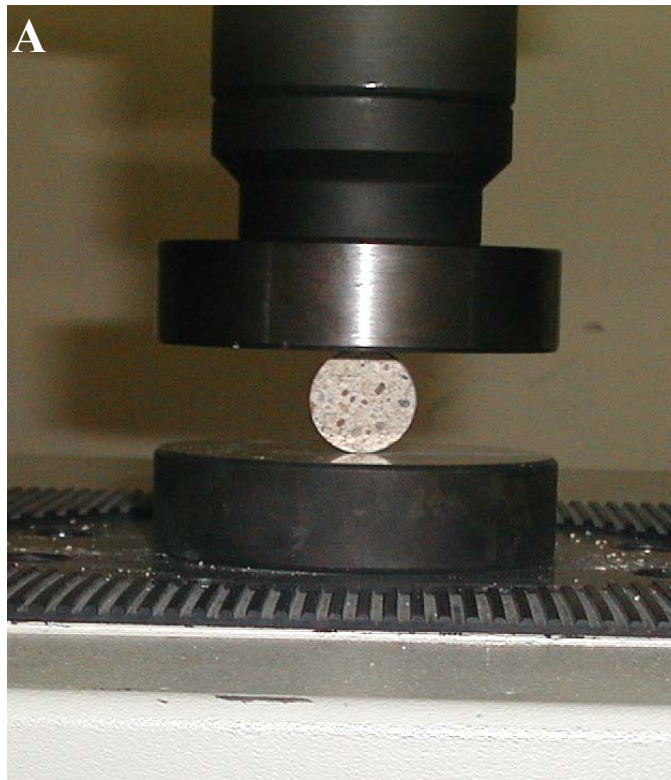
Figure 3.21 Images showing how diametrical loading was applied on a cylindrical specimen to determine its tensile strength. Image A shows the positioning of the sample before loading and image B shows the situation after loading. This sample presents a correct type of failure occurred along the axis of its diameter.
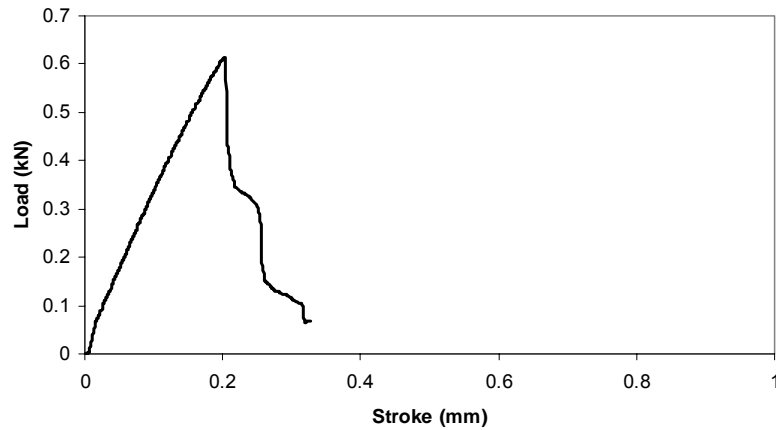
Figure 3.22 Load-stroke graph of the mortar sample of Ur.He.b., which was obtained after diametrical loading was carried out on the cylindrical specimen.

3.2.2.3. Determination of Modulus of Elasticity of Mortars

Modulus of Elasticity (Young's Modulus), which defines the rigidity of a material, is the rate of change of strain as a function of stress. It provides required information about how well a material can resist deformation under the action of external forces (Airapetov 1986). The modulus of elasticity (E) is formulated as follows:

E = Stress / Strain = σ / ε = ($\triangle$F/A) / ($\triangle$l/l_o)

where;

$\triangle$F : Failure load (kN)

A   : Area onto which force was applied (mm^2)

$\triangle$l : Change in thickness of the sample along its vertical axis (mm)

l_o : Initial thickness of the sample (mm)

Modulus of elasticity of stone and brick masonry mortars were calculated using slopes of stress-strain curves obtained from the results of uniaxial compressive strength test (ISRM 1981, Ulusay et al. 2001). Stress (σ) is the ratio of force to the area where the force is applied. Strain (ε) corresponds to the change in thickness of cube mortar samples under the action of the applied force. The relation between the stress and strain is expressed by a graph below (Figure 3.23). Slope of the curve (tanθ) gives the modulus of elasticity of that material (Figure 3.23).
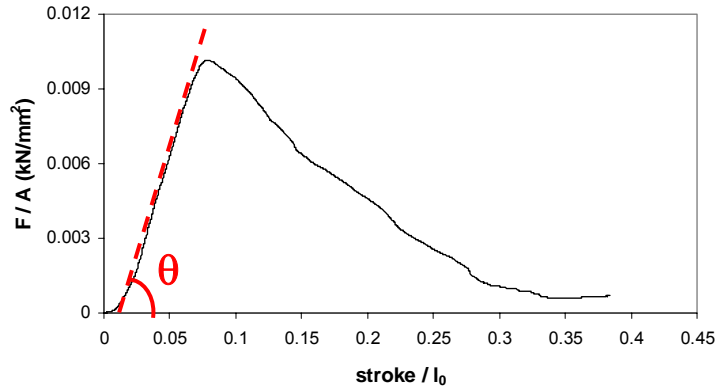
Figure 3.23 Stress (F/A)-strain (stroke/l_o) curve whose slope (tanθ) gives modulus of elasticity of the mortar sample.

3.2.3. Determination of Soluble Salts in Mortars

Soluble salts present in mortar samples were determined in order to evaluate their deterioration problems. Anion parts of the soluble salts were determined qualitatively.

3.2.3.1. Determination of Percent Soluble Salts in Mortars

Percent soluble salts in mortars were determined by an electrical conductivity meter (Black 1965). For this analysis, 1.00 g of finely-ground mortar sample was dissolved in 50 ml distilled water. After this solution was filtered, its conductivity was measured by the electrical conductivity meter (WTW MultiLine P3 pH/LF). Percentage of soluble salts within the sample was calculated using the following formula:

Soluble Salts (%) = [(A x V_{sol}) / 1000] x [100 / M_{sam}]
where;
A   = Salt concentration (mg/lt) = 640 x EC

      EC = Electrical conductivity measured by electrical conductivity meter

          (mS/cm = mmho/cm)

    640 = Constant

V_{sol} = Volume of the solution (ml)

M_{sam} = Weight of the sample (mg)

3.2.3.2. Qualitative Determination of Anion Parts of Soluble Salts

After the percent of soluble salts in mortars were calculated, anion parts of the soluble salts were determined by spot test (Black 1965, Arnold 1983, Teutonico 1988). Principle anions such as sulphate (SO_4^{-2}), chloride (Cl^-), nitrate (NO_3^-), carbonate (CO_3^{-2}), and phosphate (PO_4^{-3}) which might have been present in the solutions were determined.

3.2.4. Determination of Raw Material Compositions

Lime-aggregate ratios and particle size distributions of the aggregates were determined in order to define raw material compositions of mortars.

3.2.4.1. Determination of Lime-Aggregate Ratios of Mortars

Ratios of lime as the binder and aggregates as the filling material in mortars were determined by treatment of mortar samples with dilute hydrochloric (HCl) acid (Jedrzejevska 1981, Middendorf and Knöfel 1990). Two samples of 50-60g in weight from each mortar were prepared, dried and weighed (M_{sam}) by a precision balance. Then, the mortar samples were left under the solution of dilute hydrochloric acid (5 %) until all carbonated lime ($CaCO_3$) in the samples entirely dissolved. Aggregates remaining insoluble were filtered through a filter paper, rinsed with distilled water, dried in an oven, and then weighed (M_{agg}). Acid soluble and insoluble ratios were calculated with the following formula:

Insoluble % $= [(M_{sam} - M_{agg}) / M_{sam}] \times 100$

Acid Soluble % $= 100 -$ Insoluble %

where;

M_{sam} : Weight of the mortar sample

M_{agg} : Weight of the aggregates

Acid soluble ratio is not the exact ratio corresponding to lime ratio since both lime and calcareous aggregates that could be used in the mortars were dissolved in the

solution of dilute hydrochloric acid. Therefore, lime/aggregate ratio was calculated by the formula as follows:

Aggregate % = (100 × Insoluble %) / [((Acid Soluble % × M.W.$_{Ca(OH)_2}$) /

M.W.$_{Ca(CO_3)}$) + Insoluble %]

Lime % = 100 – Aggregate %

where;

M.W.$_{Ca(CO_3)}$: Molecular weight of Ca(CO$_3$) which is 100.

M.W.$_{Ca(OH)_2}$: Molecular weight of Ca(OH)$_2$ which is 74.

3.2.4.2. Determination of Particle Size Distributions of Aggregates

Particle size distributions of the aggregates were determined by sieve analysis in order to group these aggregates into various size ranges and to determine relative proportions of each size range (Teutonico 1988). In the first place, the aggregates were sieved through a series of sieves (Retsch mark) having the sieve sizes of 53μm, 125μm, 250μm, 500μm, 1180μm by using an analytical sieve shaker (Retsch AS200). Subsequently, each of the particles retained on each sieve was weighed respectively and each of their percentages was calculated. Lastly, their cumulative percentages were calculated.

Aggregates separated from lime were examined visually by a zoom stereo microscope (Olympus SZ40) equipped with video camera, photo micrographic system and computer. Images of the aggregates with particle sizes of >1180μm, 1180-500μm, 500-250μm and 250-125μm were taken in order to determine their physical properties in terms of their shapes and colours.

3.2.5. Determination of Pozzolanic Activity of Aggregates and Bricks

Pozzolanic activity of fine aggregates (less than 53μm), and coarse aggregates and bricks ground to the fineness of less than 53μm were determined by electrical conductivity measurements (Luxan et al. 1989). In this analysis, first of all, electrical conductivity of saturated calcium hydroxide solution of 40 ml. was measured. Then, 1.00g of sample was added into this solution. Subsequently, this mixture was kept under constant stirring for a time period of 120 seconds. Afterwards, its conductivity was

measured. Reaction took place between the sample and calcium hydroxide led to a difference in the electrical conductivity measurements of the initial and final saturated calcium hydroxide solutions. The samples leading to a difference in the electrical conductivity of more than 1.2 mS/cm presented good pozzolanicity (Luxan et al. 1989).

3.2.6. Determination of Mineralogical and Chemical Compositions, and Microstructural Properties of Lime Binders, Aggregates and Mortar Matrices

Lime binder obtained from soft carbonated lime particles in the form of white lumps in mortars, aggregates, and mortar matrices composed of lime and fine aggregates mixed firmly were analyzed in order to determine their mineralogical compositions, chemical compositions and microstructural properties.

Mineralogical compositions of lime binder, aggregates and mortar matrices were determined by X-ray Diffraction (XRD) analysis performed by using a Philips X-Pert Pro X-ray Diffractometer. The analyses were performed on carbonated lime scrubbed from mortar samples, and aggregates and mortar matrices which were ground to the fineness of less than 53μm.

Chemical compositions and microstructural properties of lime binder, aggregates and mortar matrices were determined by Philips XL 30S-FEG Scanning Electron Microscope (SEM) equipped with X-Ray Energy Dispersive System (EDS). SEM-EDS analysis was performed on the lime binder, aggregates and mortar matrices, which were ground to the fineness of less than 53μm and then pressed into pellets, in order to determine their chemical compositions.

3.2.7. Determination of Hydraulicity of Mortars by TGA

Thermogravimetric analysis (TG/DTG) was performed on total mortar samples by using Shimadzu TGA-21 thermogravimetric analyzer in order to determine hygroscopic water, structurally bound water and carbon dioxide contents, and to evaluate hydraulicity of the mortars. The thermogravimetric analysis was carried out in static nitrogen atmosphere at a temperature range of 30-1000°C with a controlled heating rate of 10°C/min. This analysis determined precise measurements of weight losses in finely-

ground mortar samples of 10-20 mg as they were heated up to 1000°C. During this heating, TGA instrument recorded loss of hygroscopic (adsorbed) water (< 120°C), loss of structural water bounded to hydraulic components (200°C – 600°C) and loss of carbon dioxide gas due to decomposition of carbonates (> 600°C).

Chapter 4

RESULTS AND DISCUSSION

Results of experimental study, which were performed on stone and brick masonry mortars, and bricks used in domes, have been given in this chapter. Densities and porosities of mortars, their mechanical properties and raw material compositions, pozzolanic activities of aggregates used in the mortars, soluble salts in the mortars, their mineralogical and chemical compositions, microstructural properties and hydraulic properties were described and discussed. Besides, basic physical properties and pozzolanic activity of the bricks used in the construction of the domes were also included in order to evaluate their role together with the mortar in structural stability of the domes.

4.1. Basic Physical Properties of Mortars and Bricks

Physical properties of mortars depend on several factors such as lime/aggregate ratios, particle size distribution of aggregates, characteristics of lime used, characteristics and shapes of aggregates used, water content and mortar preparation techniques (Cowper 2000, Eckel 1928, Davey 1961, Boynton 1966, Holmes and Wingate 1997). Therefore, determination of density and porosity values of the mortars is one of the important parameters in characterization of mortar technology.

Density and porosity values of stone masonry mortar samples collected from the studied Ottoman baths were between 1.50-1.84 g/cm^3 and 26.82-41.85 % by volume respectively (Figure 4.1). Density values of brick masonry mortars ranged between 1.40-1.72 g/cm^3 and their porosity values were in the range of 31.85% and 43.46 % by volume (Figure 4.2). All these values were in the same ranges with several historic lime mortars whose density values varied between 1.10-1.90 g/cm^3 and porosity values between 28-57 % (Papayianni and Karaveziroglou 1993, Tunçoku 1993, Franzini et al. 2000, Tunçoku 2001, Moropoulou et al. 2003, Moropoulou et al. 2004a).
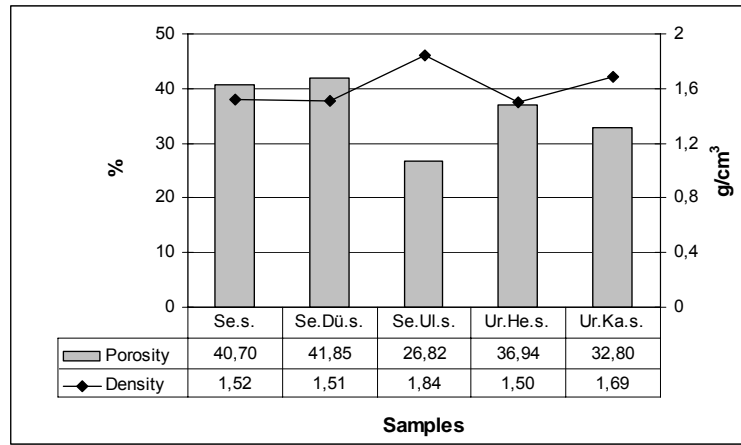
Figure 4.1 Porosity and density values of stone masonry mortars.

	Se.s.	Se.Dü.s.	Se.Ul.s.	Ur.He.s.	Ur.Ka.s.
Porosity	40,70	41,85	26,82	36,94	32,80
Density	1,52	1,51	1,84	1,50	1,69

Samples
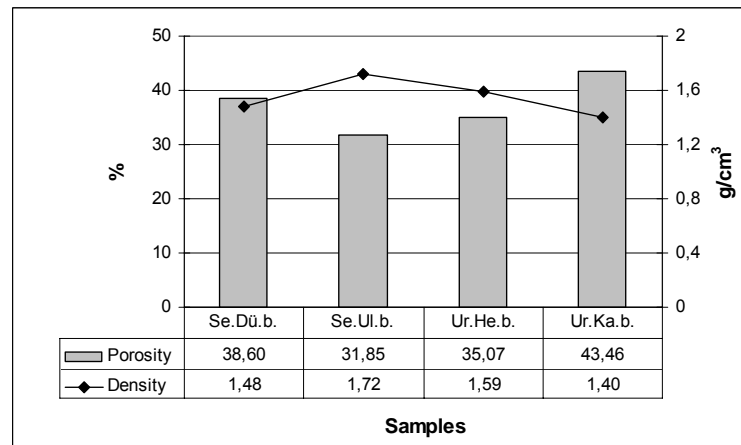
Figure 4.2 Porosity and density values of brick masonry mortars.

	Se.Dü.b.	Se.Ul.b.	Ur.He.b.	Ur.Ka.b.
Porosity	38,60	31,85	35,07	43,46
Density	1,48	1,72	1,59	1,40

Samples

Density and porosity values of stone masonry mortars used in walls and brick masonry mortars used in domes of each building were in the same ranges. While the brick masonry mortars were slightly porous than the stone masonry mortars in the baths of Ulamış and Kamanlı, the stone masonry mortars presented slightly higher porosity values than the brick masonry mortars in the baths of Düzce and Hersekzade.

Physical properties of bricks used in historic buildings depend on several factors such as mineralogical compositions, preparation techniques, firing temperature and etc. Bricks as masonry units were extensively used with lime mortars in the construction of many historic buildings since they are porous and have good compatibility with the lime mortars. Therefore, structural behaviour of the domes depends on physical and mechanical properties of both bricks and lime mortars (Moropoulou et al. 2002b). Thus, density and porosity values of bricks should be determined in order to evaluate structural behaviour of the domes.

Density values of bricks used in the domes of the examined baths ranged between 1.67-1.80 g/cm^3 and their porosity values ranged between 29.45 % and 35.96 % (Figure 4.3). These values were in the same ranges of bricks used in historic structures (Livingston 1993, Tunçoku 1993, Baronio et al. 1997). However, bricks used in some historic buildings could have considerably low density values and high porosity values. For instance, density and porosity of bricks used in the dome of Hagia Sophia in İstanbul were 1.5 g/cm^3 and 45 % respectively (Moropoulou et al. 2002b). Likewise, bricks used in the superstructures of some Anatolian Seljuk buildings had density values ranging between 1.20-1.60 g/cm^3 and porosity values in the range of 36-57 % (Tunçoku 2001). Use of such porous and light bricks in the superstructure could be attributed to its structural requirements in order to be resistant against earthquake stresses (Moropoulou et al. 2002b).

	Se.Dü.brick	Se.Ul.brick	Ur.He.brick	Ur.Ka.brick
Porosity	31,47	35,96	30,29	29,45
Density	1,76	1,67	1,78	1,80

Samples
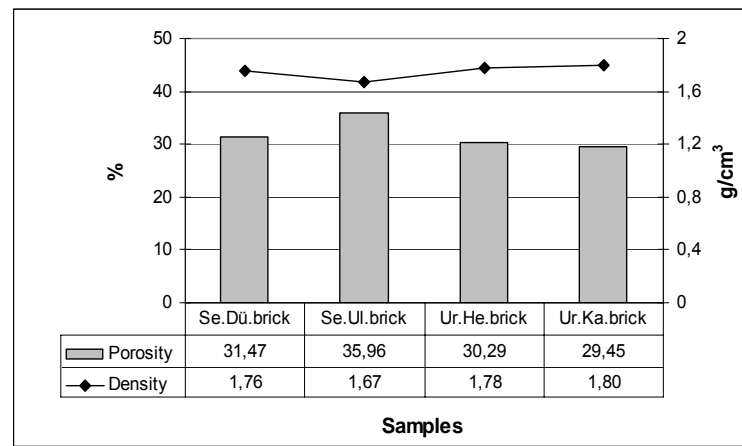
Figure 4.3 Porosity and density values of bricks used in the domes.

Brick masonry mortars and bricks, which were used in the construction of the domes of the studied baths, presented density and porosity values in the same ranges (Figures 4.4 and 4.5). When the porosity values of the mortars and bricks used in each building were compared with each other, it was found that the mortars except for the mortar of Se.Ul.b. presented slightly higher porosity values than the bricks used (Figure 4.4). As the mortars and bricks used in the domes had similar density and porosity values, the domes could be regarded as light and porous superstructures.
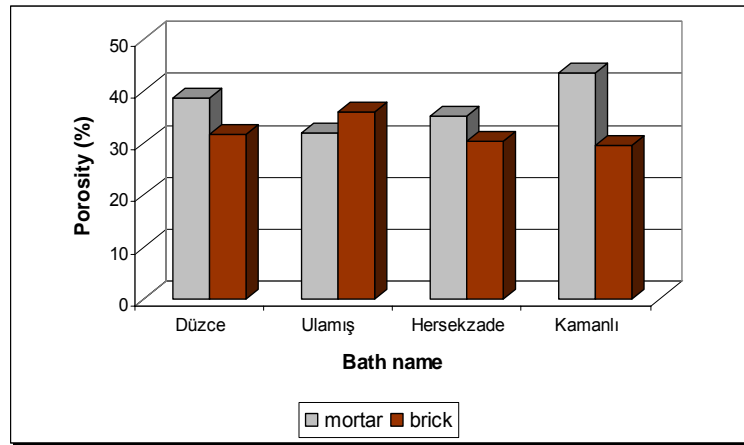
Figure 4.4 Porosity values of brick masonry mortars and bricks used in domes.
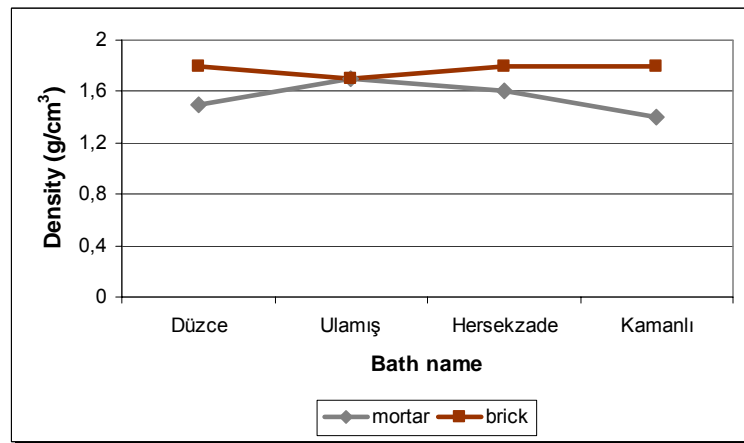
Figure 4.5 Density values of brick masonry mortars and bricks used in domes.

4.2. Basic Mechanical Properties of Mortars

One of the most important function of mortar is that it binds the masonry units into a monolithic mass and helps them to resist forces occurred in masonry. Therefore, it should have sufficient strength to hold the masonry units together and to spread loads evenly together with the masonry units (Davison 1976, Airapetov 1986, Holmes and Wingate 1997). For this reason, strength characteristics of the mortars can be regarded as important factors influencing the structural resistance of historic masonry structures. Within this context, basic mechanical properties of the mortars collected from the walls and domes of the examined Ottoman baths were determined.

Basic mechanical properties are frequently studied by compressive and tensile strength tests. Strength is described as the ability of a material to resist elastic deformation under externally applied loads which lead to internal elastic forces

(Airapetov 1986). Ultimate strength of a building material is the main strength characteristic corresponding to the highest stress which the material subjected to static (gradually applied) load can resist before breaking. The ultimate compressive and tensile strength are the primary strengths which should be resisted by building materials (Airapetov 1986). Besides, modulus of elasticity of the mortars are necessary for the evaluation of their estimated elastic behaviour that helps them to resist deformation under the action of external forces (Airapetov 1986).

4.2.1. Uniaxial Compressive Strength of Mortars

Stone masonry mortars used in the walls of the studied baths had compressive strengths values ranging between 4.2 MPa and 17.4 MPa Brick masonry mortars used in domes presented compressive strength values in the range of 8.8 MPa and 21.0 MPa (Table 4.1). While all brick masonry and some of the stone masonry mortars (Se.Ul.s. and Ur.He.s.) had relatively high compressive strengths values, rest of the stone masonry mortars of Se.Dü.s. and Ur.Ka.s. had lower values of 5.3 MPa and 4.2 MPa respectively than the rest.

Table 4.1 Compressive strength values of stone and brick masonry mortars.

Sample	Compressive Strength (MPa.)
Se.s.	*
Se.Dü.s.	5.3
Se.Ul.s.	17.4
Ur.He.s.	9.7
Ur.Ka.s.	4.2
Se.Dü.b.	16.1
Se.Ul.b.	21.1
Ur.He.b.	10.5
Ur.Ka.b.	8.8
*: not determined	

Compressive strength values of stone and brick masonry mortars of the Ottoman baths were in similar ranges with the ones of several historic lime mortars (Livingston 1993, Tunçoku 2001). Livingston recorded compressive strength values of more than 9 MPa for hydraulic mortars with pozzolanic aggregates and less than 9 MPa for non-lime containing silica at high ratios mortars (Livingston 1993). Having regard to

this, since compressive strength values of all brick masonry and some stone masonry mortars (Se.Ul.s. and Ur.He.s.) were more than 9 MPa, their values were in the same ranges with lime containing silica at high ratios mortars with pozzolanic aggregates.

4.2.2. Tensile Strength of Mortars

Tensile strength values of stone masonry mortars of the examined baths ranged between 0.7 MPa and 1.4 MPa (Table 4.2). However, brick masonry mortars presented considerably high tensile strength values being in the range of 1.0 MPa and 1.5 MPa. These values were in almost similar ranges with historic lime mortars having tensile strength values in the range of 0.5 MPa and 2 MPa (Moropoulou et al. 1996, Moropoulou et al. 2000a, Moropoulou et al. 2002a). Livingston recorded tensile strength values more than 0.7 MPa for hydraulic mortars with pozzolanic aggregates and less than 0.7 MPa for non-lime containing silica at high ratios mortars (Livingston 1993). Having regard to this, all brick masonry mortars had tensile strength values of 1 MPa and more than this which was over the lowest range of the tensile strength values given for hydraulic mortars with pozzolanic aggregates.

Table 4.2 Tensile strength values of stone and brick masonry mortars.

Sample	Tensile Strength (MPa)
Se.s.	*
Se.Dü.s.	*
Se.Ul.s.	1.4
Ur.He.s.	0.8
Ur.Ka.s.	0.7
Se.Dü.b.	1.1
Se.Ul.b.	1.5
Ur.He.b.	1.1
Ur.Ka.b.	1.0
*: not determined	

Use of the lime mortars in domes with higher tensile strength than the lime mortars used in walls could be explained with the structural behaviour of the wall and dome. State of stress in a masonry wall is primarily compression while in a masonry dome it is the combination of compression and tension (Airapetov 1986, Ünay 2001). Due to the geometry of the dome, both compressive stresses along its meridian lines and

circumferential tensile forces in the lower parts of the hemisphere occur so that its structural resistance is provided (Ünay 2001, Fielden 2001). The structural resistance of the dome depends both on its geometry and strength properties of materials used (Ünay 2001). Therefore, lime mortars having high tensile strength properties may have been used consciously in the construction of the domes of the baths.

4.2.3. Modulus of Elasticity of Mortars

Stone masonry mortars sampled from the five Ottoman baths in Seferihisar-Urla region showed modulus of elasticity values ranging between 110.5 MPa. and 1246.5 MPa (Table 4.3). Among them, the mortar of Se.Ul.s. had the highest value of 1246.5 MPa. Brick masonry mortars presented modulus of elasticity values ranging between 264.4 MPa. and 1617.6 MPa. These values were mostly lower than modulus of elasticity values of several historic lime mortars, which were in the range of 600-3000 MPa (Schafer and Hildsdorf 1993, Papayianni and Stefanidou 1997, Papayianni 1997, Tunçoku 2001, Moropoulou et al. 2000a, Moropoulou et al. 2002a). These low modulus of elasticity values are probably due to the method used.

Table 4.3 Modulus of elasticity values of stone and brick masonry mortars.

Sample	Modulus of Elasticity (MPa)
Se.s.	*
Se.Dü.s.	186.5
Se.Ul.s.	1246.5
Ur.He.s.	425.8
Ur.Ka.s.	110.5
Se.Dü.b.	966.7
Se.Ul.b.	1617.6
Ur.He.b.	493.1
Ur.Ka.b.	264.4
*: not determined	

4.3. Analysis of Soluble Salts in Mortars

Determination of soluble salts in mortars is important to understand their deterioration problems. Brick and stone masonry mortar samples had low soluble salt contents ranging between 0.30 % and 0.78 % (Figures 4.6 and 4.7). Main anion parts of

soluble salts in the mortar samples were determined to be chloride (Cl⁻). These values show that the lime and aggregates used in the mortars contain little amount of soluble salts.
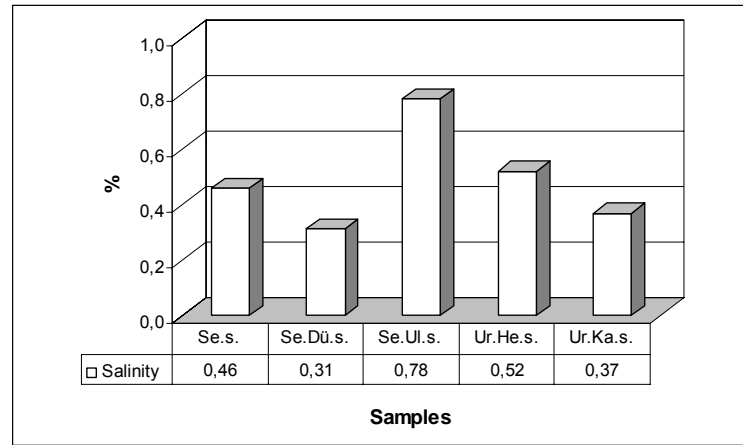
Figure 4.6 Soluble salt content (%) in stone masonry mortars.
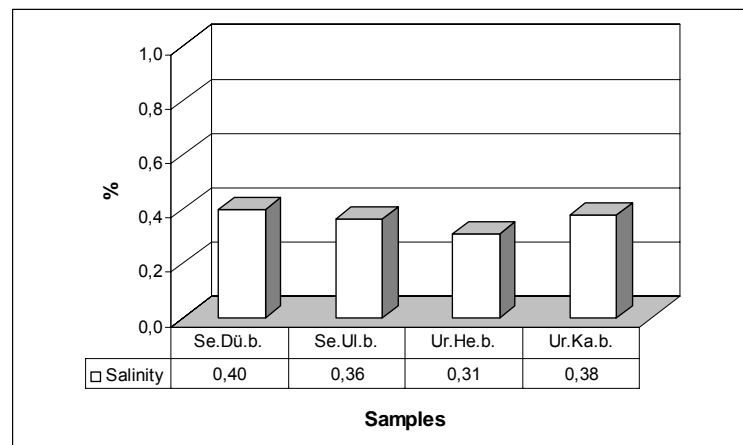
Figure 4.7 Soluble salt content (%) in brick masonry mortars.

4.4. Raw Material Compositions of Mortars

Binder-aggregate ratios and particle size distributions of the aggregates were determined in order to describe raw material compositions of mortars.

4.4.1. Lime-Aggregate Ratios of Mortars

Ratio of lime and aggregates used in mortars is an important parameter influencing physical, mechanical and durability characteristics of the mortars. While lime provides

the binding material, aggregates act as a filling material that prevents shrinkage and consequent cracking during the drying of the mortars, and impart strength, hardness and a certain degree of porosity to the mortars (Eckel 1928, Davey 1961). The lime and aggregates should be in the right proportion so that the mortar with good workability, durability and strength is produced (Cowper 2000, Eckel 1928).

Stone and brick masonry mortars collected from the examined Ottoman baths presented various lime/aggregate ratios ranging between 1:4 and 2:3 by weight (Figures 4.8 and 4.9). These ratios were in similar ranges with lime/aggregate ratios of several historic lime mortars (Moropoulou et al. 1995, Papayianni 1997, Bakolas et al. 1998, Moropoulou et al. 2000a, Moropoulou et al. 2000b, Tunçoku 2001, Moropoulou 2002a). Since calcareous aggregates in the stone masonry mortar sample of Ur.He.s. were determined by XRD and SEM analyses, lime/aggregate ratio of this mortar is smaller than their exact ratios. This is because both lime and calcareous aggregates were dissolved in dilute HCl solution while separating the aggregates from the lime binder.
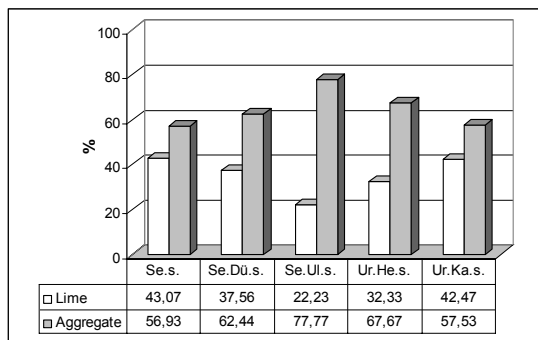
Sample	Lime/aggregate ratio
Se.s.	2:3
Se.Dü.s.	2:3
Se.Ul.s.	1:3,5
Ur.He.s.	1:2
Ur.Ka.s.	2:3

Figure 4.8 Lime-aggregate ratios of stone masonry mortars.
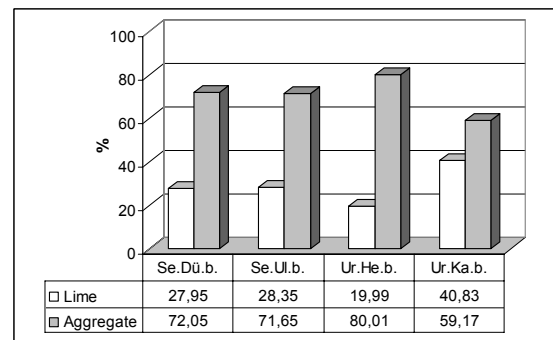
Sample	Lime/aggregate ratio
Se.Dü.b.	1:2,5
Se.Ul.b.	1:2,5
Ur.He.b.	1:4
Ur.Ka.b.	2:3

Figure 4.9 Lime-aggregate ratios of brick masonry mortars.

Stone masonry mortars presented high lime percent ranging between 32 % and 43 % except for the mortar of Se.Ul.s which had a lower binder percent of 22 % (Figure 4.8). However, brick masonry mortars except for the one of Ur.Ka.b. were composed of lower percent of lime in the range of 20 % and 28 % when compared with the stone masonry mortars (Figure 4.9). These values differed from lime percents of

mortars used in some Anatolian Seljuk buildings where brick masonry mortars contained higher ratios of lime binder than stone masonry mortars (Tunçoku 2001).

4.4.2. Particle Size Distributions of Aggregates Used in Mortars

Particle size distributions of aggregates are critical in the properties of the mortars. The aggregates should be composed of a wide range of particle sizes which are equally and evenly distributed so that spaces between larger grains are filled with smaller ones. Otherwise, the mortar will be of low quality (Davey 1961, Holmes and Wingate 1997).

Aggregates used in stone and brick masonry mortars of the five historic Ottoman baths had almost similar particle size distributions with each other (Figures 4.10 and 4.11). The aggregates with particle sizes greater than 1180 μm composed the largest fraction of the total aggregates. This largest fraction ranged between 44 % and 64 % in stone masonry mortars, and 38-67 % in brick masonry mortars. Fine aggregates whose particle sizes were less than 125 μm comprised the fraction ranging between 0.84 % and 5 % within the total aggregates. Since calcareous aggregates used in the stone masonry mortar sample of Ur.He.s. were dissolved in dilute HCl solution, exact ratios of such aggregates could not be included in the particle size distributions of its aggregates.
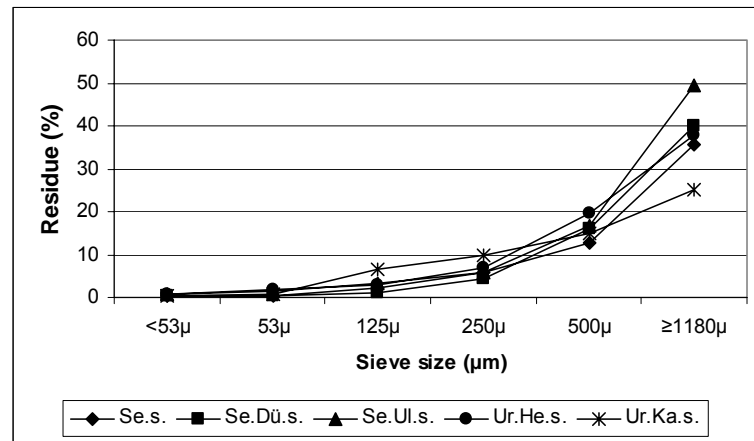
Figure 4.10 Particle size distribution curves of the aggregates used in stone masonry mortars.
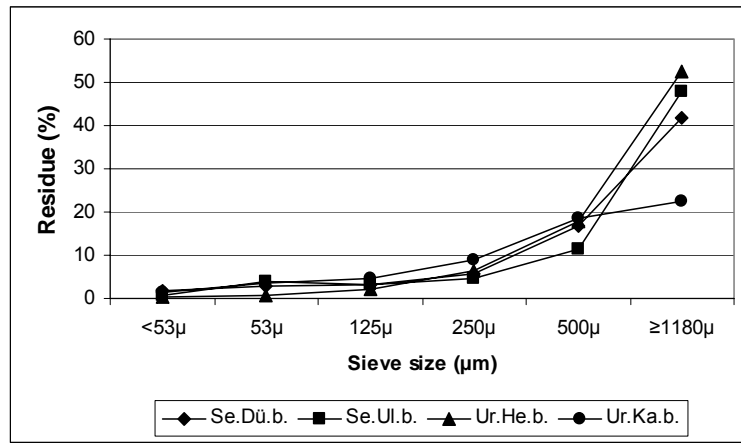
Figure 4.11 Particle size distribution curves of the aggregates used in brick masonry mortars.

Stereo microscopic observations revealed that aggregates used in stone and brick masonry mortars were mostly semi-round (Figures 4.12-4.16). However, they differed from each other in terms of colour. The ones used in the stone masonry mortars of Se.s., Se.Dü.s. and Ur.Ka.s. were mainly glassy, and had brown and grey colour. In the mortars of Se.Ul.s., Se.Ul.b. and Se.Dü.b., the aggregates were dull and greyish and white in colour. The mortars of Ur.He.s., Ur.He.b. and Ur.Ka.b. had aggregates being dull and white, grey and light brown in colour (Figures 4.12-4.16). These were more porous and lighter than the rest.
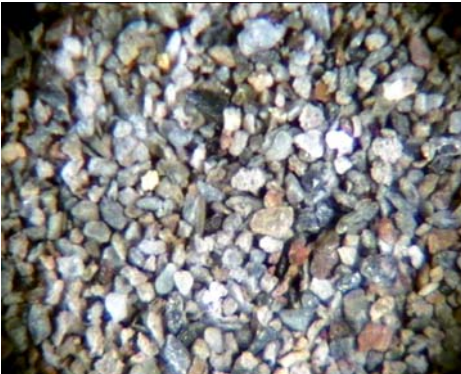
Particle size	Aggregates of Se.s.
>1180μm	
1180-500 μm	
500-250 μm	
250-125 μm	

Figure 4.12 Stereo microscope images of the aggregates used in the mortar sample of Se.s., which were grouped according to the particle sizes of >1180 μm, 1180-500 μm, 500-250 μm and 250-125 μm by sieve analysis.
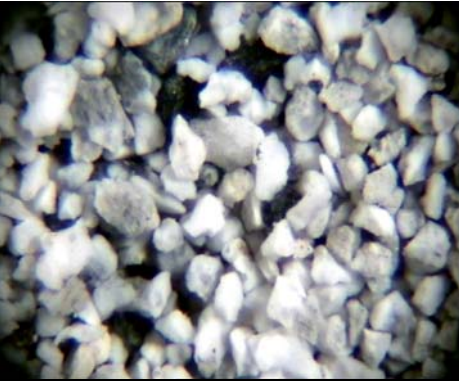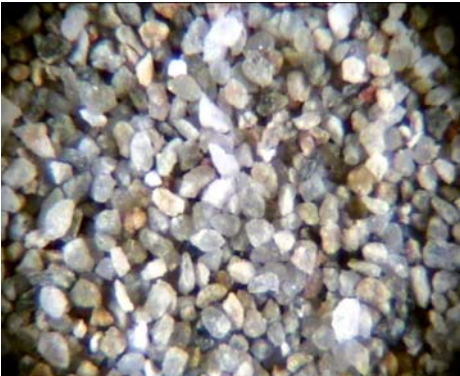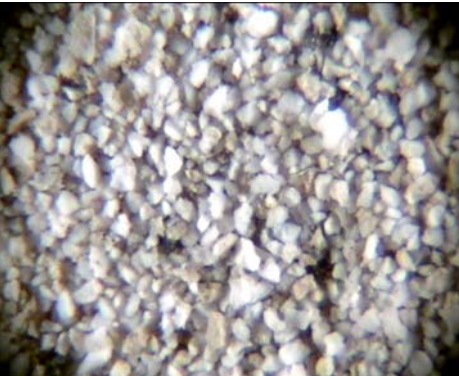
Particle size	Aggregates of Se.Dü.s.	Aggregates of Se.Dü.b.
>1180µm		
1180-500 µm		
500-250 µm		
250-125 µm		

Figure 4.13 Stereo microscope images of the aggregates used in the mortar samples of Se.Dü.s. and Se.Dü.b., which were grouped according to the particle sizes of >1180 µm, 1180-500 µm, 500-250 µm and 250-125 µm by sieve analysis.
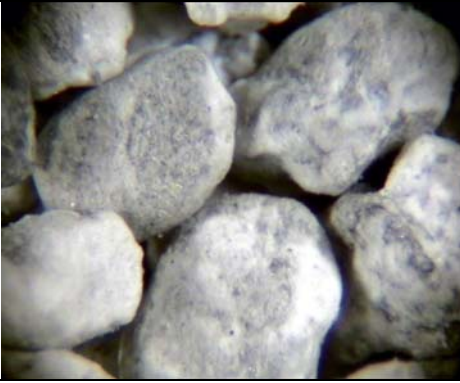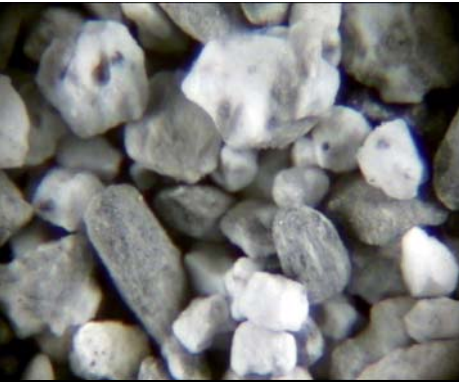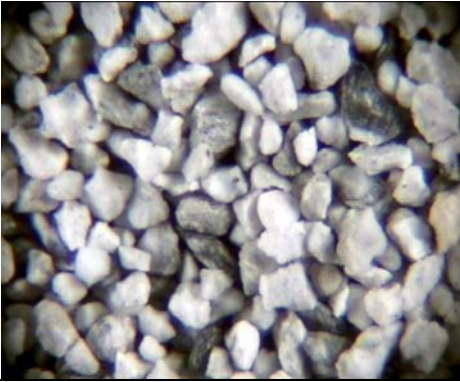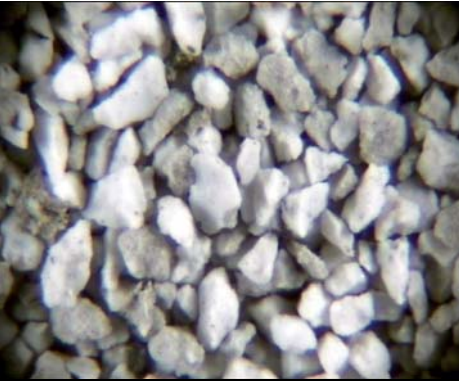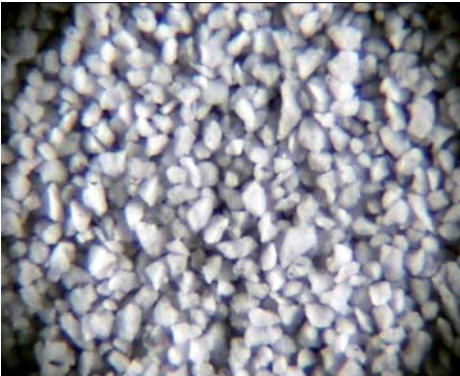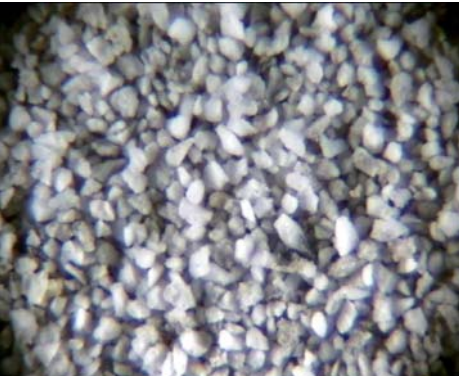
Particle size	Aggregates of Se.Ul.s.	Aggregates of Se.Ul.b.
>1180µm		
1180-500 µm		
500-250 µm		
250-125 µm		

Figure 4.14 Stereo microscope images of the aggregates used in the mortar samples of Se.Ul.s. and Se.Ul.b., which were grouped according to the particle sizes of >1180 µm, 1180-500 µm, 500-250 µm and 250-125 µm by sieve analysis.
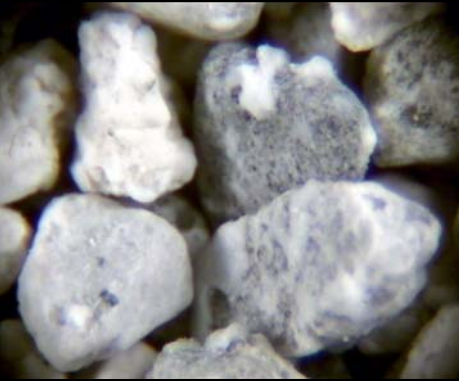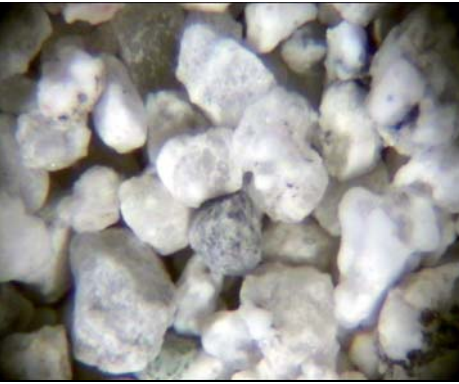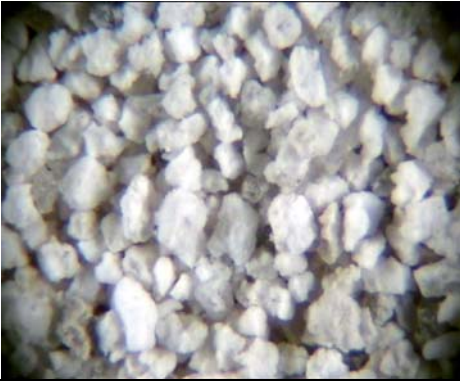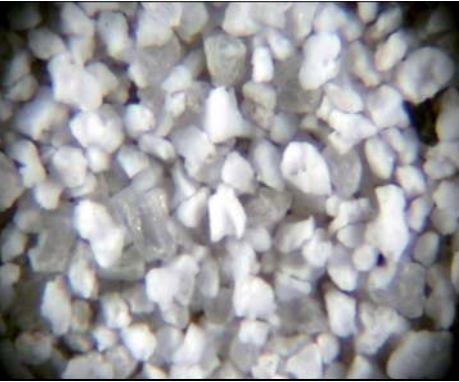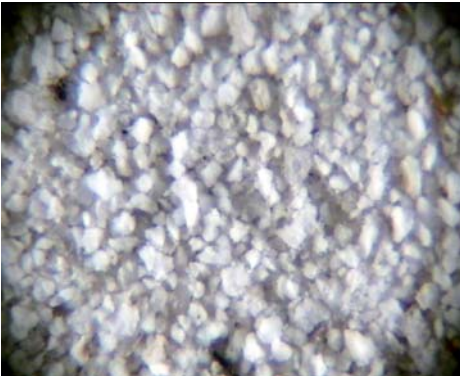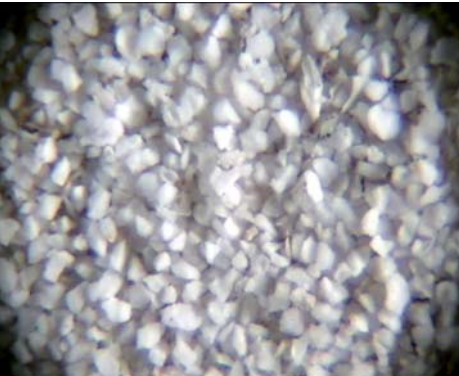
Particle size	Aggregates of Ur.He.s.	Aggregates of Ur.He.b.
>1180μm		
1180-500 μm		
500-250 μm		
250-125 μm		

Figure 4.15 Stereo microscope images of the aggregates used in the mortar samples of Ur.He.s. and Ur.He.b., which were grouped according to the particle sizes of >1180 μm, 1180-500 μm, 500-250 μm and 250-125 μm by sieve analysis.
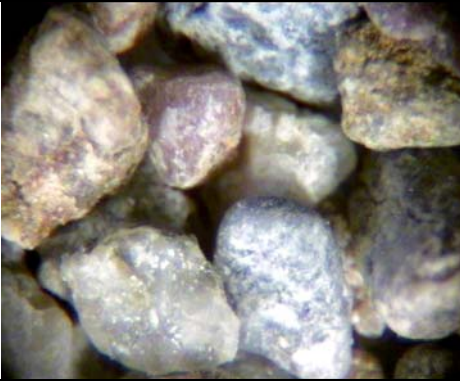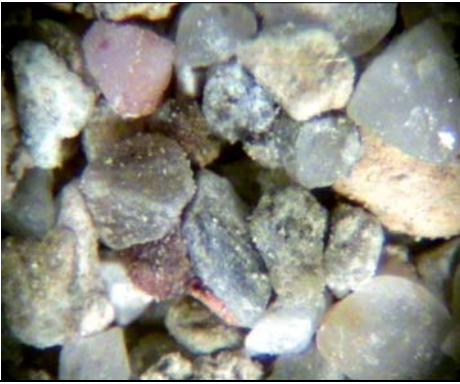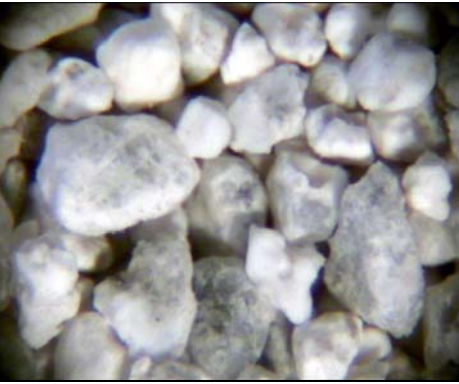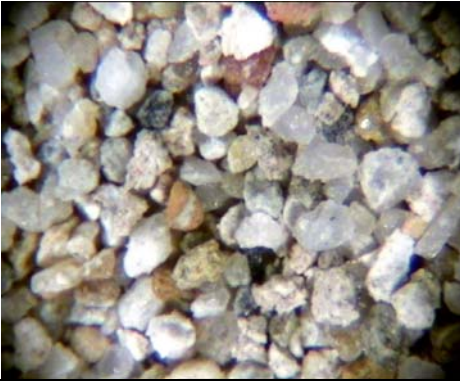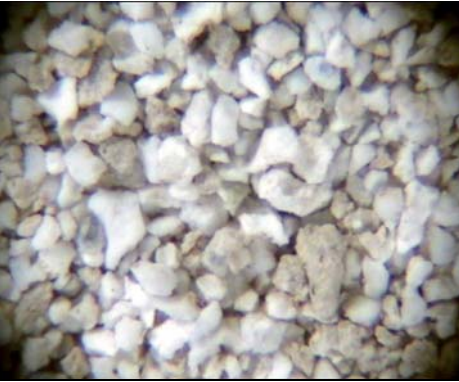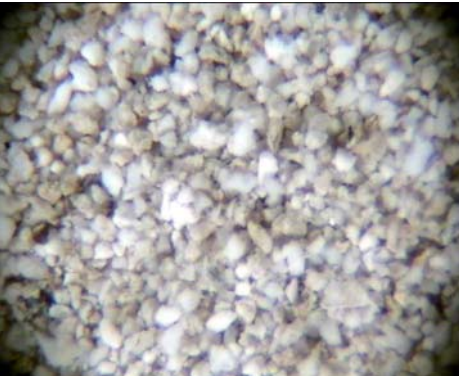
Particle size	Aggregates of Ur.Ka.s.	Aggregates of Ur.Ka.b.
>1180μm		
1180-500 μm		
500-250 μm		
250-125 μm		

Figure 4.16 Stereo microscope images of the aggregates used in the mortar samples of Ur.Ka.s. and Ur.Ka.b., which were grouped according to the particle sizes of >1180 μm, 1180-500 μm, 500-250 μm and 250-125 μm by sieve analysis.

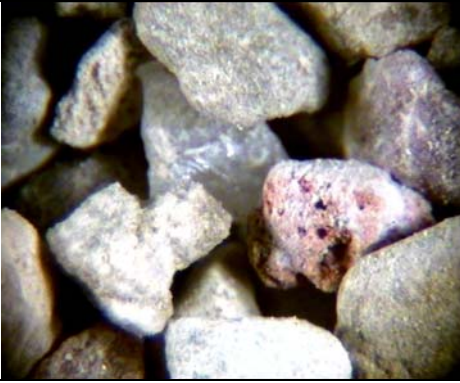All the aggregates from each particle size had similar properties in terms of colour within a single mortar sample (Figures 4.12-4.16). Furthermore, in terms of stone and brick masonry mortars used in each bath, aggregates used in the mortars of Ur.He.s.-Ur.He.b. and Se.Ul.s.-Se.Ul.b. had the same colour with each other (Figures 4.14 and 4.15). However, in each bath of Düzce and Kamanlı, aggregates used in the stone and brick masonry mortars have different colour properties (Figures 4.13 and 4.16). When the aggregates used in each stone and brick masonry mortars of the baths were compared with each other, it was observed that the aggregates of the mortars of Se.s., Se.Dü.s. and Ur.Ka.s., the ones of the mortars of Se.Ul.s., Se.Ul.b. and Se.Dü.b., and the aggregates of the mortars of Ur.He.s., Ur.He.b. and Ur.Ka.b. had same colour properties with each other (Figures 4.12-4.16). Therefore, it could be deduced that the aggregates of the each three group may be of the same source.

4.5. Pozzolanic Activity of Aggregates and Bricks

Pozzolanic activities of aggregates influence physical, mechanical and microstructural properties of lime mortars. Aggregates with pozzolanic activity may contribute to a degree of pozzolanic reaction with lime, which might acquire hydraulic properties to the lime mortars and provide high strength properties to them (Lea 1940, Moropoulou et al. 2000b). Besides, bricks with pozzolanic activity can give rise to a degree of pozzolanic reaction with the lime mortar. Such reaction can produce hydraulic reaction products at the interface between the bricks and lime mortar, which improves their adhesion.

Pozzolanic activity measurements revealed the results that fine aggregates of all mortars had good pozzolanicity. Difference in electrical conductivity measurements of calcium hydroxide solutions before and after they were mixed with the fine aggregates was more than 1.2 mS/cm (Figure 4.17). This was the value accepted as the lowest limit of good pozzolanicity (Luxan et al. 1989). Although all fine aggregates had good pozzolanicity, the ones of the stone masonry mortar samples of Se.s., Se.Dü.s. and Ur.Ka.s. showed the lowest pozzolanicity values of 1.3 mS/cm (Figure 4.17). These pozzolanic activity values of the fine aggregates are relatively higher than those of the ones used in some Anatolian Seljuk buildings (Tunçoku 2001).
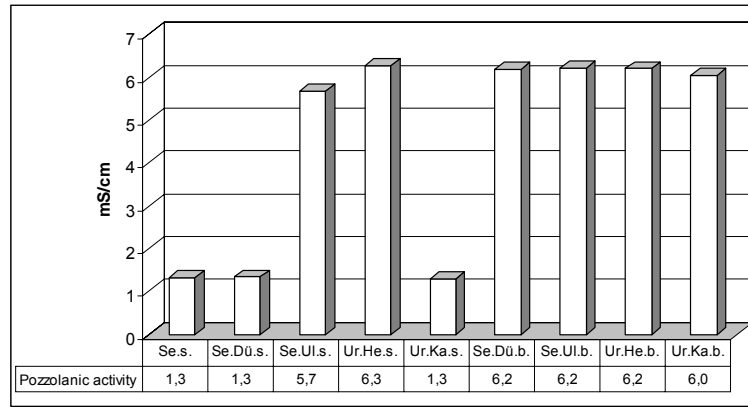
Figure 4.17 Pozzolanic activity measurements of fine aggregates (less than 53 µm).

Coarse aggregates except for the ones used in the mortars of Se.s., Se.Dü.s. and Ur.Ka.s. had good pozzolanicity with the values ranging between 1.3 mS/cm and 1.9 mS/cm (Figure 4.18). Although their pozzolanic activity values were lower than their fine aggregates, such aggregates could be accepted as good pozzolanas. However, the coarse aggregates of the three mortar samples of Se.s., Se.Dü.s. and Ur.Ka.s. had poor pozzolanicity due to their pozzolanicity values of 0.7 mS/cm and 0.8 mS/cm which were less than 1.2 mS/cm (Figure 4.18). These three mortar samples were the ones whose fine aggregates had the lowest pozzolanic activity values among the fine aggregates.
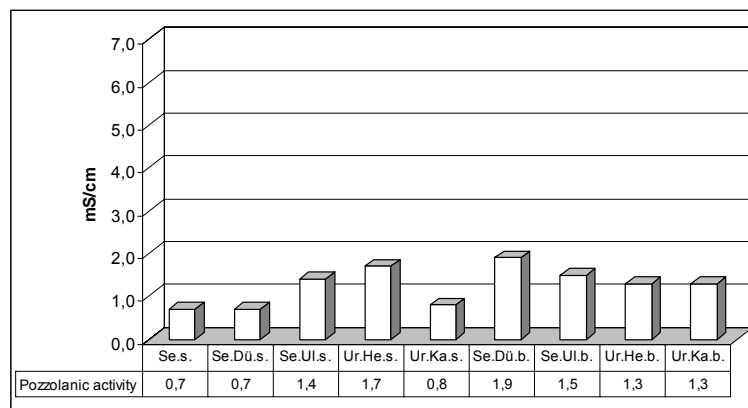
Figure 4.18 Pozzolanic activity measurements of coarse aggregates.

Pozzolanic activity measurements of bricks used in the construction of the domes revealed the results that they had poor pozzolanicity since their pozzolanicity values ranged between 0.5 mS/cm and 0.8 mS/cm (Figure 4.19). In spite of this, there could be pozzolanic reactions between the bricks and lime mortar.
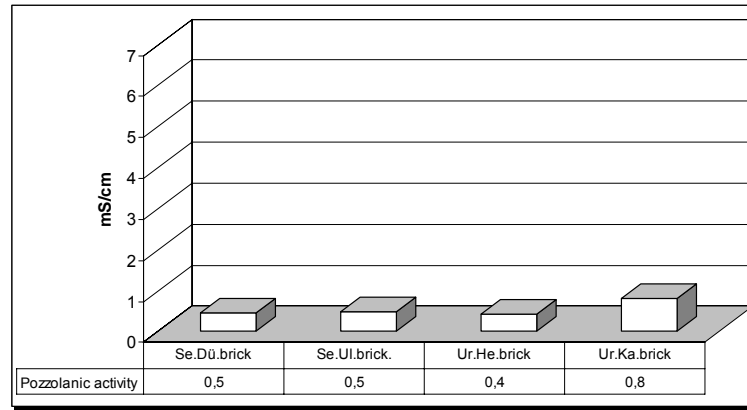
Figure 4.19 Pozzolanic activity measurements of bricks used in domes.

4.6. Mineralogical and Chemical Compositions and Microstructural Properties of Lime Binders, Aggregates and Mortar Matrices

Mineralogical and chemical compositions of lime binders and aggregates are important parameters that influence physical and mechanical properties of lime mortars (Lea 1940, Boynton 1966, Holmes and Wingate 1997). Microstructural properties of the lime such as its particle size influence plasticity and carbonation of the lime mortar (Navarro et al. 1998, Cazalla et al. 2000). Chemical compositions and microstructural properties of aggregates also influence the physical, mechanical and hydraulic properties of the lime mortars (Cowper 2000, Lea 1940, Holmes and Wingate 1997). Therefore, mineralogical and chemical compositions, and microstructural properties of the lime binders, aggregates and mortar matrices were included in this section.

4.6.1. Mineralogical and Chemical Compositions and Microstructural Properties of Lime Binders

Small, white, round and soft fragments called white lumps could be considered to represent the binding materials used in the mortars (Bruni et al. 1997). Mortar samples of Se.Dü.s., Ur.Ka.b., Ur.He.s., Ur.Ka.s. and Se.s. were the ones where the white lumps could be easily observed (Figure 4.20). However, rest of the mortars (Se.Dü.b., Se.Ul.s., Se.Ul.b. and Ur.He.b.) had white lumps being less in amount and with very small sizes (Figures 4.21 and 4.22). Therefore, required carbonated lime could not be scrubbed from these four mortar samples in order to determine their mineralogical compositions. Only chemical compositions of the white lumps within these mortars could be analyzed by SEM-EDS analysis.
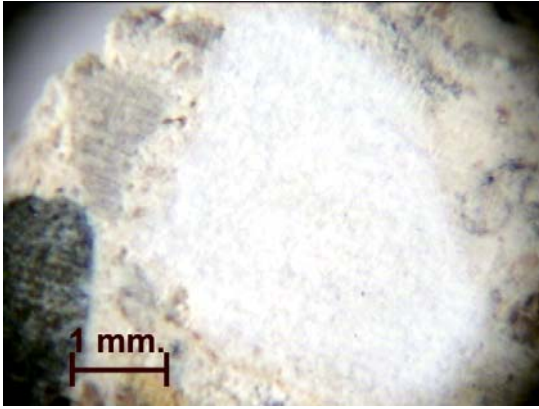
Figure 4.20 Stereo microscope image of the white lump in the stone masonry mortar sample of Ur.He.s.

Figure 4.21 Stereo microscope image of the white lump in the stone masonry mortar sample of Se.Ul.s.
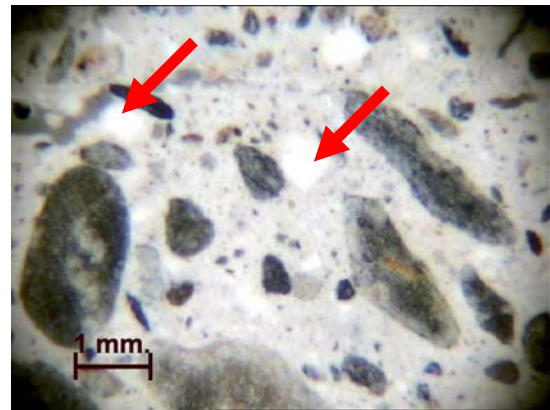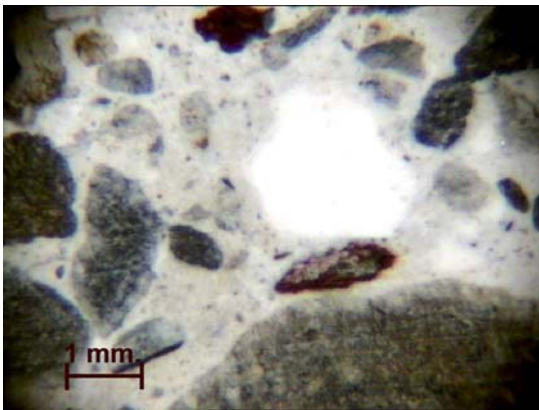
Figure 4.22 Stereo microscope images of the white lumps in the brick masonry mortar sample of Se.Ul.b.

Mineralogical and chemical compositions of white lumps were determined by XRD and SEM-EDS analysis. XRD patterns of the white lumps indicated only calcite peaks. The white lump of the mortar of Ur.Ka.s. was determined by SEM-EDS analysis to be composed of calcium oxide (CaO) with an approximate proportion of 100 %. Therefore, the lime used in this mortar could be considered to be almost pure lime (Figure 4.23). EDS analysis of the white lumps taken from the mortar samples of Se.Dü.s., Se.s. and Ur.He.s. recorded high amounts of calcium oxide ranging between 93 % and 97 % (Figures 4.24, 4.25 and 4.26). These results showed that lime used in these mortars could be regarded as high-calcium lime (Eckel 1928, Cowper 2000). On the other hand, EDS analysis of the white lumps taken from the mortar samples of Se.Ul.s., Se.Ul.b., Se.Dü.b. and Ur.Ka.b., revealed the results that they contained high proportions of silicon dioxide (SiO_2) ranging between 11 % and 28 % (Figures 4.28-4.31). High proportions of silicon dioxide in these white lumps could be derived

from siliceous limestone from which the lime was produced. Even though SEM-EDS analysis recorded silicon dioxide, their presence could not be detected in the XRD analyses. This might be due to the fact that silicon dioxide being present in these white lumps was not in a crystal structure but in an amorphous state. Therefore, any minerals including silica could not be detected in their XRD patterns. However, SEM images indicated the presence of calcium-silicate-hydrate (C-S-H) formations in the white lumps with high proportions of silicon dioxide (Figure 4.32). Therefore, such white lumps may be composed of lime having hydraulic character. Furthermore, mortars containing white lumps with high proportions of silicon dioxide had higher mechanical properties than the ones containing white lumps composed of high-calcium lime (Tables 4.1 and 4.2). This may be due to the hydraulic character of the lime binder with high proportions of silicon dioxide, which could acquire hydraulic character to these mortars (Eckel 1928, Cowper 2000).
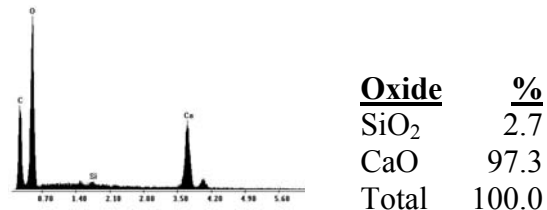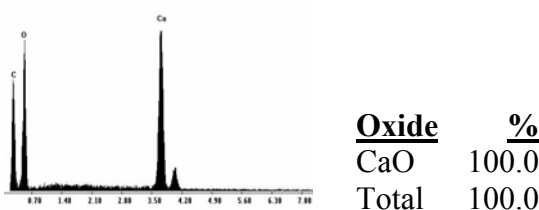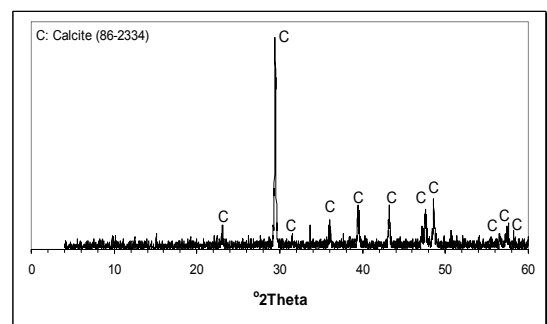
Figure 4.23 XRD pattern, EDX spectrum and elemental composition (%) of the white lump composed of high-calcium lime (Ur.Ka.s.).

Oxide	%
CaO	100.0
Total	100.0

Figure 4.24 XRD pattern, EDX spectrum and elemental composition (%) of the white lump composed of high-calcium lime (Se.Dü.s.).

Oxide	%
SiO_2	2.7
CaO	97.3
Total	100.0

Microstructural investigations carried out by SEM revealed that white lumps composed of high calcium lime consisted of micritic calcite crystals (Figures 4.25, 4.26 and 4.27). However, white lumps composed of lime containing silica at high ratios consisted of calcite crystals having different crystal structures (Figures 4.29-4.32).
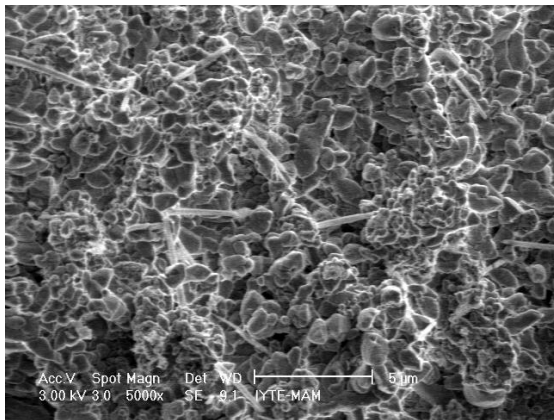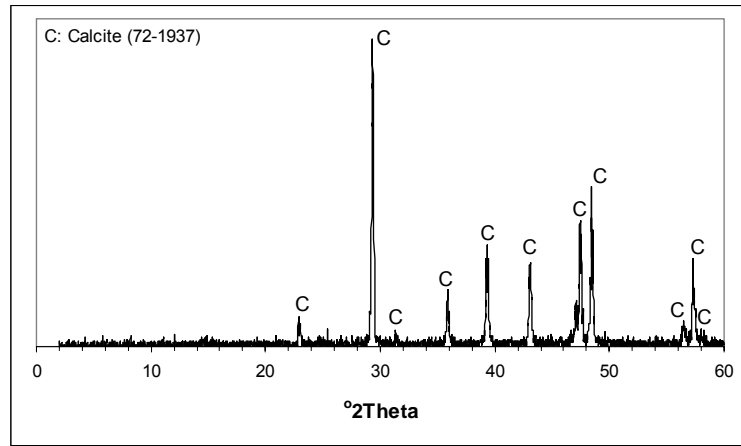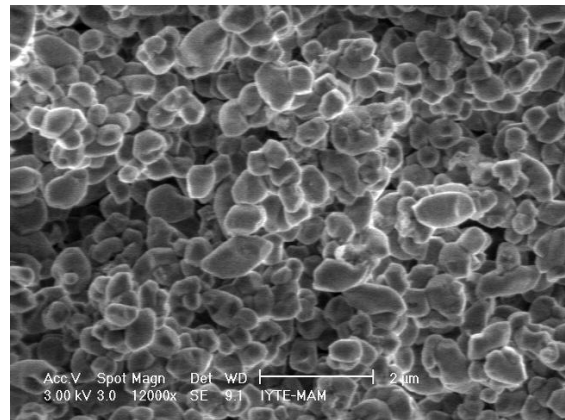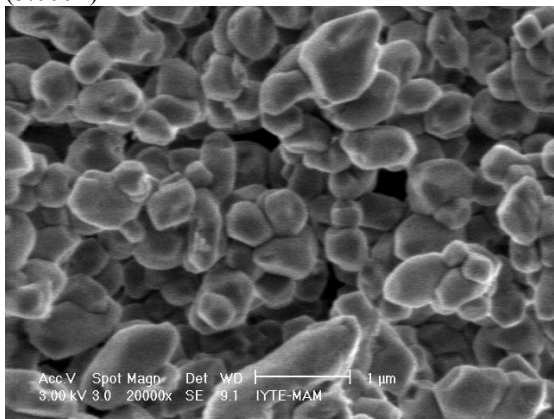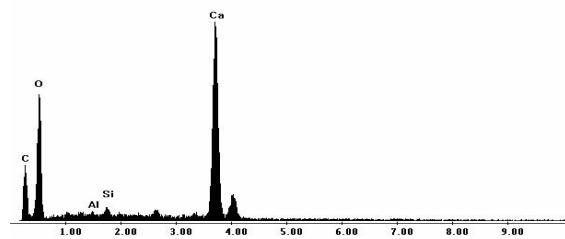
Figure 4.25 XRD pattern, SE (secondary electron) images of micritic calcite crystals in the white lump, EDX spectrum and elemental composition (%) of the white lump composed of high-calcium lime (Se.s.).
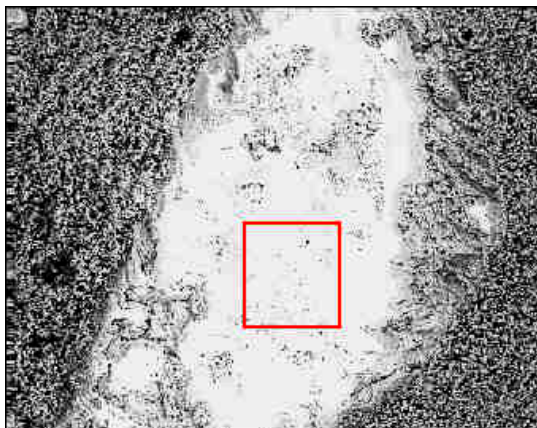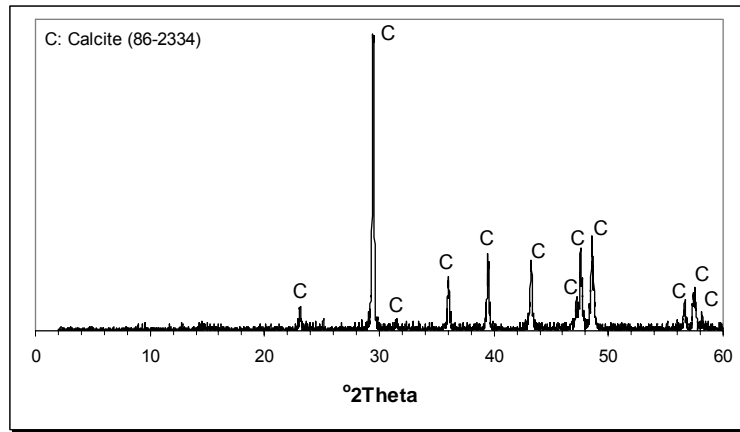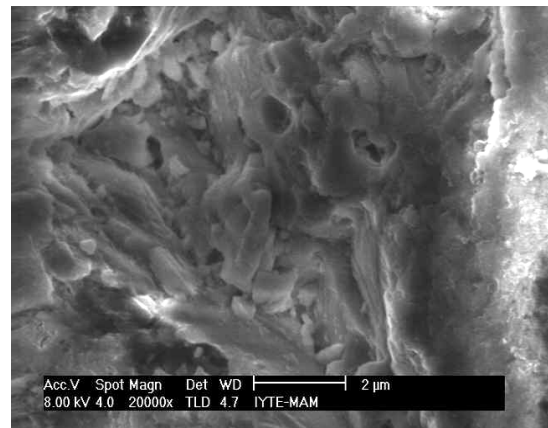
(1000×)   (20.000×)
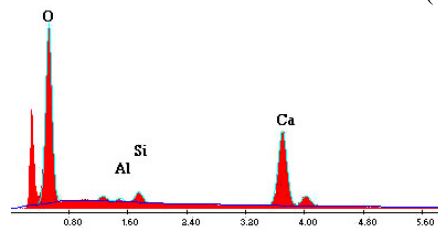
Oxide	%
Al$_2$O$_3$	1.4
SiO$_2$	3.5
CaO	95.1
Total	100.0

Figure 4.26 XRD pattern, SE images of the white lump, SE image (20.000×) of micritic calcite crystals in the white lump, EDX spectrum and elemental composition (%) of the white lump composed of high-calcium lime (Ur.He.s.).
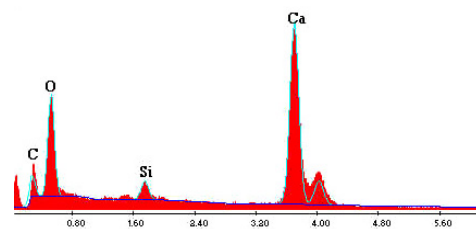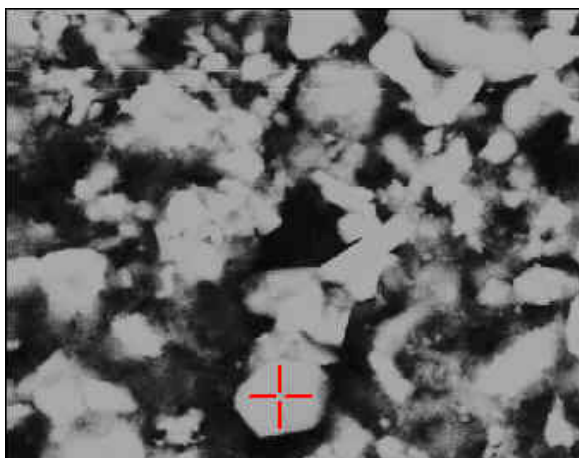
Element	%
C	14.8
O	54.7
Si	1.3
Ca	29.2
Total	100.0

Figure 4.27 BSE (back-scattered electron) image and elemental composition (%) of micritic calcite crystals in the white lump composed of high-calcium lime (Ur.He.b.).

Oxide	%
Al$_2$O$_3$	3.6
SiO$_2$	19.2
CaO	77.2
Total	100.0
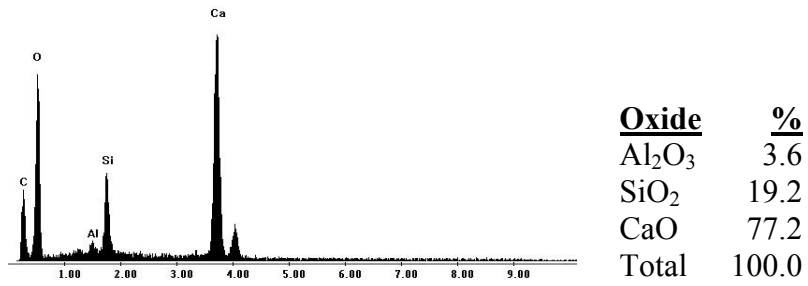
Figure 4.28 EDX spectrum and elemental composition (%) of the white lump composed of lime containing silica at high ratios (Se.Dü.b.).

C: Calcite (86-2334)

°2Theta
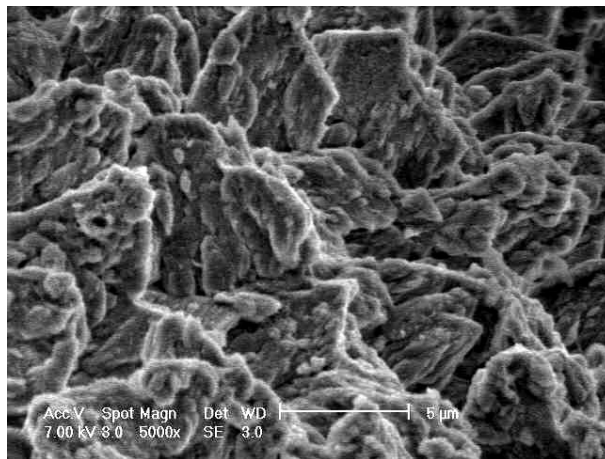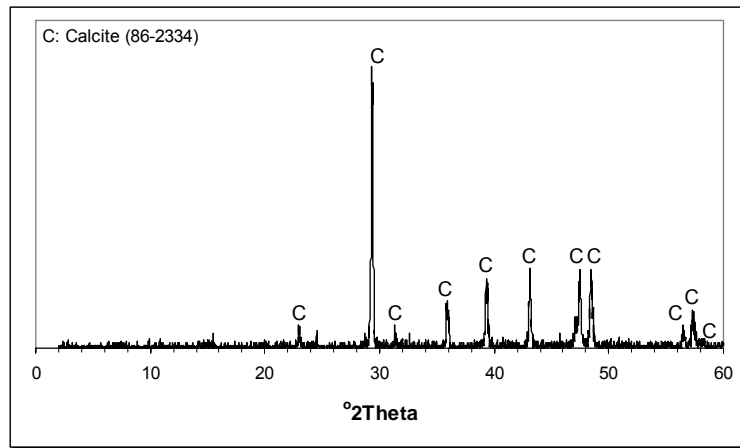
(5000×)

Oxide	%
Al$_2$O$_3$	3.0
SiO$_2$	23.6
CaO	73.4
Total	100.0

Figure 4.29 XRD pattern, SE image and elemental composition (%) of micritic calcite crystals in the white lump composed of lime containing silica at high ratios (Ur.Ka.b.).

Figure 4.30 XRD pattern, SE image, EDX spectrum and elemental composition (%) of the white lump composed of lime containing silica at high ratios (Se.Ul.s.).
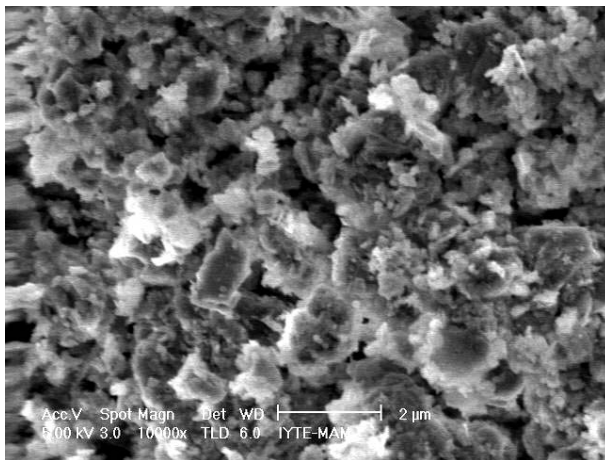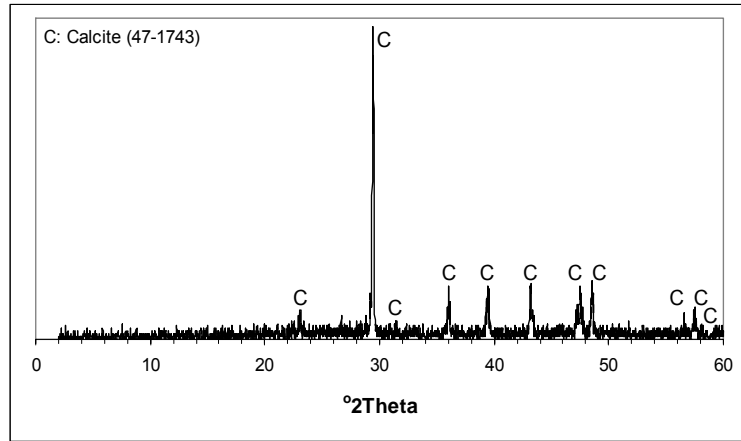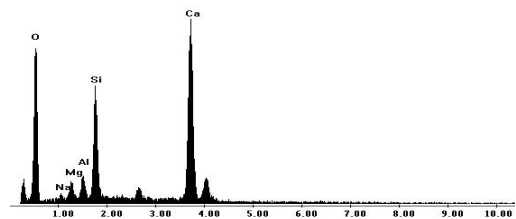
Oxide	%
Na_2O	1.2
MgO	4.1
Al_2O_3	5.6
SiO_2	28.3
CaO	60.8
Total	100.0

(10.000×)

Oxide	%
Al₂O₃	3.7
SiO₂	11.2
CaO	85.1
Total	100.0
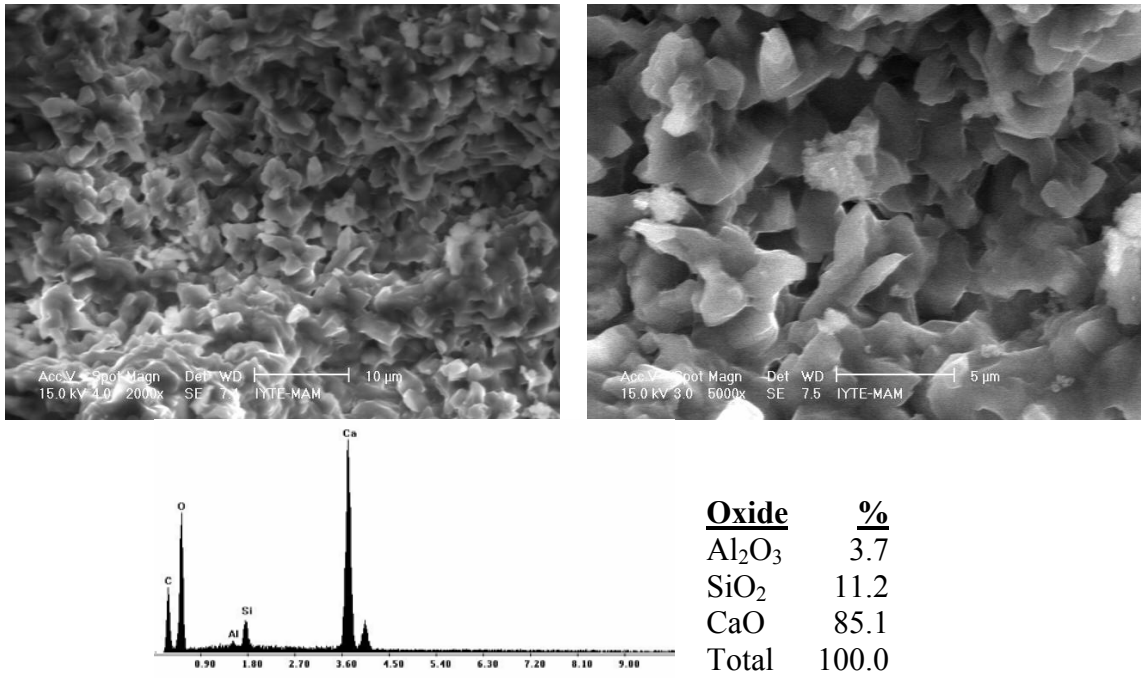
Figure 4.31 SE images (2.000× and 5.000× respectively) of micritic calcite crystals in the white lump, EDX spectrum and elemental composition (%) of the white lump composed of lime containing silica at high ratios (Se.Ul.b.).

(2500×)

(5000×)

(10.000×)
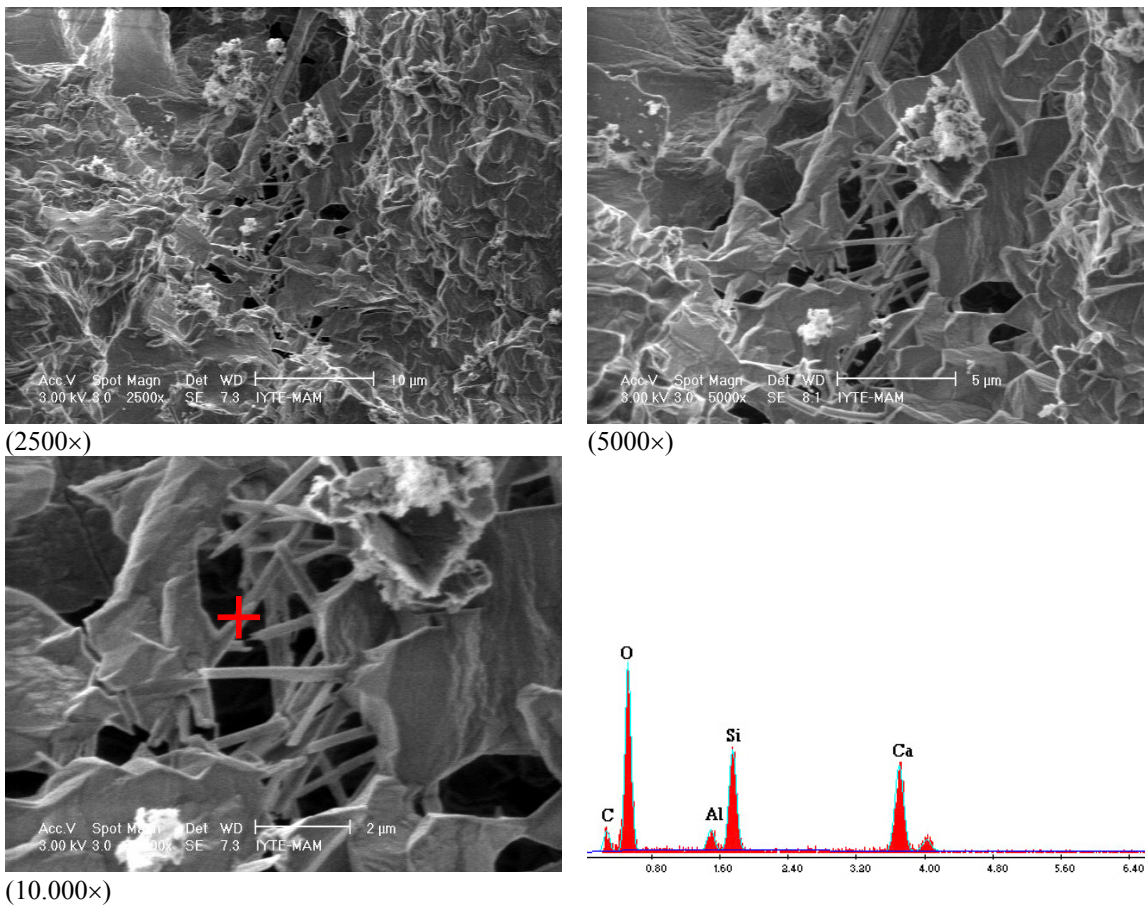
Figure 4.32 SE images and EDX spectrum of calcium-silicate-hydrate (C-S-H) formations in the white lump composed of lime containing silica at high ratios (Se.Ul.b.).

4.6.2. Mineralogical and Chemical Compositions and Microstructural Properties of Aggregates

In this section, mineralogical and chemical compositions, and microstructural properties of coarse aggregates and fine aggregates less than 53 μm used in stone and brick masonry mortars of the Ottoman baths were included in this section.

4.6.2.1. Mineralogical and Chemical Composition and Microstructural Properties of Coarse Aggregates

XRD patterns of coarse aggregates indicated that they were composed of quartz (Figures 4.33-4.38), potassium feldspars (Figures 4.33-4.37 and 4.39) and albite as the primary minerals, and muscovite, hematite (Figures 4.34, 4.35, 4.37 and 4.40), illite and kaolinite as the secondary minerals. Although the coarse aggregates except for the ones of Se.s., Se.Dü.s. and Ur.Ka.s. had pozzolanic activity, broad band indicating the presence of amorphous materials was not observed between 20-30$^{°}$ in their XRD patterns (Figures 4.34, 4.35 and 4.37). This may be explained by little amount of amorphous materials contained in their compositions.
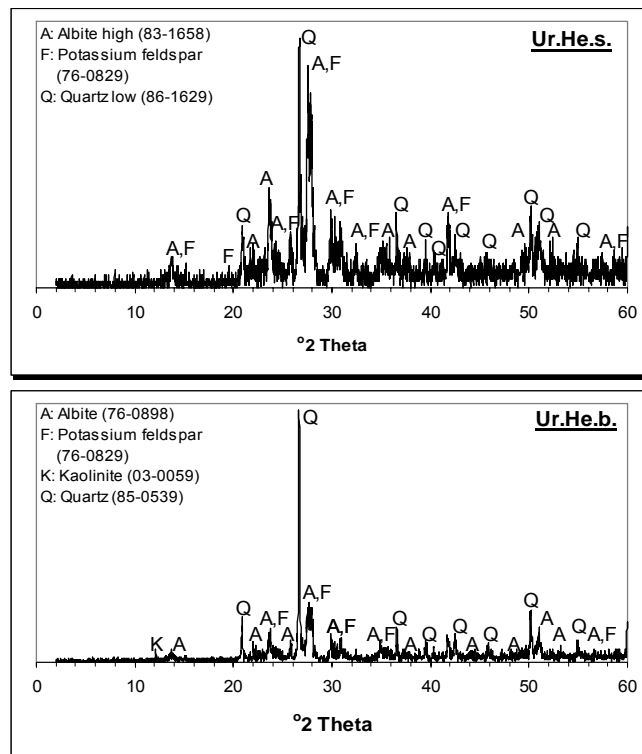
Figure 4.33 XRD patterns of the coarse aggregates used in the stone masonry mortar of Ur.He.s. and brick masonry mortar of Ur.He.b.
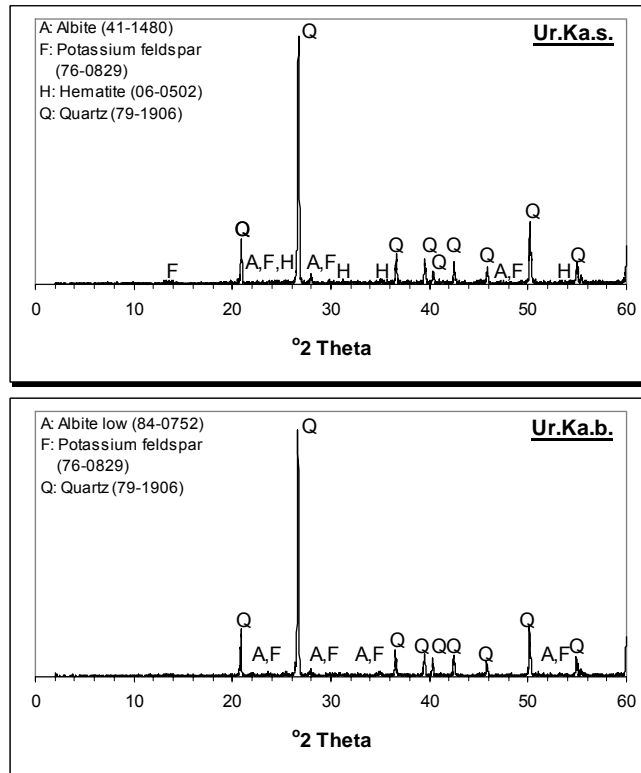
Figure 4.34 XRD patterns of the coarse aggregates used in the stone masonry mortar of Ur.Ka.s. and brick masonry mortar of Ur.Ka.b.

Figure 4.35 XRD patterns of the coarse aggregates used in the stone masonry mortar of Se.Dü.s. and brick masonry mortar of Se.Dü.b.

Figure 4.36 XRD patterns of the coarse aggregates used in the stone masonry mortar of Se.Ul.s. and brick masonry mortar of Se.Ul.b.
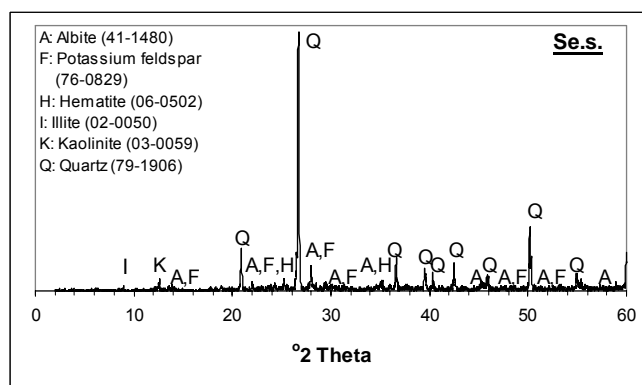
Figure 4.37 XRD pattern of the coarse aggregates used in the stone masonry mortar of Se.s.

76
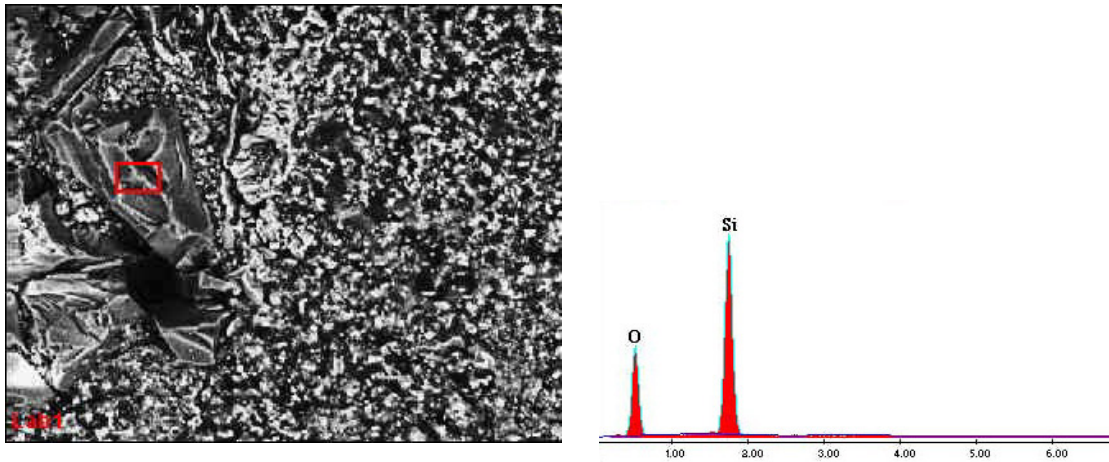
Figure 4.38 BSE image (1500×) and EDX spectrum of the quartz crystals.
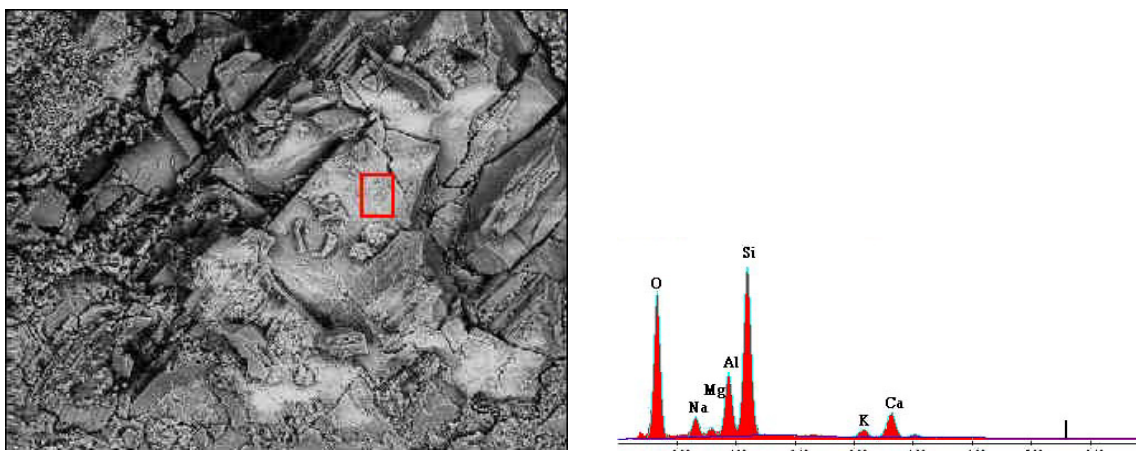
Figure 4.39 BSE image (1000×) and EDX spectrum of feldspar crystals.
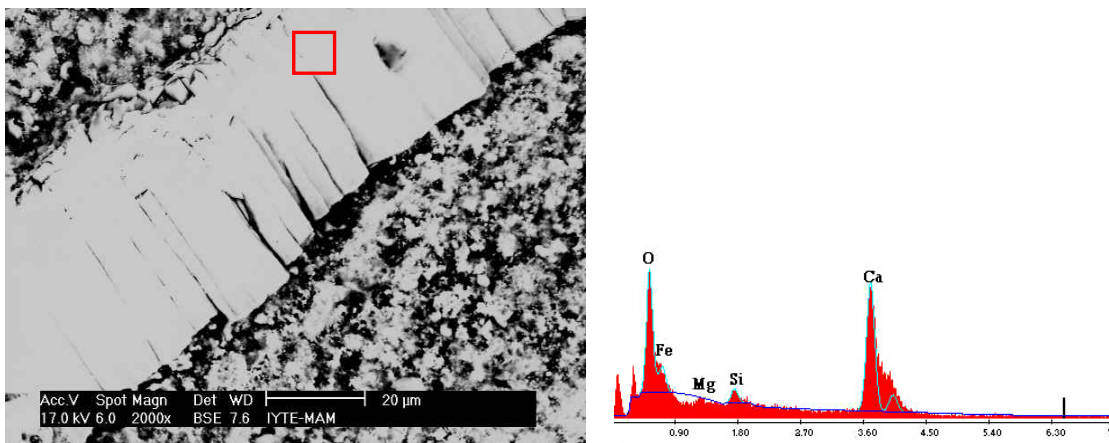
Figure 4.40 BSE image (2000×) and EDX spectrum of iron-rich crystals.

EDS analyses indicated that coarse aggregates contained high proportions of silicon dioxide (53.6-80.6 %) and aluminium oxide (9.7-19.1 %), and mostly low ratios of iron oxide, sodium oxide and potassium oxide (Table 4.4). The chemical composition results of aggregates supported their mineralogical compositions determined by XRD.

Table 4.4 Elemental compositions of coarse aggregates used in the mortars.

Coarse aggregates	Elemental Composition (%)					
	Na$_2$O	MgO	Al$_2$O$_3$	SiO$_2$	K$_2$O	Fe$_2$O$_3$
Se.s.c-agg.	2.4	4.5	15.0	64.1	2.6	11.4
Se.Dü.s.c-agg.	2.7	5.3	19.1	53.6	2.8	16.5
Se.Ul.s.c-agg.	2.0	2.6	17.7	66.5	4.0	7.2
Ur.He.s.c-agg.	4.4	1.5	15.0	68.5	5.2	5.3
Ur.Ka.s.c-agg.	1.5	2.0	9.7	78.7	1.9	6.2
Se.Dü.b.c-agg.	2.1	2.7	15.9	69.0	3.2	7.1
Se.Ul.b.c-agg.	2.1	2.0	17.4	69.2	3.8	5.5
Ur.He.b.c-agg.	4.3	1.1	14.9	72.3	5.4	2.0
Ur.Ka.b.c-agg.	1.7	1.9	9.7	80.7	1.7	4.3

SEM analyses indicated that stone masonry mortar of Ur.He.s. contained two types of calcareous aggregates. The first one contained calcium oxide with a percent of 44.5 and magnesium oxide with a percent of 33 (Figure 4.41). The other one was rich in calcium oxide (57 %), silicon dioxide (24 %) and aluminium oxide (11 %) (Figure 4.42). SEM images indicated the presence of fossils in this aggregate (Figure 4.43). Both of these calcareous aggregates differed from lime used in this mortar with their microstructures (Figure 4.44).

(2500×)

(5000×)

Oxide	%
Na$_2$O	1.1
MgO	33.1
Al$_2$O$_3$	7.0
SiO$_2$	10.9
Cl$_2$O	3.4
CaO	44.5
Total	100.0
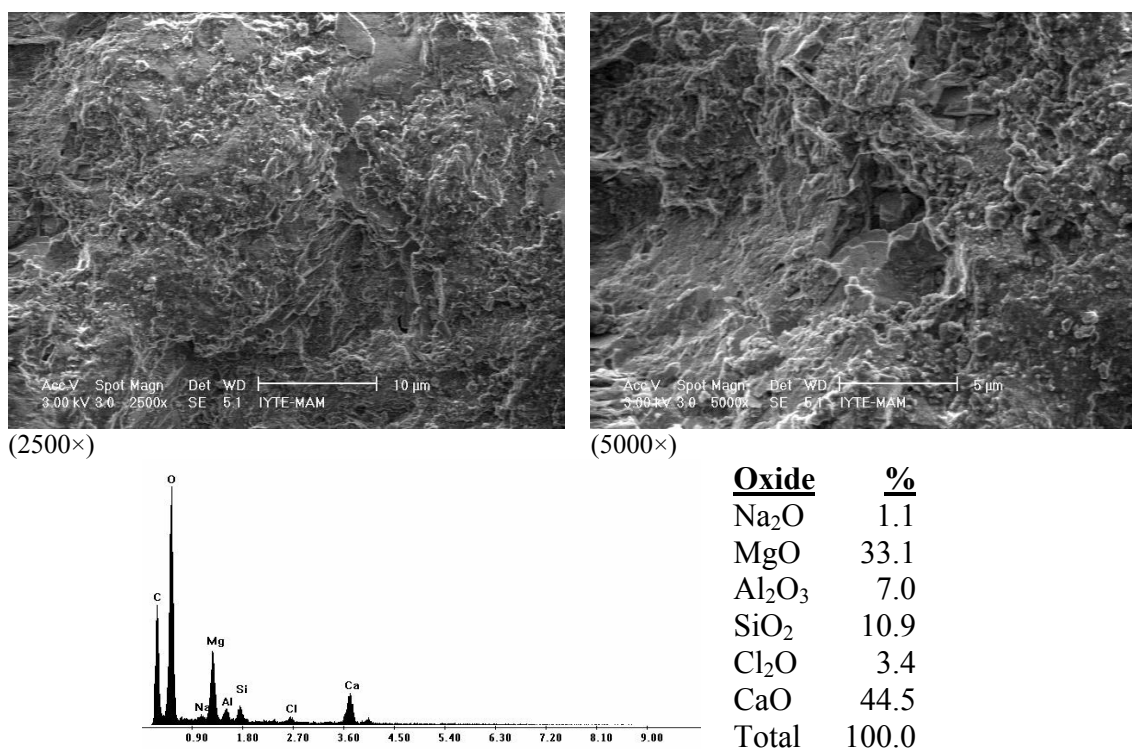
Figure 4.41 SE images, EDX spectrum and elemental composition (%) of the calcareous aggregate used in the stone masonry mortar of Ur.He.s.
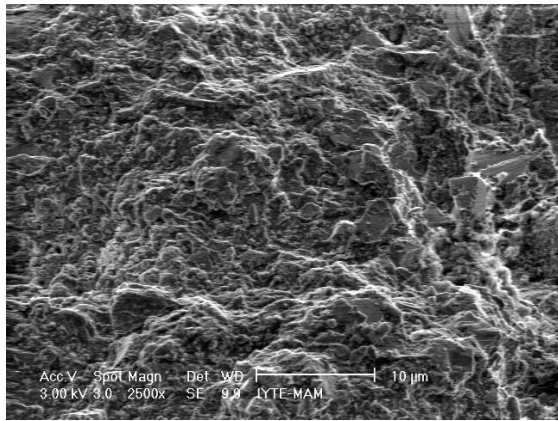
(2500×)
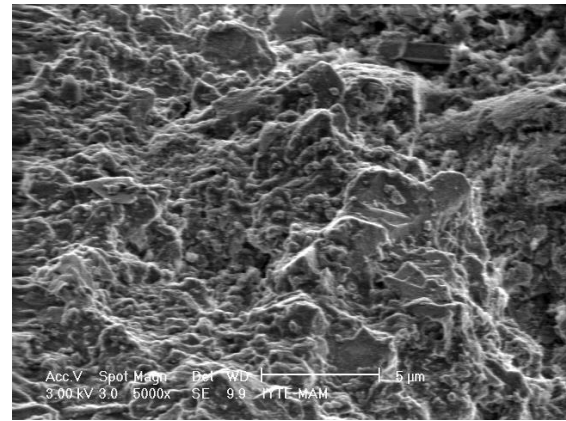
(5000×)
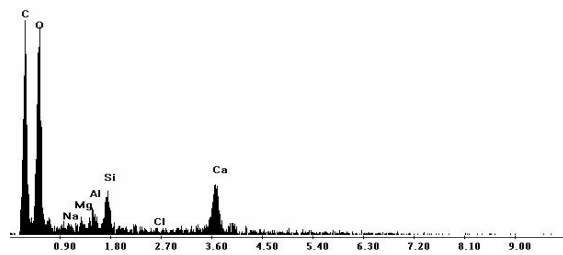
Oxide	%
Na$_2$O	2.3
MgO	4.1
Al$_2$O$_3$	10.7
SiO$_2$	24.0
Cl$_2$O	1.6
CaO	57.3
Total	100.0

Figure 4.42 SE images, EDX spectrum and elemental composition (%) of the calcareous aggregate used in the stone masonry mortar of Ur.He.s.
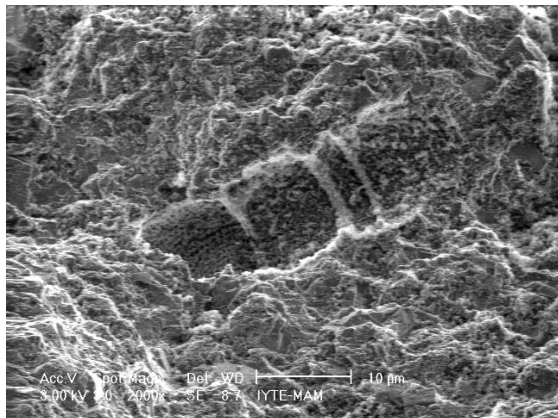
(2000×)
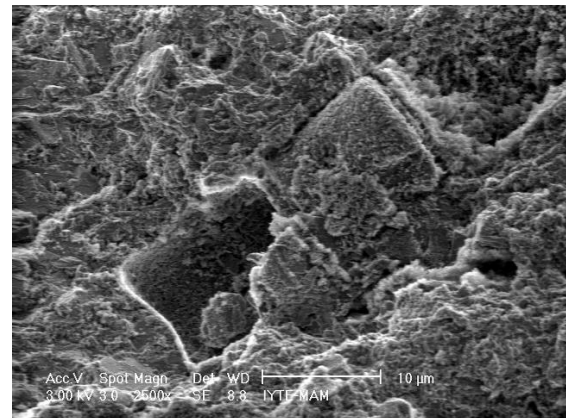
(2500×)
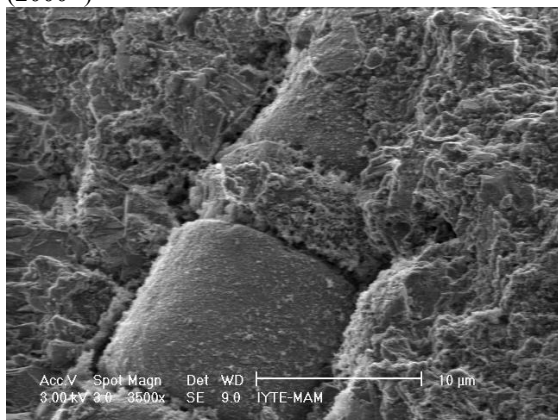
(3500×)
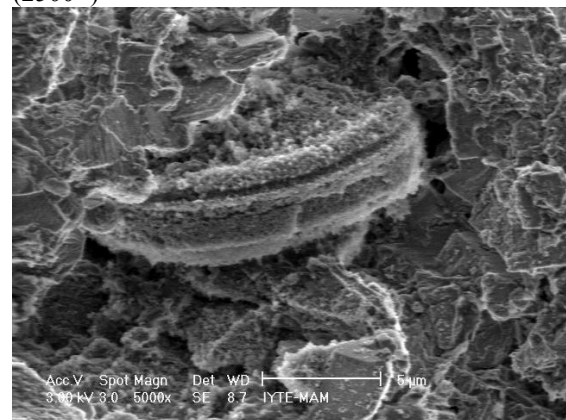
(5000×)

Figure 4.43 SE images of fossils in the calcareous aggregate used in the stone masonry mortar of Ur.He.s.
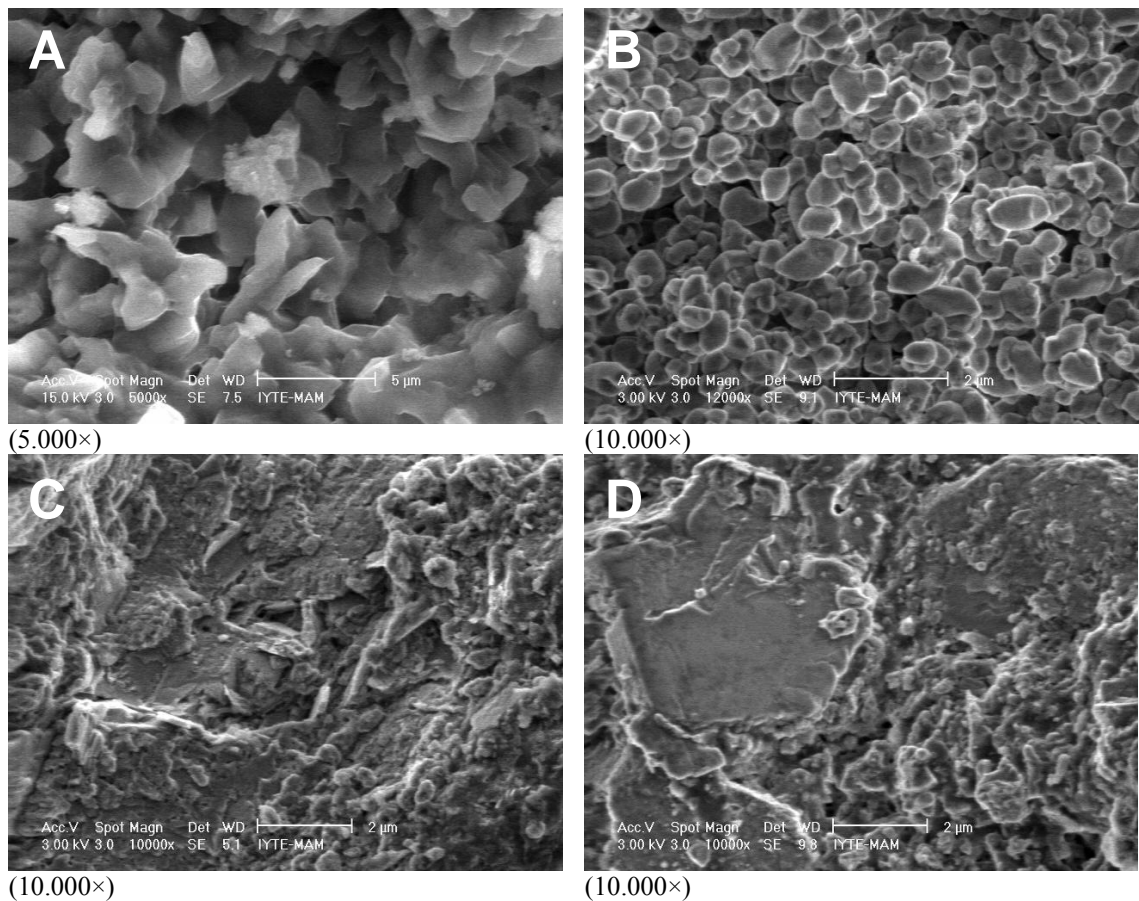
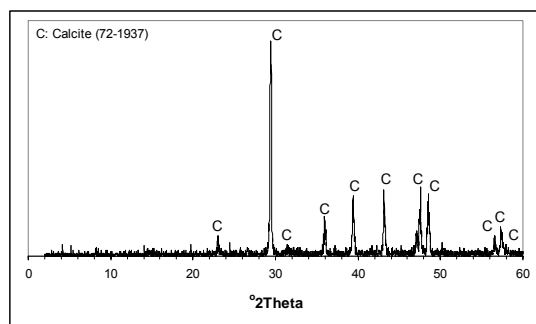**Figure 4.44** SE images of microstructures of the white lump composed of lime containing silica at high ratios (A), the one composed of high-calcium lime (B), and calcareous aggregates (C, D).

4.6.2.2. Mineralogical and Chemical Compositions and Microstructural Properties of Fine Aggregates

Fine aggregates (less than 53 μm), which were mainly composed of quartz, albite, potassium feldspar, muscovite and hematite minerals, had almost similar mineralogical compositions with their coarse aggregates (Figures 4.45-4.49). However, broad band observed between 20-30° in the XRD patterns of the fine aggregates of all brick masonry and some stone masonry mortars (Ur.He.s. and Se.Ul.s.) indicated the presence of amorphous materials at high proportions (Figuress 4.45-4.49). Therefore, better pozzolanicity of these fine aggregates than their coarse aggregates could be explained by the presence of these amorphous materials at high proportions in these fine aggregates.
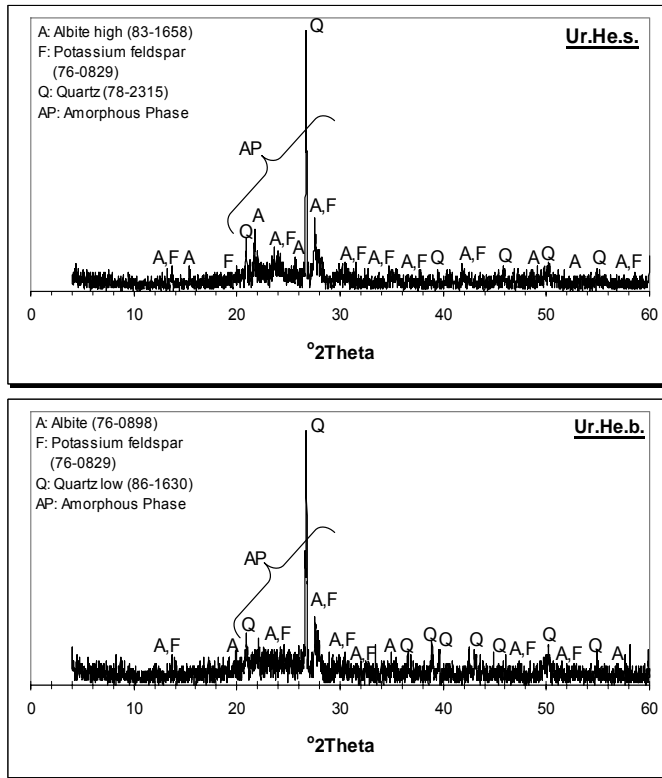
Figure 4.45 XRD patterns of the fine aggregates used in the stone masonry mortar of Ur.He.s. and brick masonry mortar of Ur.He.b.
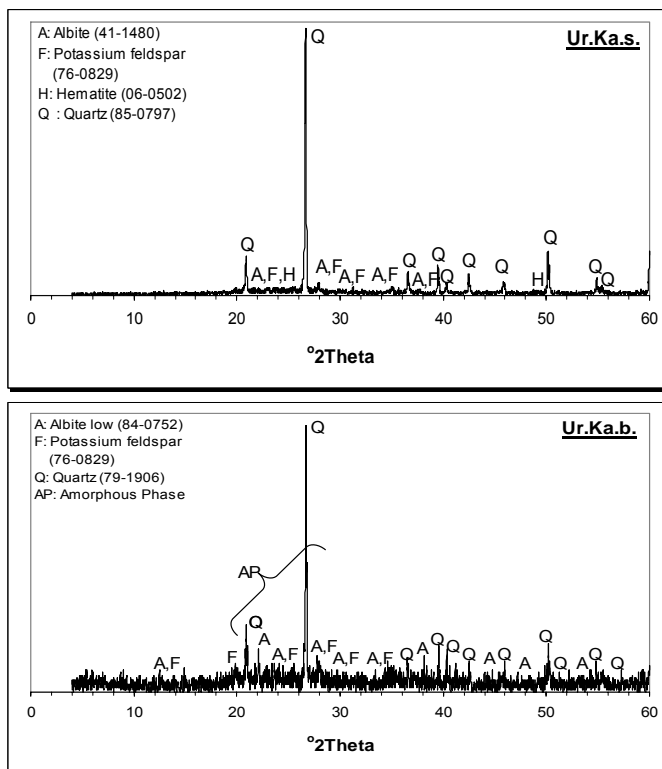
Figure 4.46 XRD patterns of the fine aggregates used in the stone masonry mortar of Ur.Ka.s. and brick masonry mortar of Ur.Ka.b.
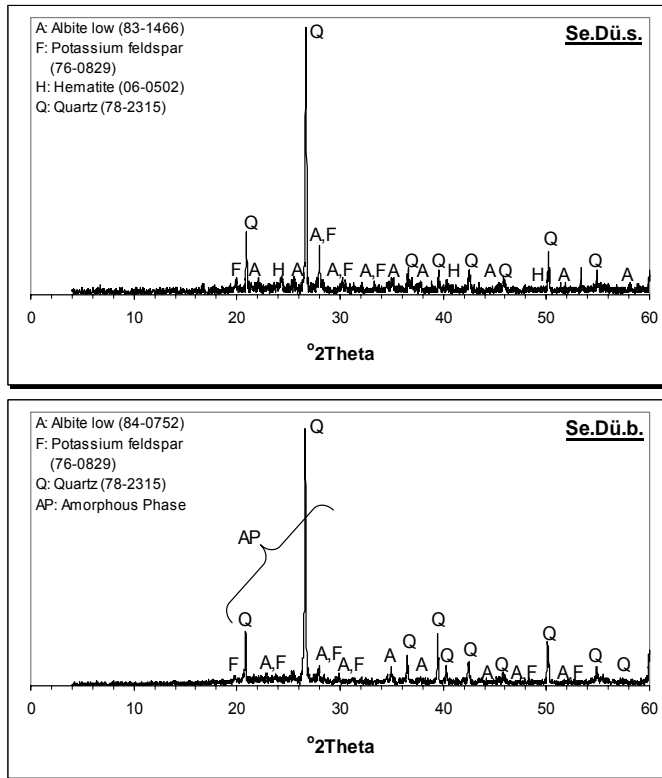
Figure 4.47 XRD patterns of the fine aggregates used in the stone masonry mortar of Se.Dü.s. and brick masonry mortar of Se.Dü.b.
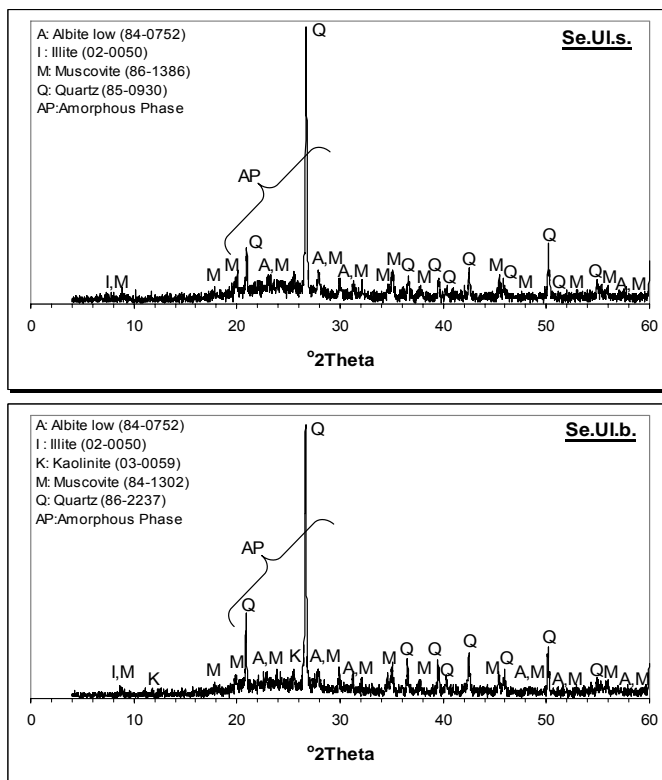
Figure 4.48 XRD patterns of the fine aggregates used in the stone masonry mortar of Se.Ul.s. and brick masonry mortar of Se.Ul.b.
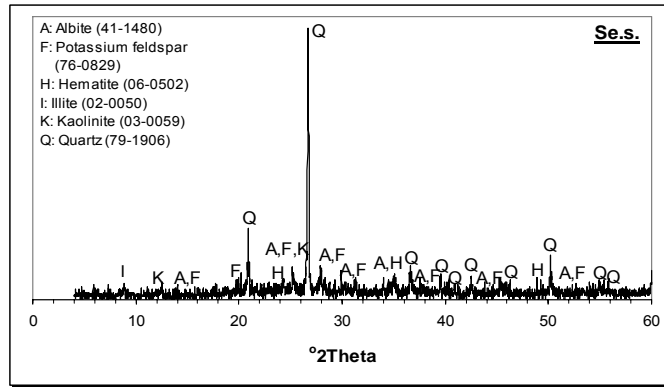
Figure 4.49 XRD pattern of the fine aggregates used in the stone masonry mortar of Se.s.

SEM-EDS analysis indicated that fine aggregates with high pozzolanic activity contained high proportions of silicon dioxide ranging between 82.5-92.5 % and aluminium oxide ranging between 5.64-17.15 % (Table 4.5). The silicon dioxide and aluminium oxide percents in the aggregates of He.s., He.b. and Ka.b. were higher than the ones of the aggregates of Ul.s., Ul.b. and Dü.b. Apart from silicon dioxide and aluminium oxide, the fine aggregates contained sodium oxide, potassium oxide and magnesium oxide in less proportion (Table 4.5). Only the fine aggregates (Se.s., Se.Dü.s. and Ur.Ka.s.) having the lowest pozzolanic activity contained iron oxide ranging between 11.49 % and 16.32 % (Table 4.5). Amount of silicon dioxide and aluminium oxide in these fine aggregates is also lower than the one of the pozzolanic aggregtaes. Low pozzolanic activity of these fine aggregates may be explained by the presence of high amounts of iron oxide and less amount of silicon dioxide and aluminium oxide.

Table 4.5 Elemental compositions of fine aggregates used in the mortars.

Fine aggregates	Elemental Composition (%)					
(less than 53μm)	Na_2O	MgO	Al_2O_3	SiO_2	K_2O	Fe_2O_3
Se.s.f-agg.	2.3	4.0	15.8	60.3	2.0	15.6
Se.Dü.s.f-agg.	2.4	3.7	17.2	58.4	2.0	16.3
Se.Ul.s.f-agg.	1.0	*	10.0	87.1	1.9	*
Ur.He.s.f-agg.	1.3	1.0	6.7	89.6	1.4	*
Ur.Ka.s.f-agg.	1.4	2.4	13.8	69.1	1.8	11.5
Se.Dü.b.f-agg.	0.7	*	8.7	89.2	1.4	*
Se.Ul.b.f-agg.	0.8	1.3	12.9	82.5	2.4	*
Ur.He.b.f-agg.	1.1	*	5.6	92.5	0.8	*
Ur.Ka.b.f-agg.	1.0	*	8.0	90.0	1.0	*
*: *not detected*						
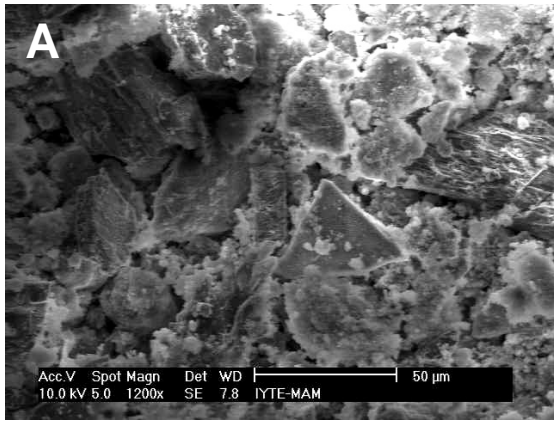
Less porous fine aggregates (1200×).
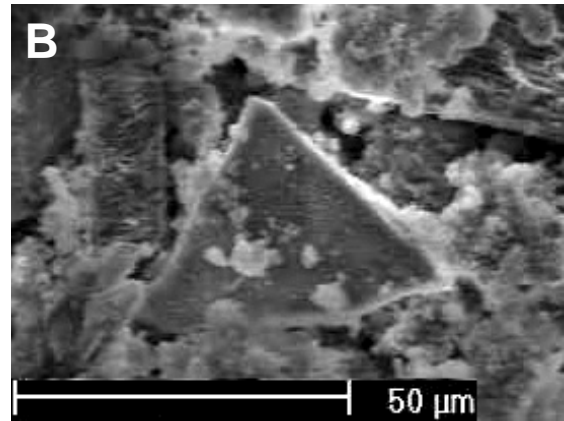
Less porous fine aggregates.
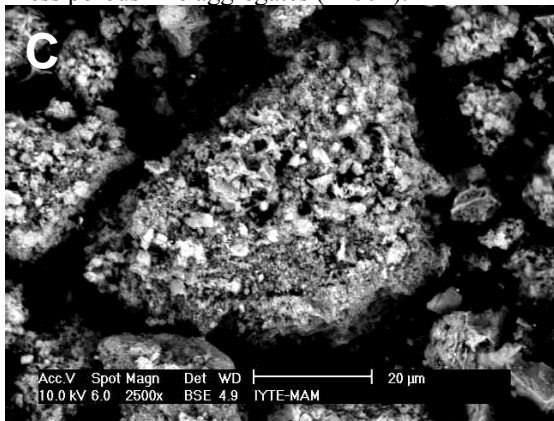
Porous fine aggregates (2500×).
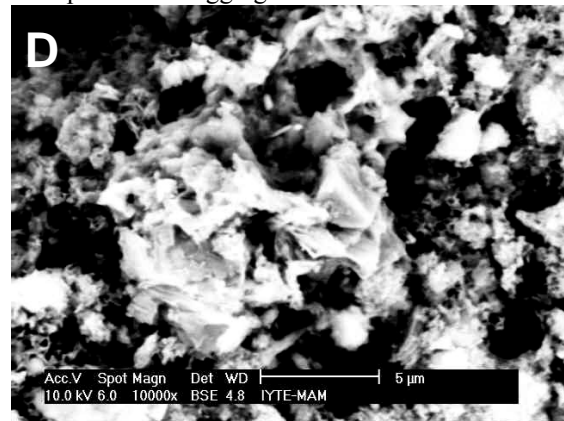
Small pores in the fine aggregates (10.000×).
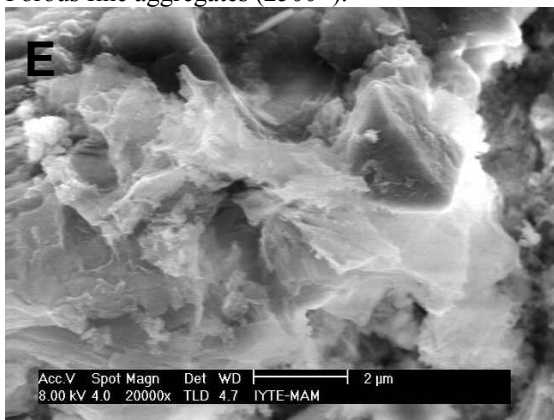
(20.000×)
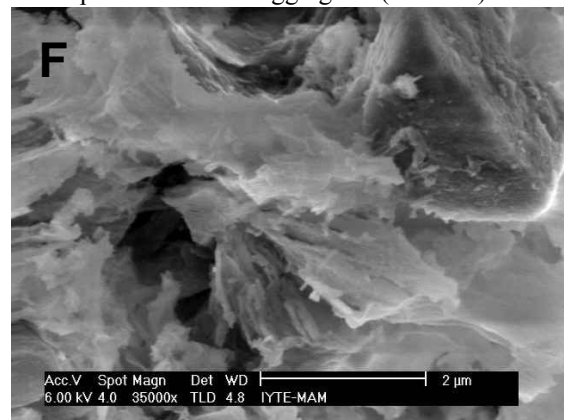
(35.000×)
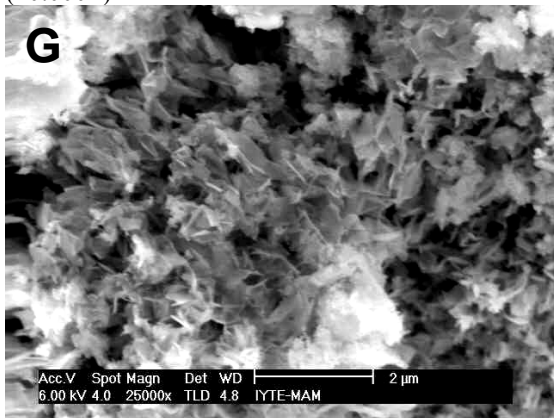
(25.000×)
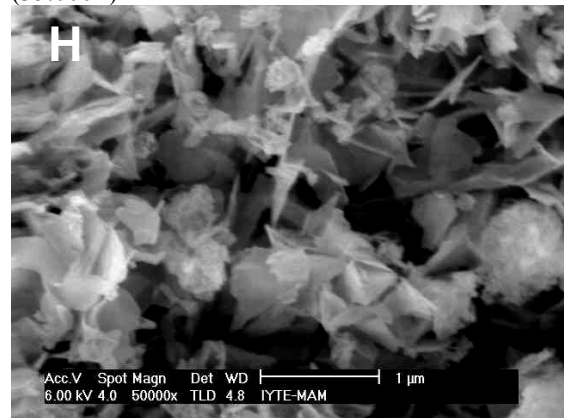
(50.000×)

Figure 4.50 SE images of microstructure of pozzolanic fine aggregates (less than 53µm).

Figure 4.50 shows SEM images of microstructures of fine aggregates. Porous and non porous fine aggregates were observed in the SEM images (Figure 4.50-A, B, C). Porous aggregates have small size of pores ranging between 1 and 4 micron (Figure 4.50-D). The crystals were composed of blade edges (Figure 4.50-E, F). This provided large specific surface area (Figure 4.50-G, H) so that the fine aggregates were tightly adhered to the lime and high amounts of pozzolanic reaction products were produced.

All the coarse aggregates belonging to each stone and brick mortar sample had almost similar mineralogical and chemical compositions, and colour properties with their fine aggregates. In spite of these similarities, most of the fine aggregates are richer in amorphous materials than their coarse aggregates observed in XRD analyses. Amount of silicon dioxide and aluminium oxide in the fine aggregates is also higher than the one of their coarse aggregates. This indicates why these fine aggregates had higher pozzolanic activity than their coarse aggregates. Considering these results, the pozzolanic fine aggregates could be present in the same source with the coarse aggregates. This is different from pozzolanic fine aggregate usage in mortars of some Seljuk buildings since these fine aggregates obtained from a different source were added in the coarse aggregates (Tunçoku 2001).

Having regard to mineralogical and chemical compositions, and colour properties of aggregates, three different aggregate types were identified in the mortars. The first aggregate type is primarily composed of quartz, albite, muscovite and potassium feldspar minerals, has high proportions of silicon dioxide and aluminium oxide and is grey and white in colour. Aggregates of this type were used in the mortars of Se.Ul.s, Se.Ul.b and Se.Dü.b. The second aggregate type consists primarily of quartz, albite and potassium feldspar minerals, has high proportions of silicon dioxide and aluminium oxide and is white, grey and light brown in colour. Such aggregates were used in the mortars of Ur.He.s., Ur.He.b. and Ur.Ka.b. The third aggregate type composed of primarily quartz, albite, hematite and potassium feldspar minerals has high amounts of iron oxide and is brown and grey in colour. The aggregates of this type were used in the stone masonry mortars of Se.s., Se.Dü.s. and Ur.Ka.s. These results indicate that while source of the first aggregate type can be in Seferihisar region, source of the second aggregate type is probably in Urla region. The third aggregate type can be from a source near to these two towns. Moreover, the first and second aggregate types are the ones whose coarse and fine aggregates have good pozzolanicity.

4.6.3. Mineralogical and Chemical Compositions and Microstructural Properties of Mortar Matrices

Mineralogical compositions of the mortar matrices composed of lime and fine aggregates were determined by XRD analysis in order to observe possible hydraulic reaction products occurred among pozzolanic fine aggregates and lime. Calcite and quartz as the primary minerals, and muscovite and albite as the secondary minerals were observed in their XRD patterns (Figures 4.51-4.55). Calcite originated from the carbonated lime, and other minerals of quartz, muscovite and albite from the fine aggregates. The hydraulic reaction products between lime and pozzolanic aggregates were not observed in the XRD patterns. This may be due to overlapping of principal peaks of calcite and the hydraulic reaction products.
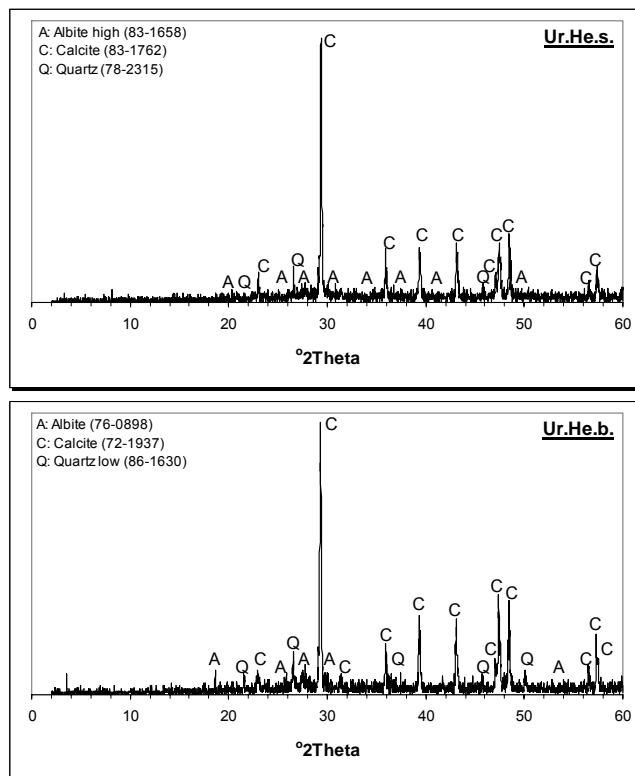
Figure 4.51 XRD patterns of the mortar matrices of the stone masonry mortar of Ur.He.s. and brick masonry mortar of Ur.He.b.
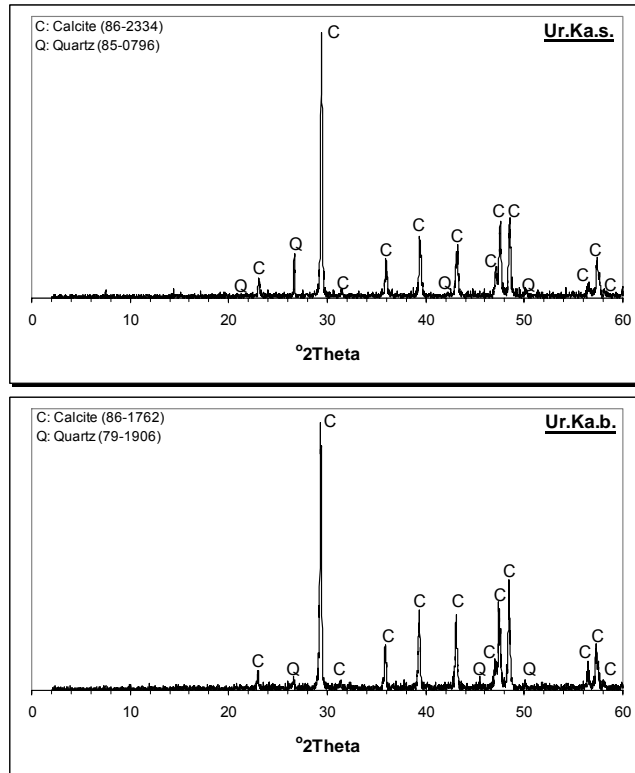
Figure 4.52 XRD patterns of the mortar matrices of the stone masonry mortar of Ur.Ka.s. and brick masonry mortar of Ur.Ka.b.
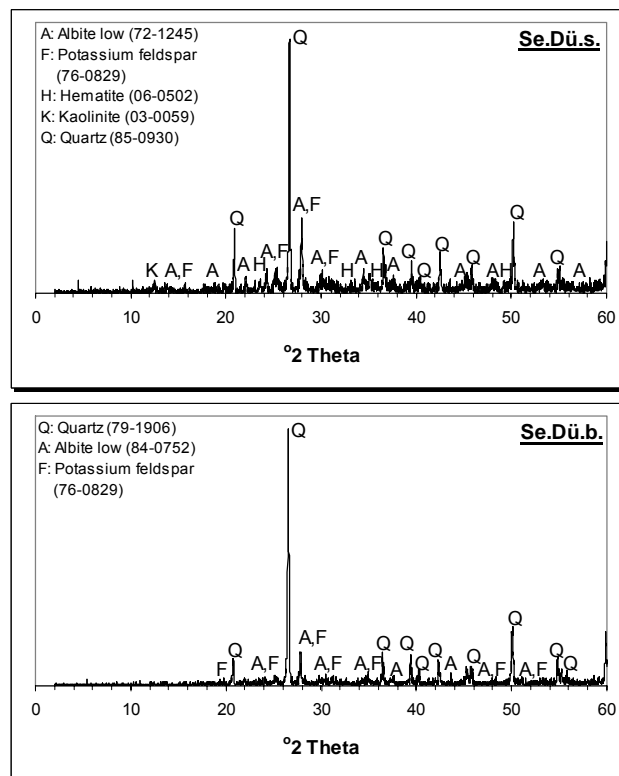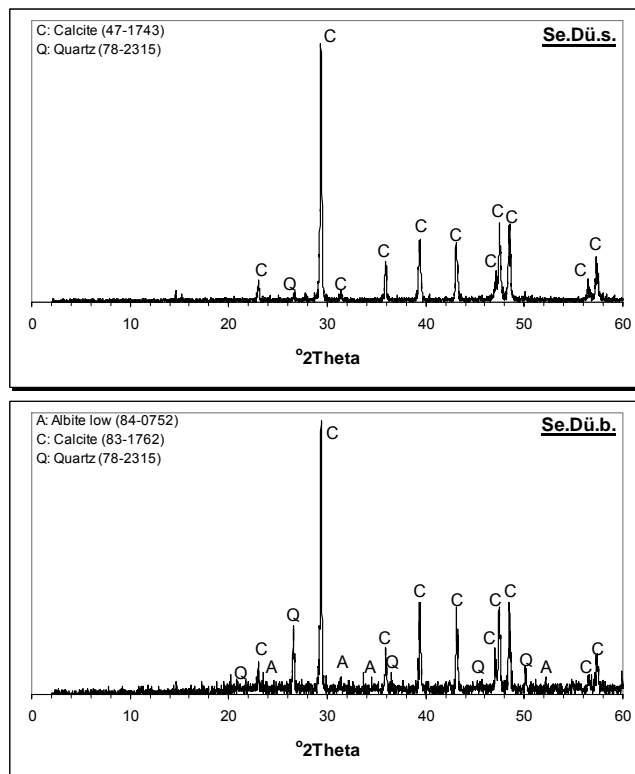

Figure 4.53 XRD patterns of the mortar matrices of the stone masonry mortar of Se.Dü.s. and brick masonry mortar of Se.Dü.b.
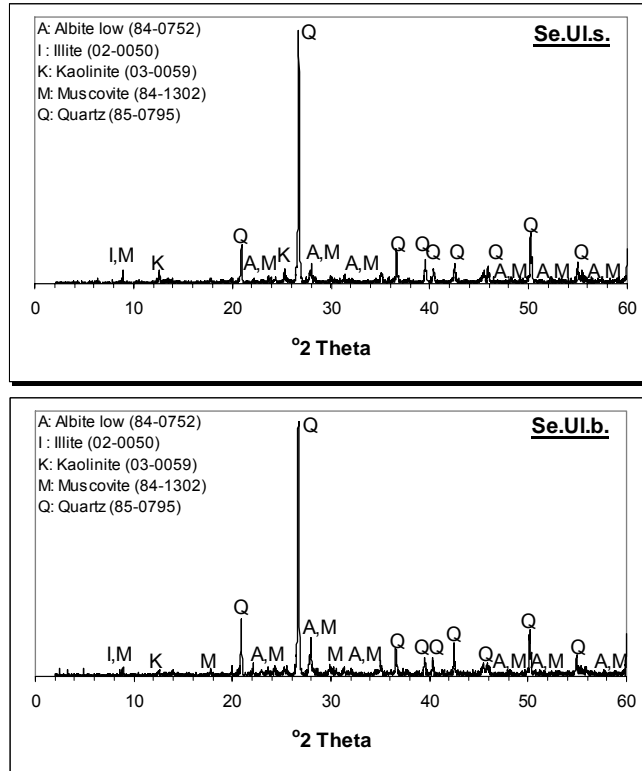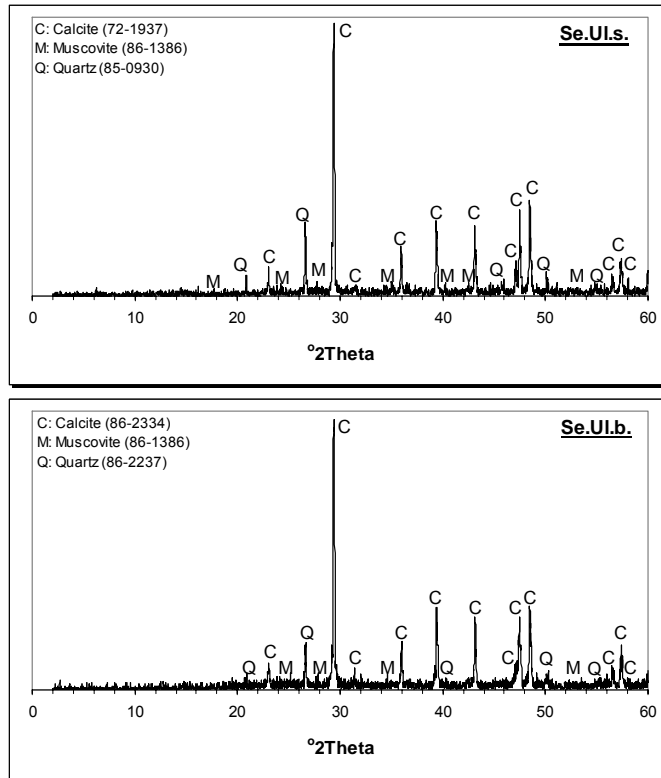
Figure 4.54 XRD patterns of the mortar matrices of the stone masonry mortar of Se.Ul.s. and brick masonry mortar of Se.Ul.b.
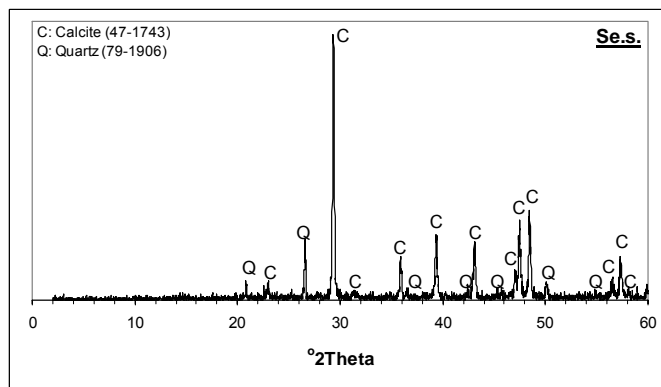

**Figure 4.55** XRD pattern of the mortar matrices of the stone masonry mortar of Se.s.

Aggregates of stone and brick masonry mortars except for the ones of Se.s., Ka.s. and Dü.s. were firmly embedded in mortar matrices (Figures 4.56-4.71). This may be due to well mixing process of aggregates with lime and pozzolanic properties of aggregates. This consequently provided good adhesion of the aggregates with lime.
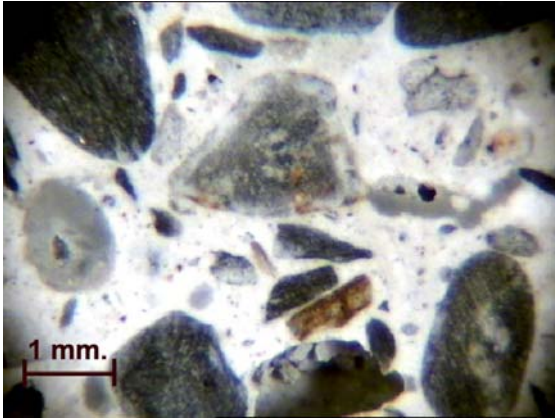
Figure 4.56 Stereo microscope image showing good adhesion of the aggregates with lime (Se.Ul.b.).
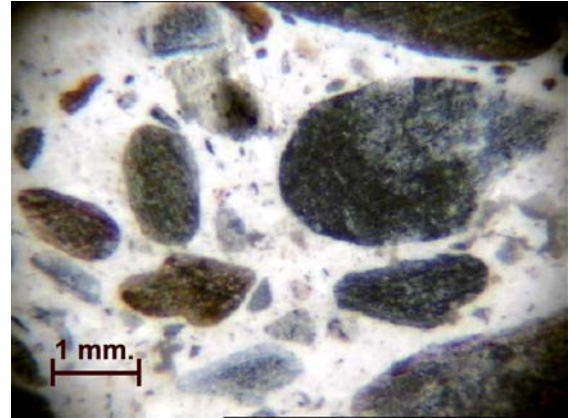
Figure 4.57 Stereo microscope image showing good adhesion of the aggregates with lime (Se.Ul.s.).
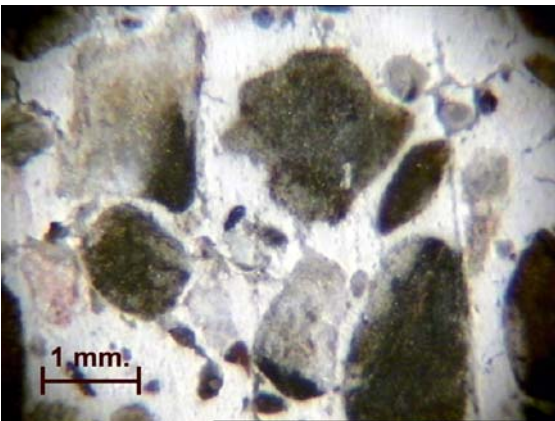
Figure 4.58 Stereo microscope image showing good adhesion of the aggregates with lime (Se.Dü.b.).
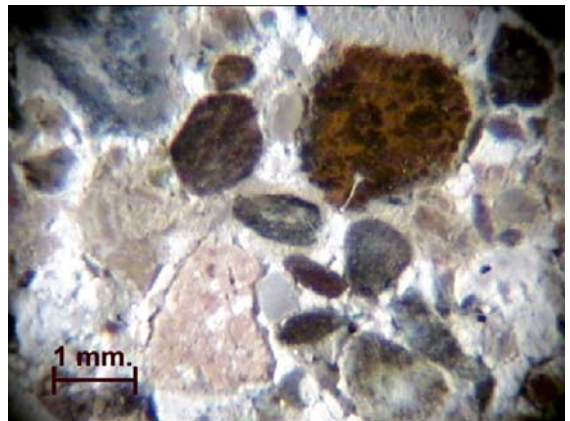
Figure 4.59 Stereo microscope image showing poor adhesion of the aggregates with lime (Se.Dü.s.).
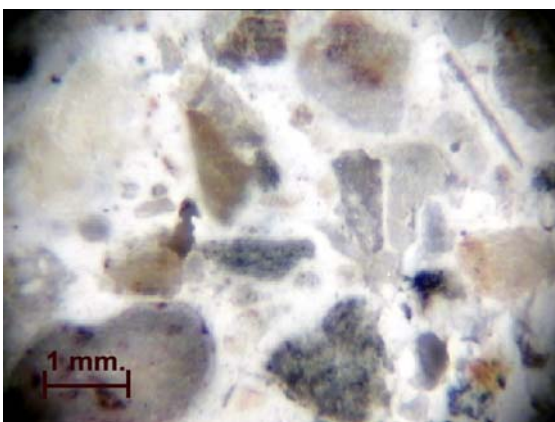
Figure 4.60 Stereo microscope image showing good adhesion of the aggregates with lime (Ur.He.b.).
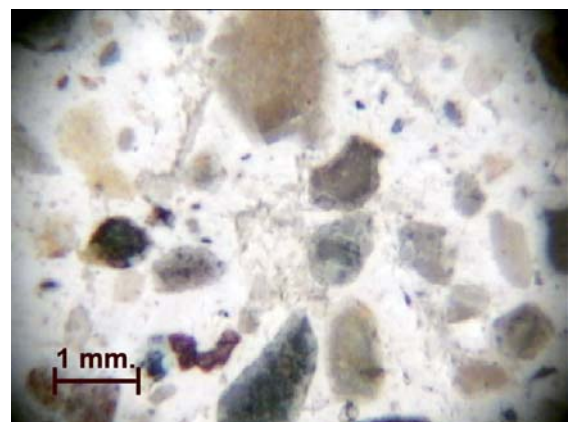
Figure 4.61 Stereo microscope image showing good adhesion of the aggregates with lime (Ur.He.s.).
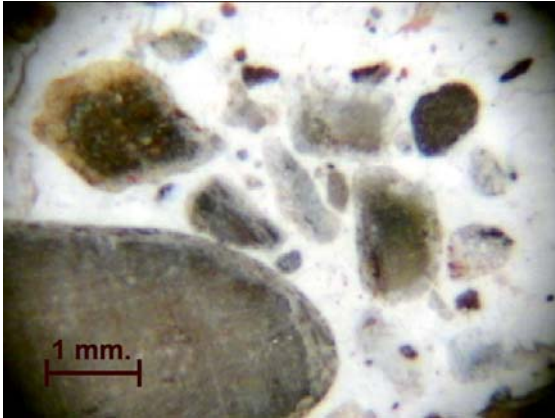
Figure 4.62 Stereo microscope image showing good adhesion of the aggregates with lime (Ur.Ka.b.).
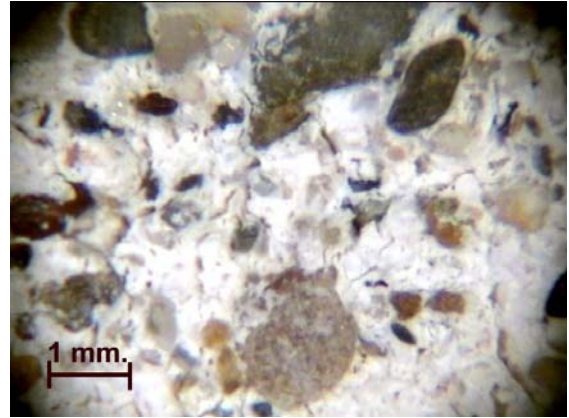
Figure 4.63 Stereo microscope image showing poor adhesion of the aggregates with lime (Ur.Ka.s.).
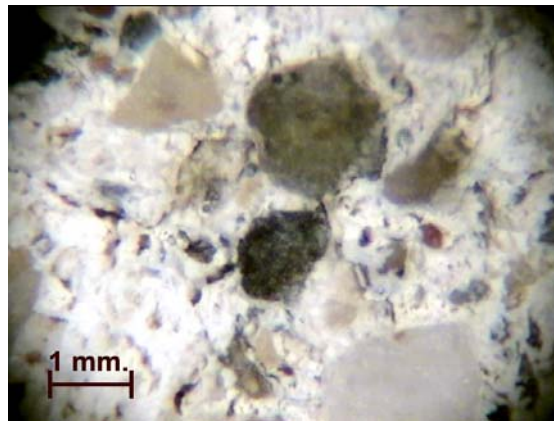
Figure 4.64 Stereo microscope image showing poor adhesionof the aggregates with lime (Se.s.).
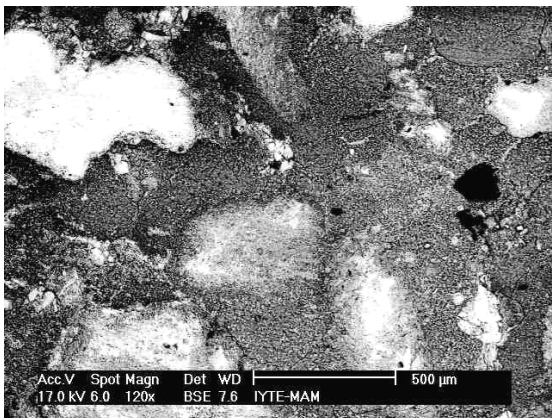
Figure 4.65 BSE image (120×) showing good adhesion of the aggregates with the mortar matrix (Ur.He.b).
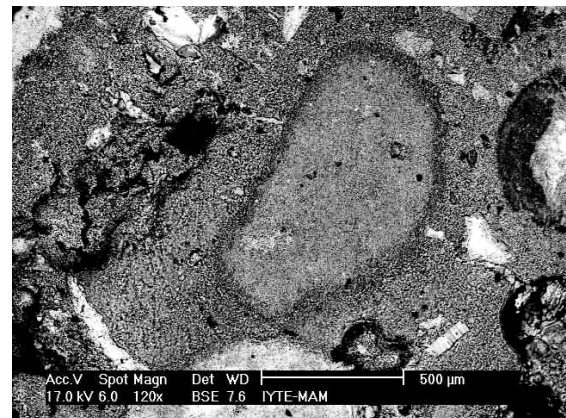
Figure 4.66 BSE image (120×) showing good adhesion of the aggregates with the mortar matrix (Ur.He.s).
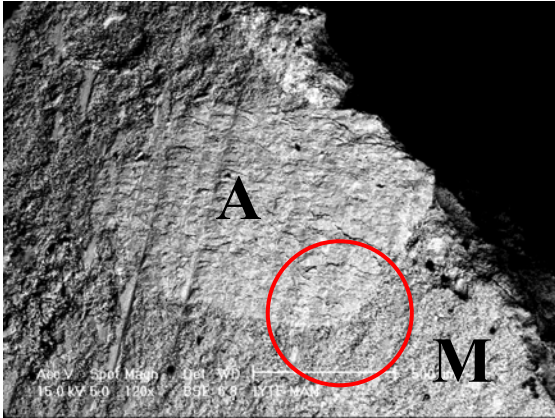
Figure 4.67 BSE image (80×) showing good adhesion of an aggregate (A) with the mortar matrix (M) (Se.Ul.s.).

Figure 4.68 Detailed BSE image (500×) of the left-handed image, showing how well the aggregate (A) was adhered to the mortar matrix (M).
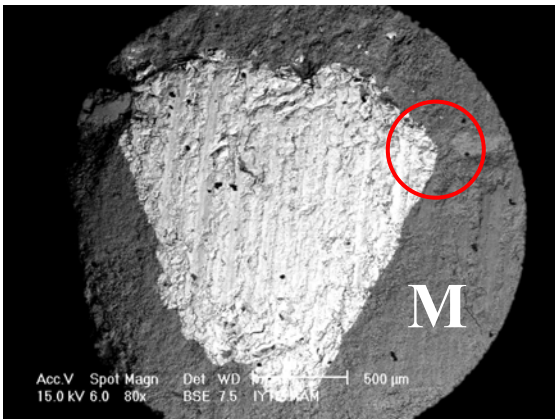
Figure 4.69 BSE image (80×) showing good adhesion of an aggregate (A) with the mortar matrix (M) (Se.Ul.b.).
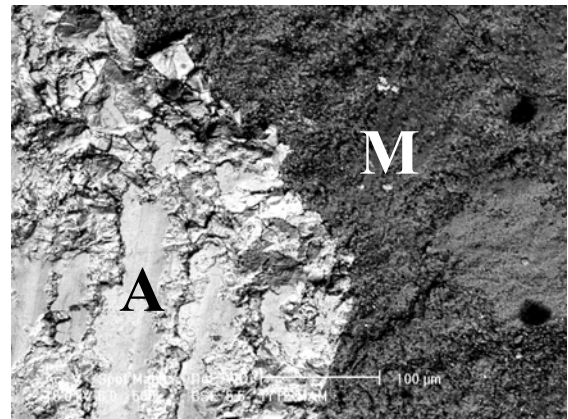
Figure 4.70 Detailed BSE image (500×) of the left-handed image, showing how well the aggregate (A) was adhered to the mortar matrix (M).
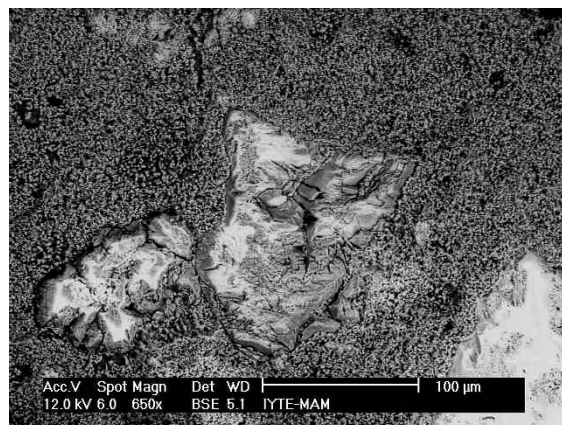
Figure 4.71 BSE image (650×) showing poor adhesion of the aggregates with the mortar matrix (Se.Dü.s.).

Microstructural characteristics and chemical compositions of interfaces observed in lime mortars having good-adhered aggregates (1180–53 micron) with lime were determined by SEM-EDS analyses (Figure 4.72 and 4.73). SEM analyses indicated that these interfaces were thin irregular boundaries (up to 50 micron) being free from pores and cracks (Figure 4.73). SEM-EDS analyses recorded calcium (Ca), silica (Si) and alumina (Al) elements in these interfaces (Figure 4.74). From the aggregates towards the mortar matrix, calcium content increased while silica and alumina contents decreased (Figure 4.74). In the mortar matrices with fine aggregates, calcium reached its highest content. Higher silica and alumina contents at the interfaces than the mortar matrices could be due to pozzolanic reactions occurred among the lime and pozzolanic aggregates. This most probably imparted high strength properties to these mortars (Lea 1940, Moropoulou et al. 2000b, Moropoulou et al. 2002a).
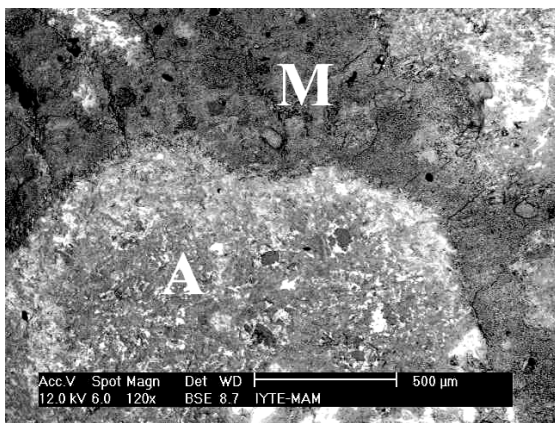
(120×)

Figure 4.72 BSE image showing good adhesion between the aggregate (A) and mortar matrix (M) (Se.Dü.b.).
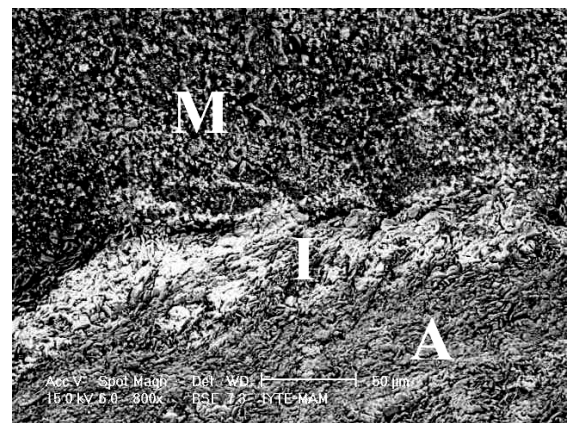
(800×)

Figure 4.73 BSE image of the interface (I) between the aggregate (A) and mortar matrix (M) (Se.Dü.b.).
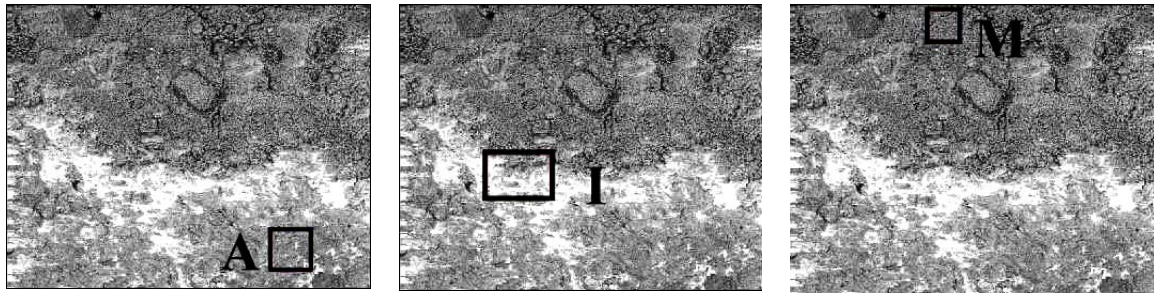
Element	%	Element	%	Element	%
O	48.0	O	49.4	O	52.8
Na	4.4	Na	3.7	Mg	2.9
Al	9.7	Al	8.5	Al	3.8
Si	31.4	Si	25.6	Si	14.5
K	4.3	K	3.2	Cl	0.9
Ca	2.2	Ca	8.1	Ca	25.1
Total	100.0	Mg	1.5	Total	100.0
		Total	100.0		

Figure 4.74 BSE images (350×) and elemental composition (%) of the aggregate (A), interface (I) and lime matrix (M) of the stone masonry mortar of Ur.He.s.

Microstructural properties of mortar matrices with fine aggregates (less than 53 micron) were determined by SEM analysis. The mortar matrices showed homogeneous microstructure with their fine pores whose sizes ranged between 2 μm and 10 μm (Figure 4.75). It was determined by phase analysis of SEM images that the fine pores commonly formed 31-43 % of the whole matrices (Figures 4.76, 4.77 and 4.78). These homogenous microstructures of the mortar matrices indicated a well mixing process of the lime with the pozzolanic fine aggregates.
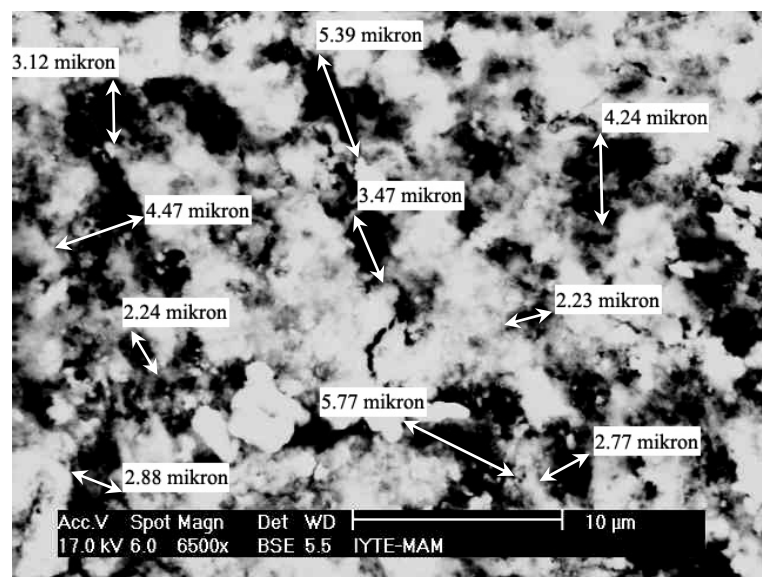
Figure 4.75 BSE image (6500×) of the pore sizes of the mortar matrix of the brick masonry mortar of Ur.He.b.
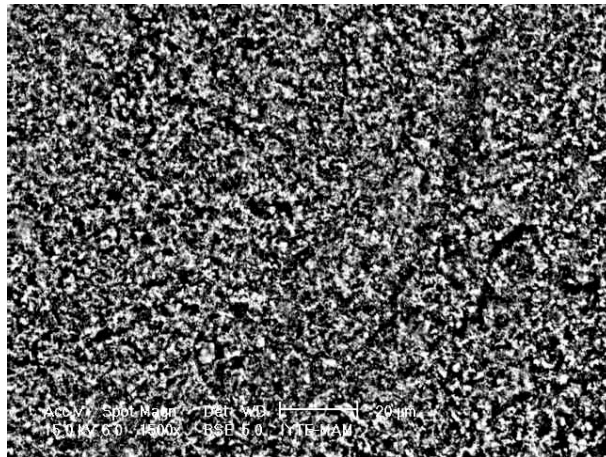
Oxide	%
Al_2O_3	5.1
SiO_2	52.5
CaO	42.4
Total	100.0

Figure 4.76 BSE image (1500×) and elemental composition (%) of the mortar matrix of the brick masonry mortar of Se.Dü.b.
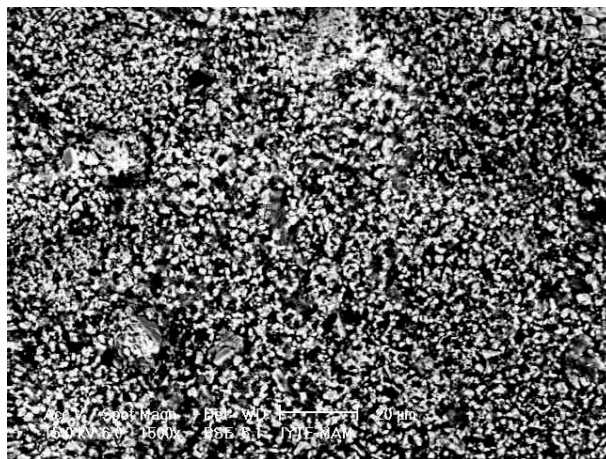
Oxide	%
Al_2O_3	9.7
SiO_2	31.3
CaO	56.4
MgO	2.6
Total	100.0

Figure 4.77 BSE image (1500×) and elemental composition (%) of the mortar matrix of the brick masonry mortar of Ur.He.b.
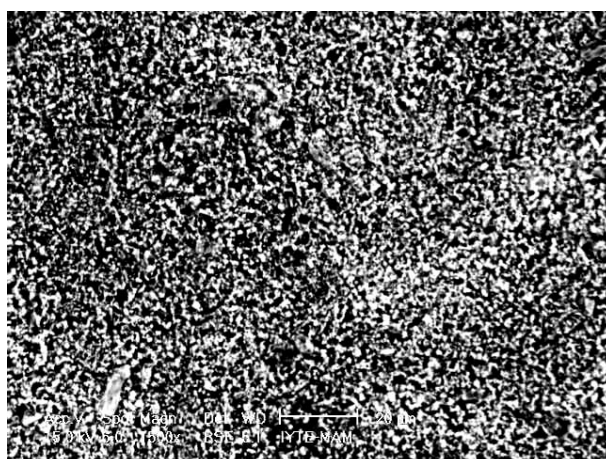
Oxide	%
Al_2O_3	9.3
SiO_2	40.1
CaO	44.9
MgO	5.7
Total	100.0

Figure 4.78 BSE image (1500×) and elemental composition (%) of the mortar matrix of the stone masonry mortar of Ur.He.s.

SEM-EDS analysis indicated that mortar matrices had calcium oxide contents ranging between 34 % and 56 %, silicon dioxide contents between 31 % and 58 %, and aluminium oxide contents between 5 % and 10 % (Figures 4.76-4.80). Silica in the mortar matrices containing high-calcium lime could be derived from pozzolanic fine aggregates (less than 53μm) containing silica. However, high silica in the other mortar matrices could be attributed to the presence of silica in their lime binders and also pozzolanic fine aggregates (less than 53μm) containing silica.

Oxide	%
Al_2O_3	7.3
SiO_2	58.4
CaO	34.3
Total	100.0
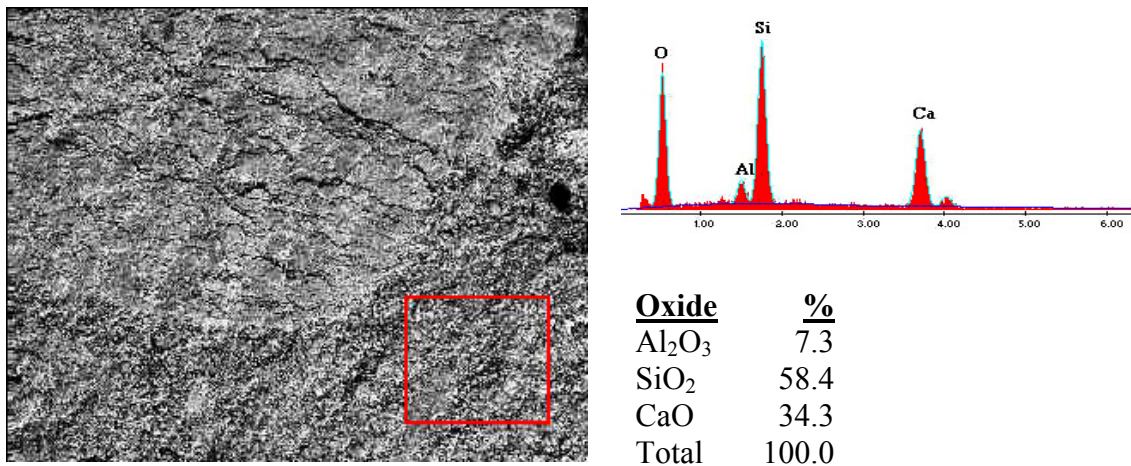
Figure 4.79 BSE image, EDX spectrum and elemental composition (%) of the mortar matrix of the stone masonry mortar of Se.Ul.s.

Oxide	%
Al_2O_3	6.3
SiO_2	52.5
CaO	41.2
Total	100.0
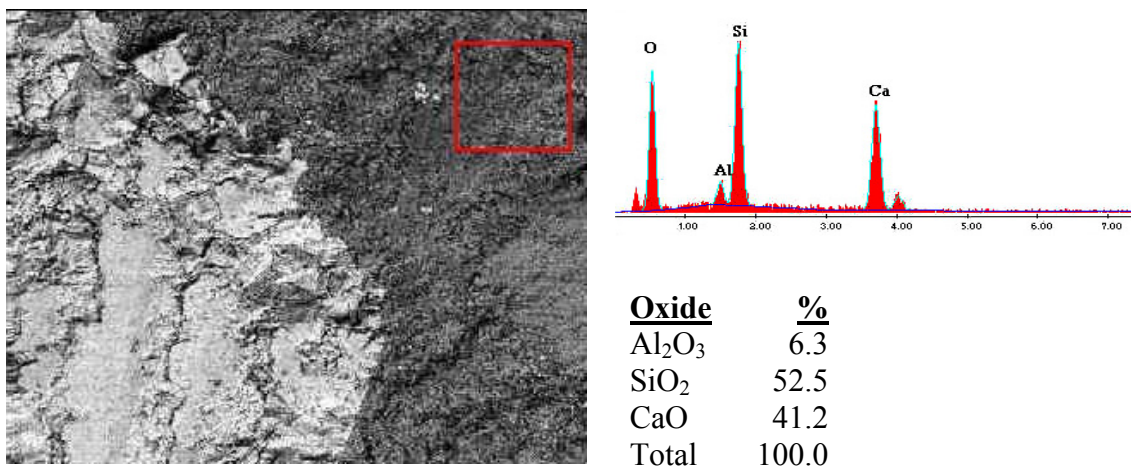
Figure 4.80 BSE image, EDX spectrum and elemental composition (%) of the mortar matrix of the brick masonry mortar of Se.Ul.b.

SEM analysis recorded images of gel formations in mortar matrices of all brick masonry mortars and some stone masonry mortars (Se.Ul.s. and Ur.He.s.) (Figure 4.81). This may indicate the presence of hydraulic reaction products (C-S-H, C-A-H, etc.)

occurred among lime and pozzolanic aggregates. However, XRD analysis could not detect any peaks of the hydraulic reaction products in the mortar matrices. This was most probably due to the fact that main peaks of hydraulic reaction products were overlapped with main peaks of calcite (Lewin 1981). Therefore, only calcite peaks could be recorded in the XRD patterns of these mortar matrices.

(20.000×)

(20.000×)

(50.000×)

(50.000×)

(50.000×)

(65.000×)
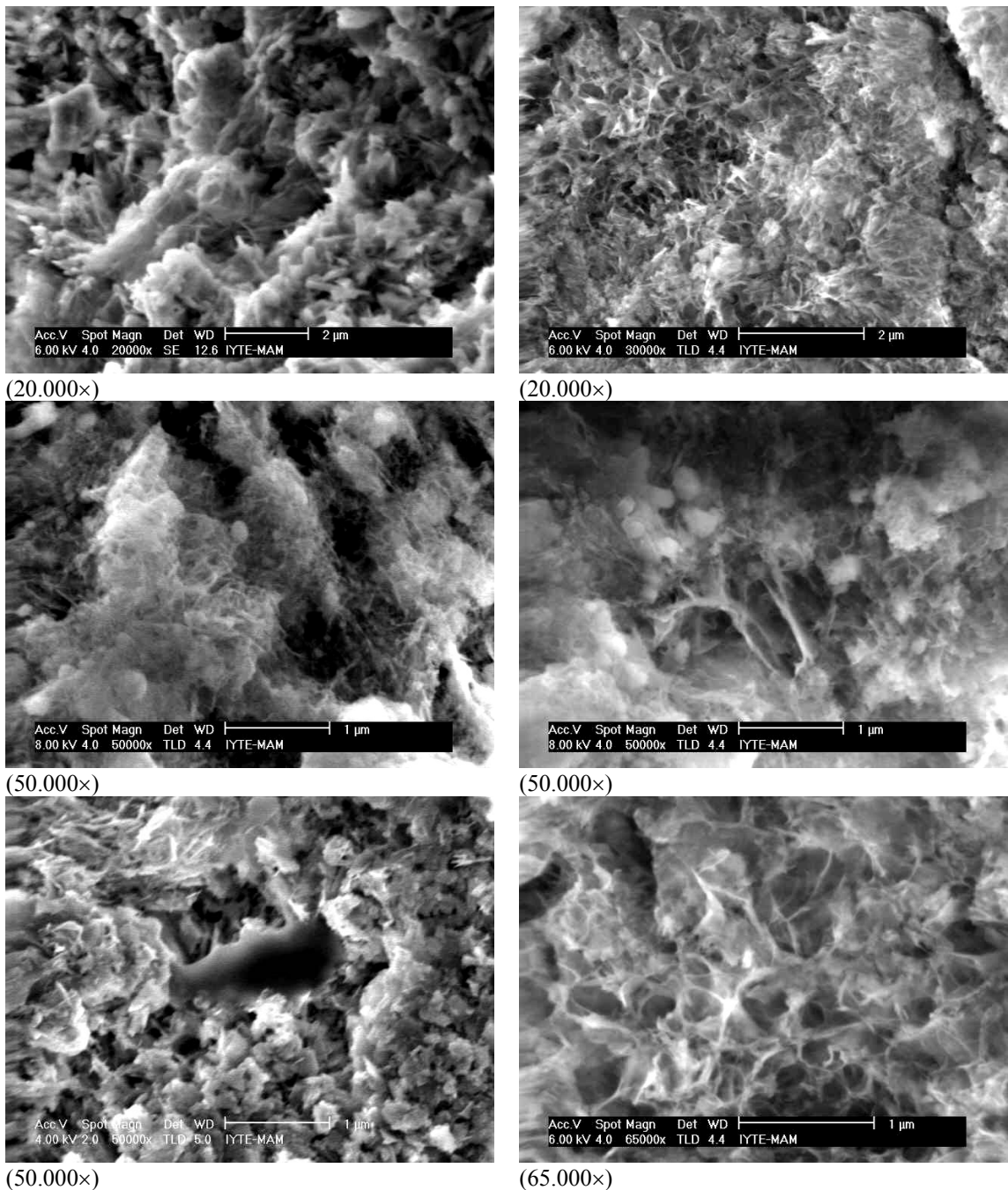
Figure 4.81 SE images of possible hydraulic reaction products within the mortar matrices of lime containing silica at high ratios mortars.

SEM images indicated that there were very fine cracks (1-5 micron) in mortar matrices with fine aggregates (less than 53μm) (Figure 4.82). This could be derived from the property of lime mortars being capable of producing many fine cracks which tolerate stresses and strains occurred in masonry (Davison 1976). Within these fine cracks and pores, fine calcite crystals were observed in SEM images (Figure 4.83). These fine calcite crystals were thought to precipitate either by a successive dissolution of carbonated lime or by carbonation of free lime by humid atmosphere of the bath and rain water permeating the masonry (Davison 1976, Holmes and Wingate 1997). This could indicate self-healing ability of the lime mortars, which contributes to survival of the masonry throughout years.
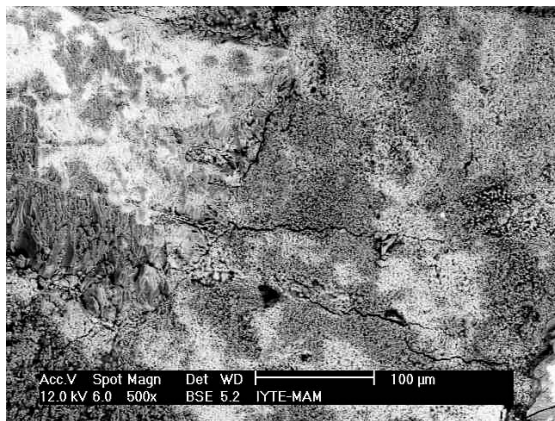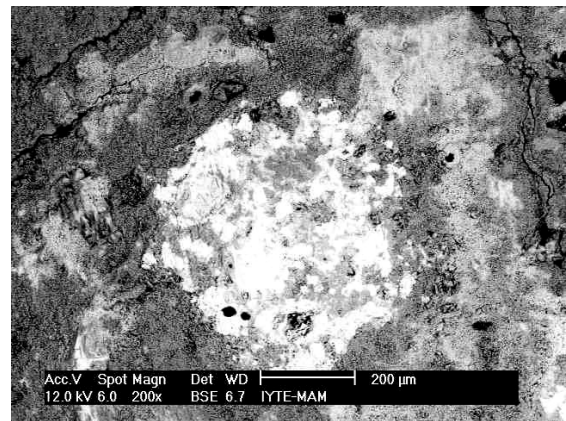
(500×)   (200×)

Figure 4.82 BSE images showing micro cracks in the mortar matrices.

(350×) (500×)

Element	%
C	20.2
O	50.1
Na	2.1
Al	2.7
Si	7.0
Ca	17.9
Total	100.0

(2500×)
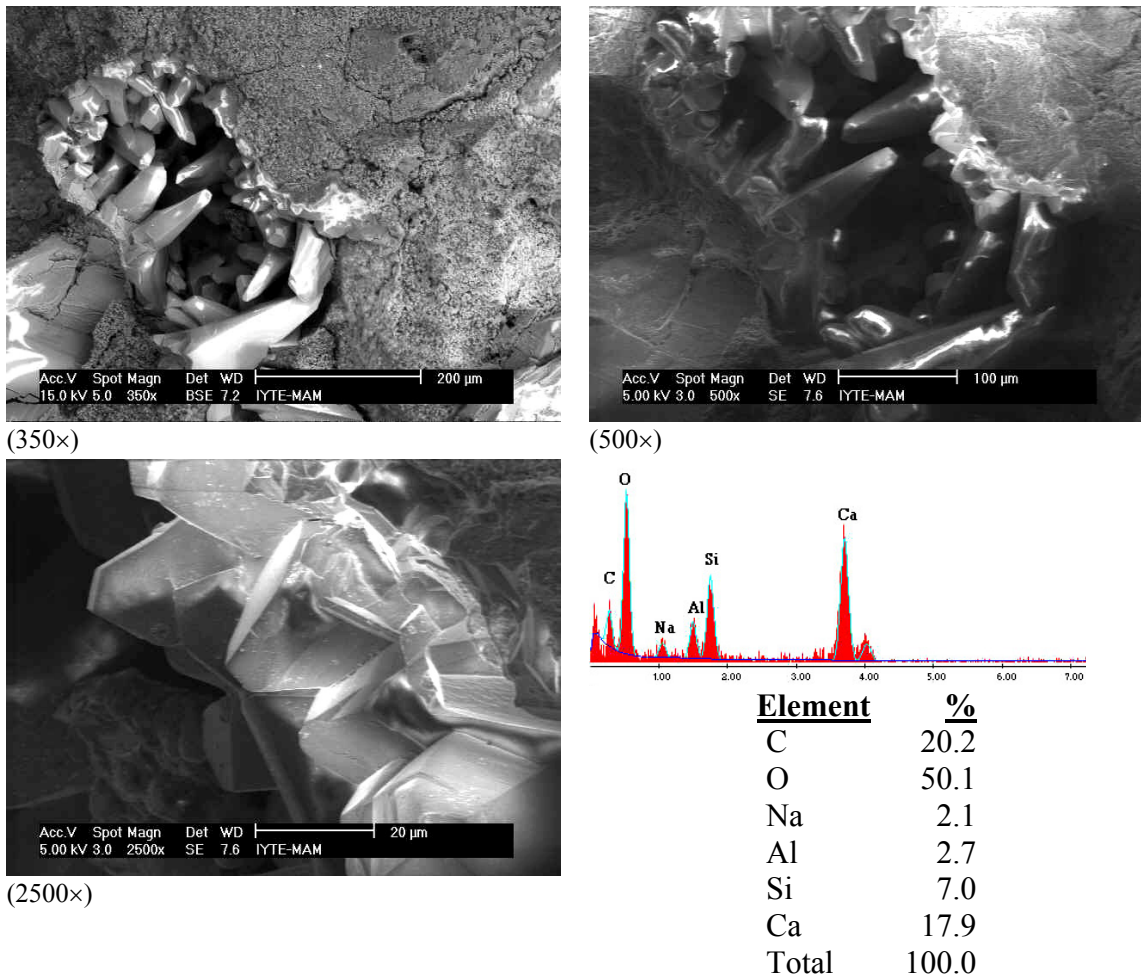
Figure 4.83 BSE images, EDX spectrum and elemental composition (%) of the calcite crystals precipitated within the pore.

4.7. Hydraulicity of Mortars by TGA

Thermogravimetric analyses (TGA) were carried out in order to evaluate hydraulic character of mortars. Percentages of weight losses at temperatures between $200^{\circ}C$ and $600^{\circ}C$, and temperatures over $600^{\circ}C$ were determined. Weight loss at the temperatures between $200^{\circ}C$ and $600^{\circ}C$ was mainly due to loss of structurally bound water (H_2O) of hydraulic reaction products (C-S-H, C-A-H, etc.) (Bakolas et al. 1998, Moropoulou et al. 2000b). Weight loss at the temperatures over $600^{\circ}C$ was mainly attributed to the release of carbon dioxide gas (CO_2) during the decomposition of calcium carbonates (Bakolas et al. 1998, Moropoulou et al. 2000b).

Thermal analysis results of several lime mortars from different periods revealed the results that non-lime containing silica at high ratios mortars commonly contained CO_2 over 30 % and structurally bound water (H_2O) lower than 3 %. However, in lime containing silica at high ratios mortars, CO_2 content was less than 30 % and H_2O

content more than 3 % (Maravelaki-Kalaitzaki et al. 2002, Moropoulou et al. 2002a, Moropoulou et al. 2000b). Having regard to these results, hydraulicity of lime mortars was commonly evaluated by the ratio of CO_2/H_2O. This ratio varied between 1 and 10 for lime containing silica at high ratios mortars and between 10 and 35 for non-lime containing silica at high ratios mortars (Moropoulou et al. 2003, Maravelaki-Kalaitzaki et al. 2002a, Moropoulou et al. 2000b). The hydraulicity of the lime mortars corresponds to low ratio of CO_2/H_2O. Therefore, it could be deduced that there is an inverse relationship between the hydraulicity (CO_2/H_2O) and CO_2 %.

Stone masonry mortars of Se.s. and Ur.Ka.s. contained structurally bound water of 1.5 % and 3 % and carbon dioxide 30 % and 33 % respectively (Table 4.6, Figures 4.85 and 4.86). Their CO_2/H_2O ratios were over 10 (Table 4.6). Therefore, these two stone masonry mortars could be regarded as non-lime containing silica at high ratios mortars. However, rest of the stone masonry mortars and all brick masonry mortars had higher percents of structurally bound water ranging between 3-5 %, lower percents carbon dioxide ranging between 11-23 % and CO_2/H_2O ratios being less than 10 (Table 4.7, Figures 4.84-4.87). These results indicated that all brick masonry and some stone masonry mortars (Ur.He.s. and Se.Ul.s.) could be regarded as lime containing silica at high ratios mortars. The hydraulic character of these mortars could be mainly attributed to hydraulic reactions took place among pozzolanic coarse and fine aggregates and lime in the presence of water. Even though stone masonry mortar of Se.Dü.s. contained high calcium lime and aggregates with poor pozzolanicity, it had hydraulic character due to its CO_2/H_2O ratio being less than 10 (Table 4.6). Its hydraulic character could be due to organic matter that may be present in this mortar.

Table 4.6 Structurally bound water (H_2O) percents, carbon dioxide (CO_2) percents and CO_2/H_2O ratios of stone masonry mortars.

Sample	H_2O (%)	CO_2 (%)	CO_2/H_2O
Se.s.	1.55	29.67	19.14
Se.Dü.s.	2.01	17.36	8.63
Se.Ul.s.	2.03	12.27	6.04
Ur.He.s.	2.11	12.76	6.05
Ur.Ka.s.	3.15	32.56	10.34

Table 4.7 Structurally bound water (H_2O) percents, carbon dioxide (CO_2) percents and CO_2/H_2O ratios of brick masonry mortars.

Sample	H_2O (%)	CO_2 (%)	CO_2/H_2O
Se.Dü.b.	4.94	20.08	4.07
Se.Ul.b.	4.37	11.09	2.54
Ur.He.b.	4.88	19.83	4.06
Ur.Ka.b.	2.86	23.47	8.21
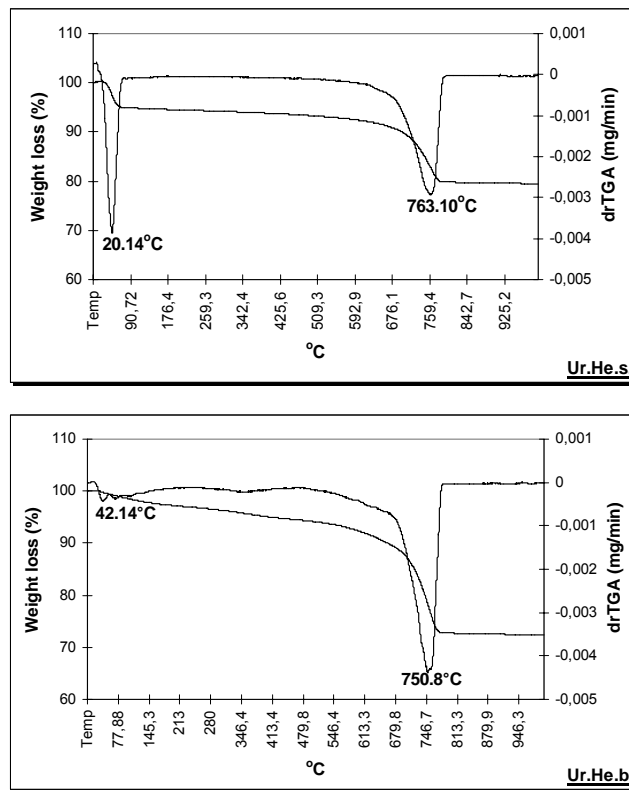
Figure 4.84 TGA-drTGA graph of the stone masonry mortar of Ur.He.s. and brick masonry mortar of Ur.He.b.
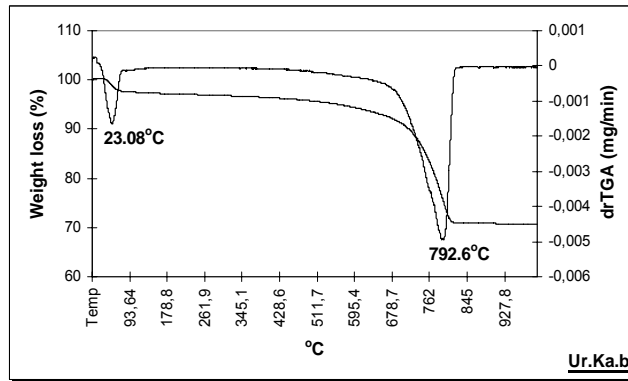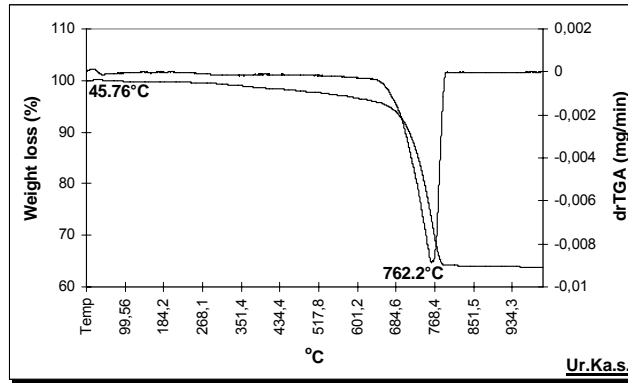
Figure 4.85 TGA-drTGA graph of the stone masonry mortar of Ur.Ka.s. and brick masonry mortar of Ur.Ka.b.
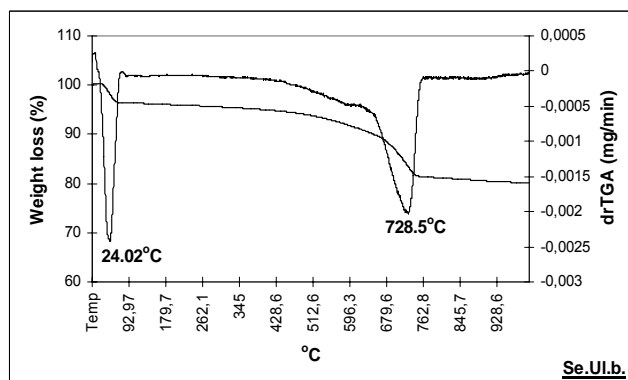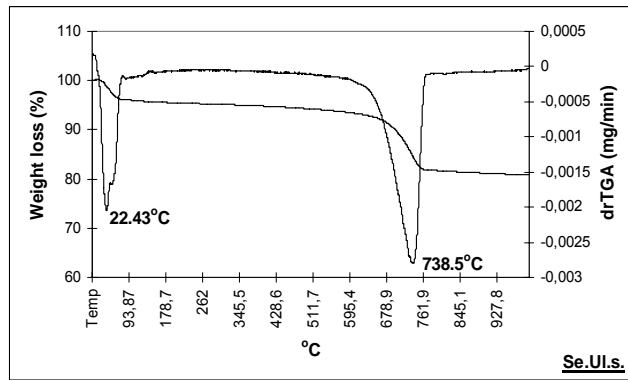
Figure 4.86 TGA-drTGA graph of the stone masonry mortar of Se.Ul.s. and brick masonry mortar of Se.Ul.b.
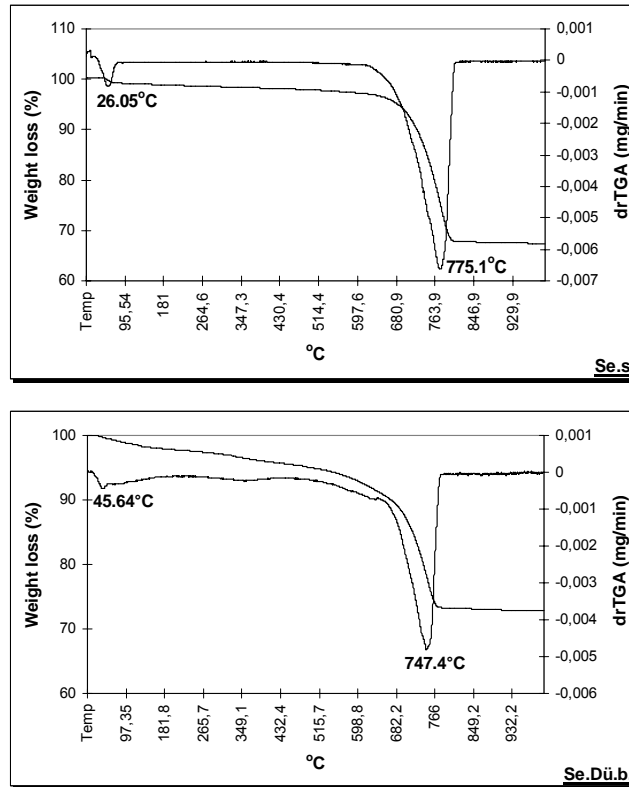
Figure 4.87 TGA-drTGA graph of the stone masonry mortar of Se.s. and brick masonry mortar of Se.Dü.b.

The inverse relationship between hydraulicity (CO_2/H_2O) and CO_2 % is generally expressed by a graph in which the ratio of CO_2/H_2O was recorded on the ordinate (y) axis and the corresponding CO_2 % on the abscissa (x) axis (Figure 4.88). Mortars having hydraulic character are concentrated at the bottom left part of this graph (Moropoulou et al. 2003, Maravelaki-Kalaitzaki et al. 2002, Moropoulou et al. 2000b). According to this, all brick masonry and some stone masonry mortars (Ur.He.s. and Se.Ul.s.) were concentrated at the bottom left part of the graph since they showed low percents of CO_2 but high percents of H_2O (Figure 4.88). Therefore, such mortars were included within the area of lime containing silica at high ratios mortars. However, stone masonry mortars of Se.s. and Ur.Ka.s. were concentrated at the upper right part of the graph due to their high percents of CO_2 but low percents of H_2O (Figure 4.88). Thus, they were defined as non-lime containing silica at high ratios mortars.
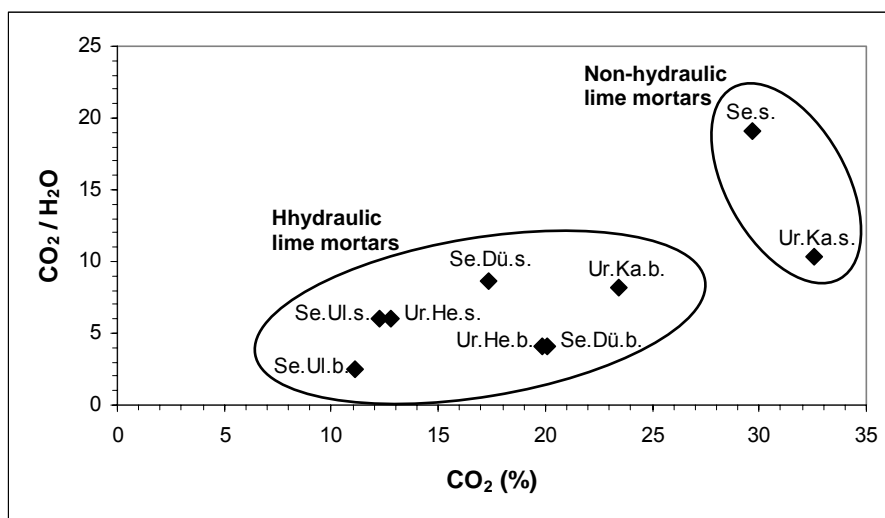
Figure 4.88 Inverse hydraulicity (CO_2/H_2O) versus CO_2 % of stone and brick masonry mortars.

4.8. Relation between Pozzolanicity of Aggregates, Mechanical Strength Properties and Hydraulicity of Mortars

Pozzolanic aggregates used in lime mortars are known to improve their mechanical strength and hydraulic properties (Lea 1940). Pozzolanic reaction, which takes place among the pozzolanic aggregates and lime in the presence of water, can produce hydraulic reaction products such as calcium-silicate-hydrates (C-S-H) and calcium-silicate-hydrates (C-A-H). Such products are the ones that acquire hydraulic properties to the lime mortars and provide high strength properties to them (Lea 1940, Moropoulou et al. 2000b). Within this context, pozzolanicity of aggregates used in the lime mortars of the Ottoman baths, mechanical strength and hydraulic properties of the lime mortars were evaluated in this section.

As seen in Figures 4.89, 4.90, 4.91 and 4.92, pozzolanic activities of aggregates used in lime containing silica at high ratios mortars and their compressive and tensile strength values were higher than those of non-lime containing silica at high ratios mortars. This could indicate that pozzolanic aggregates imparted hydraulic character to the lime mortars and the hydraulic character improved their mechanical strengths.

103
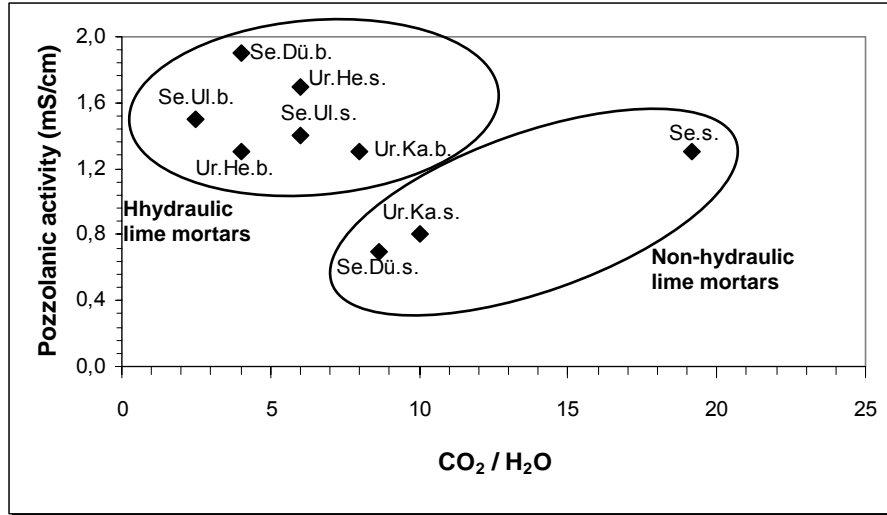
Figure 4.89 Pozzolanic activity measurements of the coarse aggregates versus hydraulicity (CO_2/H_2O) of stone and brick masonry mortars.
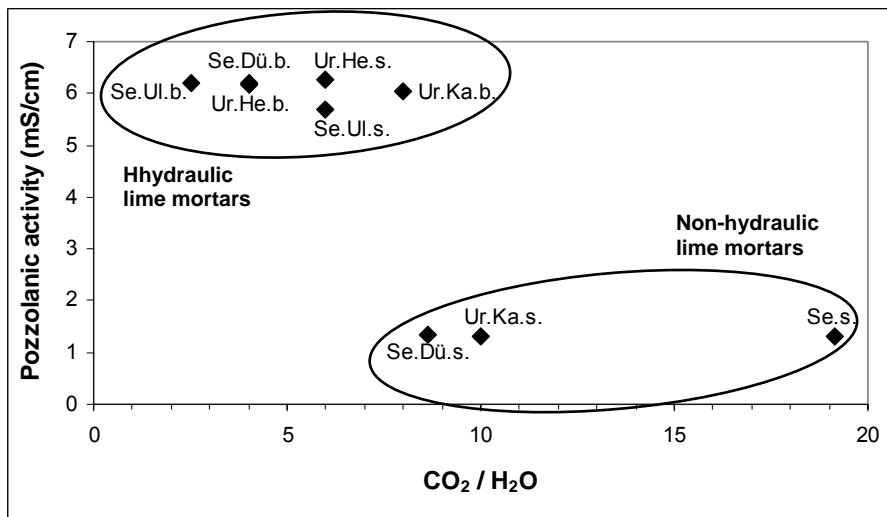
Figure 4.90 Pozzolanic activity measurements of the fine aggregates versus hydraulicity (CO_2/H_2O) of stone and brick masonry mortars.
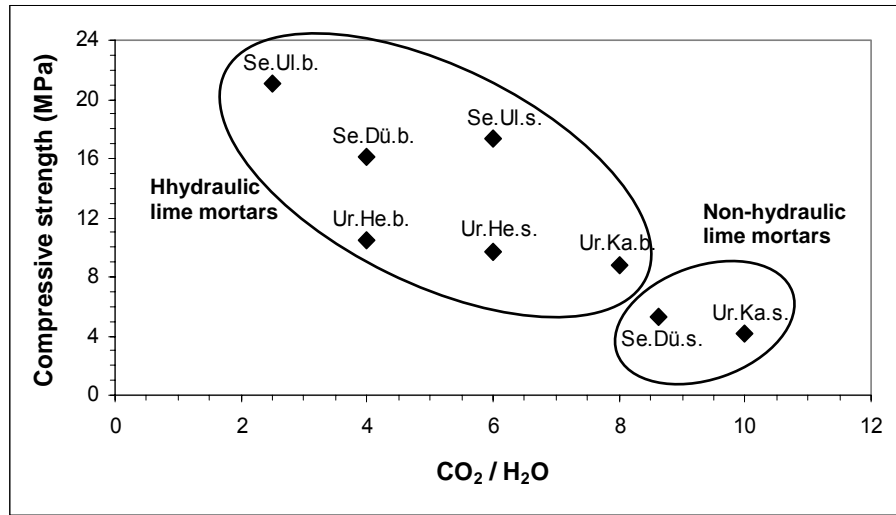
Figure 4.91 Compressive strength values versus hydraulicity (CO_2/H_2O) of stone and brick masonry mortars.
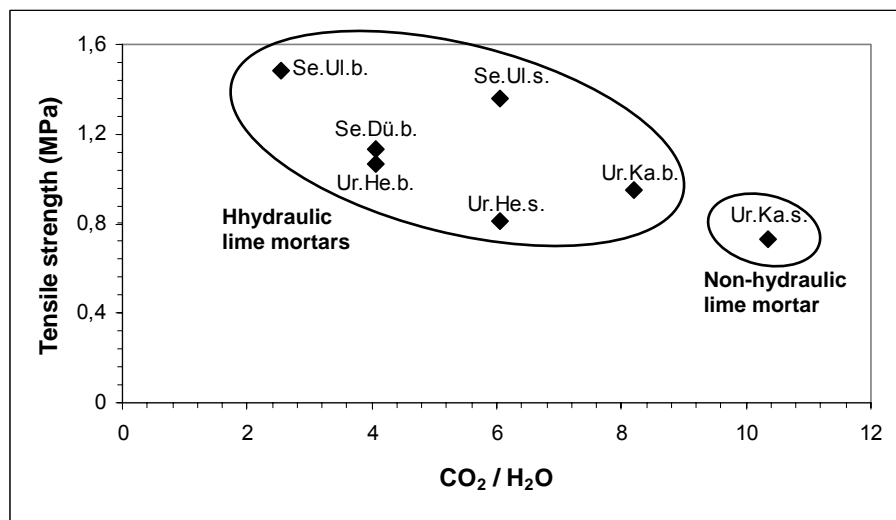
Figure 4.92 Tensile strength values versus hydraulicity (CO_2/H_2O) of stone and brick masonry mortars.

Hydraulic and mechanical properties of lime mortars used in the walls and domes of the five Ottoman baths were compared with each other to find if their production technologies changed depending on the properties of the structural elements where they were used. It was found that all brick masonry mortars having hydraulic properties presented higher compressive and tensile strength values than the stone masonry mortars (Figures 4.91 and 4.92). Such difference in stone and brick masonry mortars could be attributed to the difference in structural behaviour of the structural elements of the wall and dome. The wall works in compression. However, in the dome both compressive stresses along its meridian lines and circumferential tensile forces in the

lower parts of the hemisphere are formed (Ünay 2001, Fielden 2001). Therefore, the dome should be able to resist both of these stresses in order to provide its structural resistance. This considerably depends on the geometry of the dome and strength properties of materials used (Ünay 2001). Therefore, lime containing silica at high ratios mortars of high mechanical strength properties could be used deliberately in the construction of the domes of the Ottoman baths.

4.9. Mortar-Brick Interface

When mortar is spread over the masonry units, it starts to lose water through the absorption of the masonry units and by evaporation to the air from the surface of the joints. The former improves adhesion bonds between the masonry units and the mortar (Davison 1976).

Within this context, interface between lime mortar and bricks used in domes of the Ottoman baths were examined by both stereo microscopic observations and SEM analysis. It was found that lime mortar and bricks were tightly adhered to each other (Figure 4.93). Furthermore, along the bricks nearer to the mortar side, a dark band in 1.5-3 mm thickness was detected. SEM-EDS analysis indicated that this part contained calcium oxide at an average ratio of 8.3 % (Figure 4.93). This could be explained in a way that lime dissolved in the water of the mortar penetrated into the bricks through their pores and the subsequent carbonation of calcium hydroxide created a physical adhesion between the mortar and the bricks (Armelao et al. 2000). It was also assumed that at the interface and in the pores of the brick, a thin layer of calcium silicates could be formed due to chemical reactions among the brick constituents and calcium hydroxide (Armelao et al. 2000). The final products of calcium silicates were assumed to contribute to the strong adhesion of the lime mortar to the brick (Armelao et al. 2000). Consequently, this could be considered to contribute to the good adhesion of the bricks with the lime mortar and so to the structural resistance of the domes of the examined baths.

I
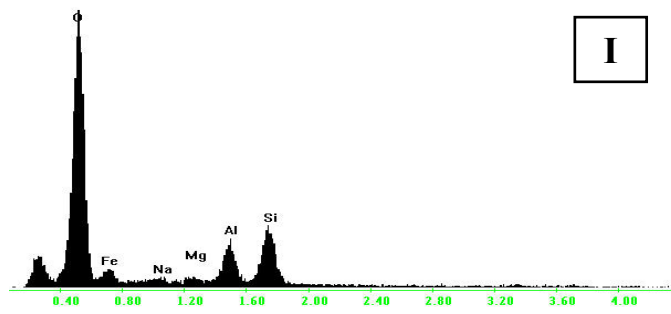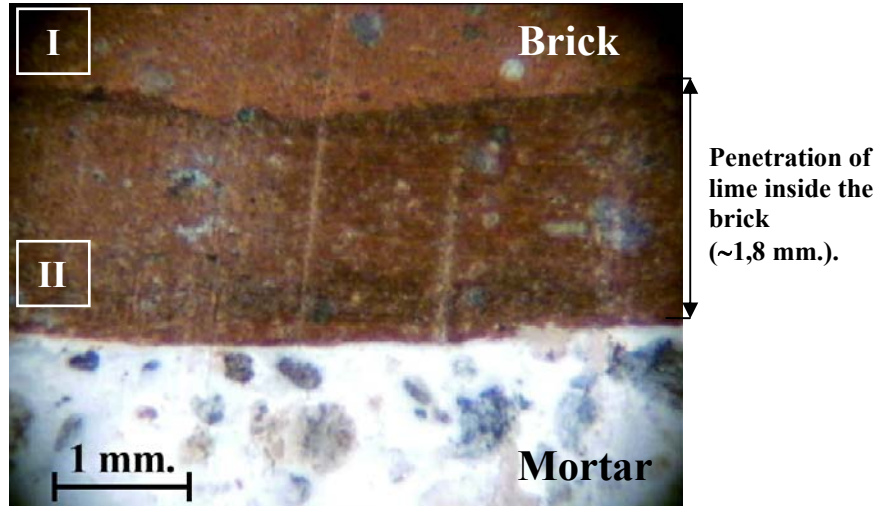
Oxide	%
Fe$_2$O$_3$	21.2
Na$_2$O	2.8
MgO	3.8
Al$_2$O$_3$	23.8
SiO$_2$	48.4
Total	100.0

II
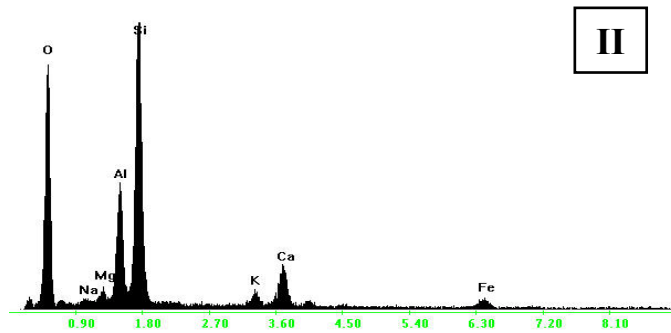
Oxide	%
Fe$_2$O$_3$	5.8
Na$_2$O	1.3
MgO	2.7
Al$_2$O$_3$	20.1
SiO$_2$	59.5
K$_2$O	2.3
CaO	8.3
Total	100.0

Figure 4.93 Stereo microscope image showing adhesion between brick and lime mortar used in domes, EDX spectra and elemental compositions (%) of the brick (I) and its part into which lime penetrated (II).

Chapter 5

CONCLUSIONS

Characterization of lime mortars used in the walls and domes of some Ottoman baths in Seferihisar-Urla region near İzmir have been carried out to understand the mortar characteristics which will be necessary for the production of intervention mortars to be used in their restoration.

Mortars used in the walls and domes of the examined Ottoman baths are lime mortars whose lime/aggregate ratios range between 1:4 and 2:3.

All brick masonry mortars used in the domes are hydraulic lime mortars having higher mechanical strength properties than those of the stone masonry mortars most of which are non-hydraulic lime mortars used in the walls. Such difference can be explained with the structural behaviour of the dome derived from its geometry.

Aggregates from a common source were used in the mortars and their particle size distributions are almost the same. Fine and coarse aggregates in each mortar were used from the same source since their mineralogical and chemical compositions are similar with each other. However, the fine aggregates have higher proportions of amorphous materials and are richer in silicon dioxide (SiO_2) and aluminium oxide (Al_2O_3) than their coarse aggregates. Therefore, the fine aggregates have higher pozzolanic activity than their coarse aggregates in all mortars.

Due to the use of pozzolanic aggregates and lime containing silica at high ratios, all brick masonry mortars are hydraulic lime mortars. Therefore, they have high compressive and tensile strength values. In non-hydraulic lime mortars used in the walls, high-calcium lime and aggregates having poor pozzolanicity were used.

Even though bricks used in the construction of the domes have poor pozzolanicity, they are so tightly adhered to the lime mortar that they have formed a superstructure like a monolithic mass. This could be considered to contribute to the structural stability of the domes.

Determination of characteristics of lime mortars provides preliminary information for the production of intervention mortars to be used in restoration of the examined Ottoman baths. Therefore, further studies should be carried out to produce the intervention mortars. Source of the aggregates especially the pozzolanic ones used in

the original lime mortars should be investigated in the region where the studied baths are located. In case it is not found, possible aggregate sources should be investigated in the same region and compatibility of mineralogical and chemical compositions of the found aggregates should be examined. Properties of lime to be used as the binding material in the mortars should be determined. New mortars in various lime/aggregate ratios should be produced. Then, the produced mortars should be tested in order to determine the compatible ones with those of the original mortars in terms of physical and mechanical properties.

It should be particularly important to consider that cement should never be used as the binding material or even as additive in the intervention mortars since it contains soluble salts, has high thermal expansion and makes the mortar less porous and more rigid than the original lime mortars. Therefore, its use can lead to deterioration of original building materials.

This study has shown that determination of lime mortar characteristics is of particular importance in the conservation of historic buildings for the production of intervention mortars compatible with the original lime mortars. In addition, the lime mortar characteristics can play a significant role in structural behaviour of the historic structures.

REFERENCES

1. Aardt Van J.H.P., Visser S., "Formation of hydrogarnets: Calcium hydroxide attack on feldspars and clays", *Cement and Concrete Research*, **7**, (1977), pp. 39-44.

2. Airapetov D., "*Architectural Materials Science*", Translated from the Russian by A.B. Kuznetsov, (Mir Publishers, Moscow,1986), pp. 36-40.

3. Akman M. S., Güner A., Aksoy İ. H., "Horasan Harcı ve Betonunun Tarihi ve Teknik Özellikleri," in *2. Uluslararası Türk-İslam Bilim ve Teknoloji Tarihi Kongresi, İTÜ, 28 Nisan-2 Mayıs 1986*, (Ayrıbasım, 1986), pp.101-112.

4. Aktaş A., "*Konya' daki Anadolu Selçuklu Dönemi Yapılarında Malzeme ve Teknik (Materials and Techniques in the Buildings of Anatolian Seljuk Monuments in Konya)*", Unpublished M.Sc. Thesis, Hacettepe University, Ankara, 1988.

5. Allen G., Allen J., Elton N., Farey M., Holmes S., Livesey P., Radonjic M., "*Hydraulic Lime Mortar*", (Donhead Publishing, 2003).

6. Alvarez J.I., Navarro I., Martin A., Casado Garcia P.J., "A study of the ancient mortars in the north tower of Pamplona's San Cernin church", *Cement and Concrete Research*, **30**, (2000a), pp. 1413-1419.

7. Alvarez J.I., Navarro I., Casado Garcia P.J., "Thermal, mineralogical and chemical studies of the mortars used in the cathedral of Pamplona (Spain), *Thermochimica Acta*, **365**, (2000b), pp. 177-187.

8. Armelao L., Bassan A. , Bertoncello R., Biscontin G., Daolio S., Glisenti A., " Silica glass interaction with calcium hydroxide: a surface chemistry approach", *Journal of Cultural Heritage,* **1**, (2000), pp. 375-384.

9. Arnold A., "Determination of Saline Minerals from Monuments", *GP News Letter*, **4**, (1983), pp. 4-15.

10. Ashall G., Butlin R.N., Teutonico J.M., Martin W., "Development of Lime Mortar Formulations for Use in Historic Buildings", in *Durability of Building Materials and Components 7*, Volume 1, Ed. C. Sjöström, (E & FN Spon, London, 1996), pp. 353-359.

11. Ashurst J., Ashurst N., "*Practical Building Conservation – Mortars, Plasters and Renders*", English Heritage Technical Handbook, Volume 3, (Gower Technical Press, 1998), pp. 1-15.

12. Ashurst J., Dimes F., "Mortars for Stone Buildings," in *Conservation of Building and Decorative Stone*, Volume 2, (Buttherworth-Heinemann, 1990), pp. 78-93.

13. Bakolas A., Biscontin G., Moropoulou A., Zendri E., "Characterization of structural Byzantine mortars by thermogravimetric analysis", *Thermochimica Acta*, **321**, (1998), pp. 151-160.

14. Baronio G., Binda L., Tedeschi C., "Thick mortar joints in Byzantine Buildings: Study of Their Composition and Mechanical Behaviour", in the *Proceedings of the International Conference on Studies in Ancient Structures, July 14-18, 1997, İstanbul, Turkey*, (1997), pp. 235-244.

15. Barret P., Menetrier D., Cottin B., "Study of silica-lime solution reactions", *Cement and Concrete Research*, **7**, (1977), pp. 61-67.

16. Biscontin G., Birelli M.P., Zendri E., "Characterization of binders employed in the manufacture of Venetian historical mortars", *Journal of Cultural Heritage,* **3**, (2002), pp. 31-37.

17. Black C.A., "Methods of Soil Analysis", Part 2, *American Society of Agronomy*, Madison, Wisconsin, USA, (1965).

18. Boynton R. S., *Chemistry and Technology of Lime and Limestone*, (John Wiley & Sons, New York, 1966).

19. Böke H., Akkurt S., İpekoğlu B., "Tarihi Yapılarda Kullanılan Horasan Harcı ve Sıvalarının Özellikleri", *Yapı Dergisi*, **269**, (Nisan 2004a), pp. 90-95.

20. Böke H., Akkurt S., İpekoğlu B., Uğurlu E., "Tarihi Yapıların Onarımlarında Kullanılacak Horasan Harç ve Sıvalardaki Puzolanik Malzemelerin Özelliklerinin Araştırılması", *TÜBİTAK Projesi, Kod: İÇTAG – I674*, (2004b).

21. Bruni S., Cariati F., Fermo P., Cairati P., Alessandrini G., Toniolo L. "White lumps in fifth-to seventeenth-century AD mortars from northern Italy", *Archaeometry*, **39/1**, (1997), pp. 1-7.

22. Cazalla O., Navarro C. R., Sebastian E., Cultrone G., "Aging of Lime Putty: Effects on Traditional Lime Mortar Carbonation", *Journal of American Ceramic Society*, **83**, (2000), pp. 1070-1076.

23. Charola E.A., Henriques F. M. A., "Hydraulicity in Lime Mortars Revisted", *Proceedings of the RILEM TC-167COM International Workshop: "Historic mortars: characteristics and tests"*, (Paisley, 1999), pp. 97-106.

24. Cowan H.J., "Structure in the Ancient World," in *The Master Builders – A History of Structural and Environmental Design from Ancient Egypt to the Nineteenth Century*, (John Wiley & Sons, New York, 1977), pp. 25-74.

25. Cowper A.D., *Lime and Lime Mortars*, (Donhead Publishing Ltd, Dorset, 2000, First published in 1927 for the Building Research Station by HM Stationary Office, London).

26. Davey N., "Limes and Cements, and Mortar and Concrete," in *A History of Buildings Materials*, (Phoenix House, London, 1961), pp. 97-127.

27. Davison J.I., "Mortar Technology", in the *Proceedings of the First Canadian Masonry Symposium, University of Calgary, Calgary, Alberta, 7-10 June 1976*, Division of Building Research (DBR), Paper no. 692, (1976), pp. 12-21.

28. Degrysea P., Elsena J., Waelkensb M., "Study of ancient mortars from Sagalassos (Turkey) in view of their conservation", *Cement and Concrete Research*, **32**, (2002), pp. 1457–1463.

29. Diamond S., "A review of alkali-silica reaction and expansion mechanisms (2. Reactive aggregates)", *Cement and Concrete Research*, **6**, (1976), pp. 549-560.

30. Eckel E.C., *"Cements, Limes and Plasters – Their materials, manufacture and properties"*, (John Wiley & Sons, New York, 1928), pp. 91-583.

31. EHDBL (English Heritage Directory of Building Limes), (Donhead Publications, London, 1997).

32. Elert K., Rodriguez-Navarro C., Pardo E. S., Hansen E. and Cazalla O., "Lime Mortars for the Conservation of Historic Buildings", *Studies in Conservation*, **47**, Number 1, (2002), pp. 62-75.

33. Fielden B.M, "Structural elements I: Beams, arches, vaults and domes", in *Conservation of Historic Buildings*, (Architectural Press, Oxford, 2001), pp. 37-49.

34. Franzini M., Leoni L., Lezzerini M., "A procedure for determining the chemical composition of binder and aggregate in ancient mortars: its application to mortars from some medieval buildings in Pisa", *Journal of Cultural Heritage,* **1**, (2000), pp. 365-373.

35. Gay C. M., Parker H., *"Materials and Methods of Architectural Construction"*, (John Wiley & Sons Inc., New York, 1932), pp. 14-17.

36. Gillot J.E., "Carbonation of $Ca(OH)_2$ investigated by thermal and x-ray diffraction methods of analysis", *Journal of Applied Chemistry*, **17**, (1967), pp. 185-189.

37. Goodwin J.F., West H.W., "A review of the literature on brick:mortar bond", *Proc. Br. Ceram. Soc.*, **30,** (1982), pp. 23–28.

38. Güleç A., *"Bazı Tarihi Anıt Harç ve Sıvalarının İncelenmesi (Characterization of Mortars and Platers of Some Historic Monuments)"*, Unpublished Ph.D. Thesis, İstanbul Technical University, İstanbul, 1992.

39. Güleç A., Tulun T., "Studies of Old Mortars and Plasters from the Roman, Byzantine and Ottoman period of Anatolia", *Architectural Science Review*, **39**, (1996), pp. 3-13.

40. Hansen E.F., Balen K.V., Elert K., Rodriquez-Navarro C., Simon S. "*Preservation of Lime Mortars and Plasters*", The GCI Project Bibliographies Series, (The Getty Conservation Institute, 2003).

41. Hassibi M., "An Overview of Lime Slaking and Factors That Affect The Process", *Presented to 3rd International Sorbalit Symposium*, November 3-5, 1999, New Orleans, LA USA, (1999).

42. Holmes S., Wingate M., "*Building with Lime*", (Intermediate Technology Publications, London, 1997).

43. Hughes J.J., Bartos P.M., Cuthbert S.J., Stewart R.N., Valek J., "Microstructures in historic Scottish lime mortars" in *Stone Weathering and Atmospheric Pollution Network 1997: Aspects of Stone Weathering, Decay and Conservation, Ed. M.S. Jones and R.D. Wakefield*, (Imperial College Press, London, 1998), pp. 125-137.

44. ISRM (International Society for Rock Mechanics), "*Rock Characterization, Testing and Monitoring: ISRM Suggested Methods*", (Ed. E.T. Brown, Pergamon Press, 1981), p. 211.

45. İpekoğlu B., Böke H., Hamamcıoğlu M., Akkurt S., Çizer Ö., "Tarihi Yapılarda Malzeme Bozulmasının Sınıflandırılması ve Sorunların Saptanmasına Yönelik Bir Yöntem Araştırması", *TÜBİTAK Projesi, Kod: İÇTAG – I304*, (2003).

46. Jedrzejevska H., "Ancient Mortars as Criterion in Analysis of Old Architecture", in the *Proceedings of Symposium on Mortars, Cements and Grouts Used in the Conservation of Historic Buildings, 1981, Rome*, (1981), pp. 311-329.

47. Kent R., "Role of lime cycle in historic buildings", *Building Engineer*, **70**, (1995), pp.1-2.

48. Krumnacher P.J., "*Lime and Cement Technology: Transition from Traditional to Standardized Treatment Methods*", Unpublished Master's Thesis, Virginia Polytechnic Institute and State University, Virginia, 2001.

49. Lanas J., Alvarez J.I., "Masonry repair lime-based mortars: Factors affecting the mechanical behavior", *Cement and Concrete Research*, **33**, (2003), pp. 1867–1876.

50. Lanas J., Perez Bernal J.L., Bello M.A., Alvarez Galindo J.I., "Mechanical properties of natural hydraulic lime-based mortars", *Cement and Concrete Research*, (2004), In press.

51. Lea F.M. "Investigations on Pozzolanas", *Building Research*, Technical Paper No.27, (1940), pp. 1-63.

52. Lewin S.Z., "X-Ray diffraction and scanning electron microscope analysis of conventional mortars," in the *Proceedings of Symposium on Mortars, Cements and Grouts Used in the Conservation of Historic Buildings, 1981, Rome*, (1981), pp. 101-131.

53. Livingston R., "Materials Analysis of the Masonry of the Hagia Sophia Basilica", in *Structural Repair and Maintenance of Historic Buildings*, II, (Ed. C.A. Brebbia, R.J.B Frewer, Computational Mechanics Publications, Southampton, 1993), U.K, pp. 15-32.

54. Luxan M.P., Madruga F., Saavedra J., "Rapid evaluation of pozzolanic activity of natural products by conductivity measurement", *Cement and Concrete Research*, **19**, (1989), pp. 63-68.

55. Maravelaki-Kalaitzaki P., Bakolas A., Moropoulou A., "Physico-chemical study of Cretan ancient mortars", *Cement and Concrete Research*, **2233**, (2002), pp. 1-11.

56. McKee H.J., "*Early American Masonry Materials in Walls, Floors and Ceilings: Notes on Prototypes, Sources, Preparation and Manner of Use*", (New York: Syracuse, 1971).

57. Middendorf B., Knöfel D., "Use of Old and Modern Analytical Methods for the Determination of Ancient Mortars in Northern Germany", in the *Proceedings of the 3rd Expert Meeting, Hamburg, NATO-CCMS Pilot Study on Conservation of Historic Brick Structures, Berlin, Germany*, (1990), pp. 75-92.

58. Moorehead D.R., "Cementation by the Carbonation of Hydrated Lime", *Cement and Concrete Research*, **16**, (1986), pp. 700-708.

59. Moropoulou A., Bakolas A., Bisbikou K., "Characterization of Ancient, Byzantine and Later Historic Mortars by Thermal and X-ray Diffraction Techniques", *Thermochimica Acta*, **269/270**, (1995), pp. 779-795.

60. Moropoulou A., Tsiourva Th., Bisbikou K., Biscontin G., Bakolas A., Zendri E., "Hot lime technology imparting high strength to historic mortars", *Construction and Building Materials*, **10**, (1996), pp. 151-159.

61. Moropoulou A., Biscontin G., Bakolas A., Bisbikou K., "Technology and behaviour of rubble masonry mortars", *Construction and Building Materials*, **11**, (1997), pp. 119-129.

62. Moropoulou A., Çakmak A.S., Lohvyn N., "Earthquake resistant construction techniques and materials on Byzantine monuments in Kiev", *Soil Dynamics and Earthquake Engineering*, **19**, (2000a), pp. 603-615.

63. Moropoulou A., Bakolas A., Bisbikou K., "Investigation of the technology of historic mortars", *Journal of Cultural Heritage*, **1**, (2000b), pp. 45-58.

64. Moropoulou A., Bakolas A., Aggelakopoulou E., "The effects of limestone characteristics and calcination temperature to the reactivity of the quicklime", *Cement and Concrete Research*, **31**, (2001), pp. 633-639.

65. Moropoulou A., Çakmak A.S., Biscontin G., Bakolas A., Zendri E., "Advanced Byzantine cement based composites resisting earthquake stresses: the crushed brick/lime mortars of Justinian' s Hagia Sophia", *Construction and Building Materials*, **16**, (2002a), pp. 543-552.

66. Moropoulou A., Cakmak A., Polikreti K., "Provenance and Technology Investigation of Agia Sophia Bricks, Istanbul, Turkey", *Journal of American Ceramic Society*, **85 (2)**, (2002b), pp. 366-372.

67. Moropoulou A., Polikreti K., Bakolas A., Michailidis P., "Correlation of physicochemical and mechanical properties of historical mortars and classification by multivariate statistics", *Cement and Concrete Research*, **33**, (2003), pp. 891–898.

68. Moropoulou A., Bakolas A., Anagnostopoulou S., "Composite materials in ancient structures", *Cement & Concrete Composites*, (2004a), In press.

69. Moropoulou A., Bakolas A., Moundoulas P., Aggelakopoulou E., Anagnostopoulou S., "Strength development and lime reaction in mortars for repairing historic masonries", *Cement & Concrete Composites*, (2004b), In press.

70. Navarro C. R., Hansen E., Ginell W.S., "Calcium hydroxide crystal evolution upon aging of lime putty", *Journal of American Ceramic Society*, **81**, (1998), pp. 3032-3034.

71. Papayianni I., Karaveziroglou M., "Aggregate Gradation of Ancient Mortars. Relationship to Strength and Porosity", in the *Proceedings of the International RILEM/UNESCO Congress on Conservation of Stone and Other Materials: Research-Industry-Media, June 29-July 1, 1993, Paris*, (Ed. by Thiel M.J., E & FN Spon, 1993, London), pp. 493-499.

72. Papayianni I., "Technology of Mortars and Bricks Used in Ottoman Monuments of Thessaloniki", in the *Proceedings of the International Conference on Studies in Ancient Structures, July 14-18, 1997, İstanbul, Turkey*, (1997), pp. 245-253.

73. Papayianni I., Stefanidou M., "Repair Mortars Suitable for Interventions of Ottoman Monuments", in the *Proceedings of the International Conference on Studies in Ancient Structures, July 14-18, 1997, İstanbul, Turkey*, (1997), pp. 255-264.

74. Peroni S., Tersigni G., Torraca G., Cerea S., Forti M., Guidobaldi F., Rossi-Doria P., De Rege A., Picchi D., Pietrafitta F.J., Benedetti G., "Lime based mortars for the repair of ancient masonry and possible substitutes", in *Mortars, Cements and Grouts Used in the Conservation of Historic Buildings*, (ICCROM, Rome, 1981), pp. 63-99.

75. Potgieter J.H., Potgieter S.S., Moja S.J. "An empirical study of factors influencing lime slaking. Part I: production and storage conditions", *Minerals Engineering*, **15**, (2002), pp. 201-203.

76. Ramachandran V.S., Sereda P.J., Feldman, "Delayed hydration in white-coat plaster", *Materials Research and Standards (ASTM)*, **4**, (1964), pp. 663-666.

77. Reyhan K. "*Construction Techniques and Materials of Ottoman Period Baths in Urla-Seferihisar Region*", Unpublished M.Sc. Thesis, İzmir Institute of Technology, İzmir, 2004.

78. RILEM, "Tests Defining the Structure", *Materials and Construction,* **13**, (1980), p. 73.

79. Satongar L.Ş. "*İstanbul Şehir Surları Horasan Harçları Üzerine Bir Araştırma (An Investigation on Horasan Mortars of İstanbul City Walls)*", Unpublished M.Sc. Thesis, İstanbul Technical University, İstanbul, 1994.

80. Schafer J., "The Weathering of Natural Building Stones", Department of Scientific and Industrial Research, Special Report No.18, (London, 1972), p. 149.

81. Schafer J., Hildsdorf H.K., "Ancient and New Lime Mortars – The Correlation between Their Composition, Structure and Properties", in the *Proceedings of the International RILEM/UNESCO Congress on Conservation of Stone and Other Materials: Research-Industry-Media, June 29-July 1, 1993, Paris*, (Ed. by Thiel M.J., E & FN Spon, 1993, London), pp. 605-612.

82. Sickels L.B. (1981), "Organics and Synthetics: Their Use as Additives in Mortars, Mortars, Cements and Grouts Used in the Conservation of Historic Buildings", in the *Proceedings of Symposium, 1981, Rome*, (1981), pp. 25-52.

83. SLCHS (Scottish Lime Centre for Historic Scotland), *Preparation and Use of Lime Mortars – An introduction to the principles of using lime mortars*, (Historic Scotland, Edinburgh, 1995).

84. Steward J., Glover R., Holmes S., Proudfoot T., Seeley N., "Traditional lime-mortar formulations at the National Trust", *Transactions ASCHB*, **19**, (1994), pp.21-38.

85. Swallow P., Carrington D., "Limes and Lime Mortars–Part 1", *Journal of Architectural Conservation*, **1**, (1995), pp. 7-25.

86. Teutonico J.M., "Porous Building Materials," in *A Laboratory Manual for Architectural Conservators*, (ICCROM Publishing, Rome, 1988), pp. 35-68.

87. The Nara Document on Authenticity, http://www.international.icomos.org/naradoc_eng.htm, (2004).

88. The Venice Charter, http://www.international.icomos.org/e_venice.htm, (2004).

89. The Burra Charter, http://www.icomos.org/australia/burra.html, (2004).

90. Torraca G., "Binders," in *Porous Materials Building – Materials Science for Architectural Conservation*", (ICCROM Publications, Italy, 1988), pp. 67-74.

91. Tunçoku S.S., Caner-Saltık E.N., Böke H., "Definition of the Materials and Related Problems of a XIIIth Century Anatolian Seljuk Mescid: A Case Study in Konya City", in the *Proceedings of the International RILEM/UNESCO Congress on Conservation of Stone and Other Materials: Research-Industry-Media, June 29-July 1, 1993, Paris*, (Ed. by Thiel M.J., E & FN Spon, 1993, London), pp. 368-375.

92. Tunçoku S.S., "*Characterization of Masonry Mortars Used in Some Anatolian Seljuk Monuments in Konya, Beyşehir and Akşehir*", Unpublished Ph.D. Thesis, METU, Ankara, 2001.

93. Ulusay R., Gökçeoğlu C., Binal A., "Brazilian Deney Yöntemiyle Kayaçların Çekilme Dayanımının Tayini (Dolaylı Yöntem), Tek Eksenli Sıkışma Dayanımı Deneyi, Elastisite Modülü (Young Modülü) ve Poisson Oranının Tayini", in *Kaya Mekaniği Laboratuvar Deneyleri*, (TMMOB Jeoloji Mühendisleri Odası Yayınları: 58, Ankara, 2001), pp. 69-79.

94. Ünay A. I. "Structural wisdom of architectural heritage", in the *Proceedings of ICOMOS - International Millennium Congress - More than two thousand years in the history of architecture. Ib 2.*, (Bethlehem, 2001), http://www.unesco.org/archi2000/papers.html, (2004).

95. Van Balen V., Van Gemert D., "Modelling lime carbonation", *Materials and Structures*, **27**, (1994), pp. 393-398.

96. Vicat L. J., "Mortars and Cements", (Donhead Publishing Ltd, Dorset, 2003, First published in 1837, London).

97. Wan H., Gillot J.E., "Mechanism of alkali-silica reaction and the significance of calcium hydroxide", *Cement and Concrete Research*, **21**, (1991), pp. 647-654.

98. Wingate M., "*Small-Scale Lime Burning: A Practical Introduction*", (Intermediate Technology Publications, London, 1985).

APPENDIX A

EXPERIMENTAL METHODS

Table A.1. Experimental methods carried out for the determination of characteristics of mortars and bricks.

SAMPLES	PHYSICAL PROPERTIES		MECHANICAL PROPERTIES			ANALYSIS OF SOLUBLE SALTS		RAW MATERIAL PROPERTIES		POZZOLANIC ACTIVITY	MINERALOGICAL AND CHEMICAL COMPOSITION AND MICROSTRUCTURAL PROPERTIES		HYDRAULIC PROPERTIES
EXPERIMENTAL ANALYSIS APPLIED	Density	Porosity	Uniaxial Compressive Strength	Tensile Strength	Modulus of Elasticity	Percent Soluble Salts	Quantitative Determination of Anion Parts of Soluble Salts	Lime/ Aggregate Ratio	Particle Size Distribution of Aggregates	Pozzolanic Activity Properties	Mineralogical Composition	Chemical Composition and Microstructural Properties	Structurally Bound Water and Carbon Dioxide Ratios
	Water Absorption and Hydrostatic Weighing	Water Absorption and Hydrostatic Weighing	Mechanical Test Instrument	Brazilian Test Method by Mechanical Test Instrument	Slope of Stress/Strain Graph	Electrical Conductivity Measurement	Analysis of Spot Test	Dissolution of Carbonated Lime in Dilute HCl Solution	Sieve Analysis	Electrical Conductivity Measurement	XRD Analysis	SEM-EDS Analysis	TGA Analysis
Stone Masonry Mortars													
Se.s.	■	■	*	*	*	■	■	■	■		■	■	■
Se.Dü.s.	■	■	■	*	■	■	■	■	■		■	■	■
Se.Ul.s.	■	■	■	■	■	■	■	■	■		■	■	■
Ur.He.s.	■	■	■	■	■	■	■	■	■		■	■	■
Ur.Ka.s.	■	■	■	■	■	■	■	■	■		■	■	■
Se.s.wl.											■	■	
Se.Dü.s.wl.											■	■	
Se.Ul.s.wl.											■	■	
Ur.He.s.wl.											■	■	
Ur.Ka.s.wl.											■	■	
Se.s.agg.										■	■	■	
Se.Dü.s-agg.										■	■	■	
Se.Ul.s-agg.										■	■	■	
Ur.He.s-agg.										■	■	■	
Ur.Ka.s-agg.										■	■	■	
Brick Masonry Mortars													
Se.b.											■	■	
Se.Dü.b.	■	■	■	■	■	■	■	■	■		■	■	■
Se.Ul.b.	■	■	■	■	■	■	■	■	■		■	■	■
Ur.He.b.	■	■	■	■	■	■	■	■	■		■	■	■
Ur.Ka.b.	■	■	■	■	■	■	■	■	■		■	■	■
Se.b.wl.											*	*	
Se.Dü.b.wl.											*	■	
Se.Ul.b.wl.											*	■	
Ur.He.b.wl.											*	*	
Ur.Ka.b.wl.											■	■	
Se.b.agg.											*	*	
Se.Dü.b-agg.										■	■	■	
Se.Ul.b-agg.										■	■	■	
Ur.He.b-agg.										■	■	■	
Ur.Ka.b-agg.										■	■	■	
Brick													
Se.brick											■		
Se.Dü.brick	■	■									■		
Se.Ul.brick	■	■									■		
Ur.He.brick	■	■									■		
Ur.Ka.brick	■	■									■		

*: Not determined due to inadequate sample.

APPENDIX B

BASIC PHYSICAL PROPERTIES OF MORTARS

Table B.1 Density and porosity values of stone masonry mortars.

Sample	Dry weight (g)	Saturated weight (g)	Archimedes weight (g)	Density (g/cm³)	Porosity (%)
Se.s.1	40.54	52.02	24.80	1.49	42.17
Se.s.2	43.01	54.61	26.21	1.51	40.85
Se.s.3	52.63	65.85	32.01	1.56	39.07
Se.s.				**1.52**	**40.70**
Se.Dü.s.1	20.86	26.80	12.72	1.48	42.19
Se.Dü.s.2	28.71	36.59	17.71	1.52	41.74
Se.Dü.s.3	31.05	39.51	19.18	1.53	41.61
Se.Dü.s.				**1.51**	**41.85**
Se.Ul.s.1	27.02	30.66	16.25	1.88	25.26
Se.Ul.s.2	21.99	25.27	13.22	1.82	27.22
Se.Ul.s.3	24.88	28.7	15.05	1.82	27.99
Se.Ul.s.				**1.84**	**26.82**
Ur.He.s.1	30.94	39.31	18.32	1.47	39.88
Ur.He.s.2	40.35	48.14	22.30	1.56	30.15
Ur.He.s.3	41.50	53.07	24.70	1.46	40.78
Ur.He.s.				**1.50**	**36.94**
Ur.Ka.s.1	77.85	92.89	46.53	1.68	32.44
Ur.Ka.s.2	75.43	91.02	45.67	1.66	34.38
Ur.Ka.s.3	51.62	61.05	31.18	1.73	31.57
Ur.Ka.s.				**1.69**	**32.80**

Table B.2 Density and porosity values of brick masonry mortars.

Sample	Dry weight (g)	Saturated weight (g)	Archimedes weight (g)	Density (g/cm³)	Porosity (%)
Se.Dü.b.1	40.31	48.15	22.69	1.58	30.79
Se.Dü.b.2	32.87	42.27	19.8	1.46	41.83
Se.Dü.b.3	43.26	56.54	25.78	1.41	43.17
Se.Dü.b.				**1.48**	**38.60**
Se.Ul.b.1	66.03	79.38	39.8	1.67	33.73
Se.Ul.b.2	49.10	58.53	29.59	1.70	32.58
Se.Ul.b.3	27.15	31.54	16.53	1.81	29.25
Se.Ul.b.				**1.72**	**31.85**
Ur.He.b.1	39.27	48.02	23.21	1.58	35.27
Ur.He.b.2	40.27	48.54	23.64	1.62	33.21
Ur.He.b.3	27.08	33.38	16.23	1.58	36.73
Ur.He.b.				**1.59**	**35.07**
Ur.Ka.b.1	61.17	81.15	36.53	1.37	44.78
Ur.Ka.b.2	67.80	88.4	40.31	1.41	42.84
Ur.Ka.b.3	35.39	46.08	21.08	1.42	42.76
Ur.Ka.b.				**1.40**	**43.46**

Table B.3 Density and porosity values of bricks used in domes.

Sample	Dry weight (g)	Saturated weight (g)	Archimedes weight (g)	Density (g/cm³)	Porosity (%)
Se.Dü.brick.1	19.96	23.16	11.94	1.78	28.52
Se.Dü.brick.2	12.33	14.77	7.68	1.74	34.41
Se.Dü.brick				**1.76**	**31.47**
Se.Ul.brick.1	54.53	68.12	33.62	1.58	39.39
Se.Ul.brick.2	65.67	77.80	40.52	1.76	32.54
Se.Ul.brick				**1.67**	**35.96**
Ur.He.brick.1	113.63	132.46	69.09	1.79	29.71
Ur.He.brick.2	114.43	134.50	69.46	1.76	30.86
Ur.He.brick.				**1.78**	**30.29**
Ur.Ka.brick.1	74.72	86.43	45.48	1.82	28.60
Ur.Ka.brick.2	94.63	110.79	57.48	1.78	30.31
Ur.Ka.brick.				**1.80**	**29.45**

APPENDIX C

BASIC MECHANICAL PROPERTIES OF MORTARS

Table C.1 Uniaxial compressive strength values of stone masonry mortars.

Sample	Length (mm)	Width (mm)	A (mm^2)	P (kN)	Compressive strength (MPa)
Ur.He.s.1	37.54	21.56	809.36	8.20	10.13
Ur.He.s.2	22.44	32.86	737.38	6.00	8.14
Ur.He.s.3	33.9	25.29	857.33	8.70	10.15
Ur.He.s.4	23.35	17.94	418.90	4.90	11.70
Ur.He.s.5	21.89	24.18	529.30	4.50	8.50
Ur.He.s.					**9.72**
Ur.Ka.s.1	36.94	35.24	1301.77	4.82	3.70
Ur.Ka.s.2	23.7	22.55	534.44	2.50	4.68
Ur.Ka.s.3	25.48	23.44	597.25	2.50	4.19
Ur.Ka.s.					**4.19**
Se.Dü.s.1	28.16	26.56	747.93	4.95	6.62
Se.Dü.s.2	26.78	27.72	742.34	2.53	3.41
Se.Dü.s.3	21.53	21.86	470.65	2.70	5.74
Se.Dü.s.					**5.25**
Se.Ul.s.1	19.85	20.08	398.59	2.76	6.92
Se.Ul.s.2	16.91	15.76	266.50	7.45	27.95
Se.Ul.s.					**17.44**

Table C.2 Uniaxial compressive strength values of brick masonry mortars.

Sample	Length (mm)	Width (mm)	A (mm^2)	P (kN)	Compressive strength (MPa)
Ur.He.b.1	20.59	19.66	404.80	5.23	12.92
Ur.He.b.2	23.53	24.56	577.90	6.22	10.76
Ur.He.b.3	32.98	31.77	1047.77	8.13	7.76
Ur.He.b.					**10.48**
Ur.Ka.b.1	22.04	22.57	497.44	4.70	9.45
Ur.Ka.b.2	25.59	26.67	682.49	5.50	8.06
Ur.Ka.b.					**8.75**
Se.Ul.b.1	17.42	16.89	294.22	5.63	19.14
Se.Ul.b.2	13.51	13.66	184.55	4.52	24.49
Se.Ul.b.3	18.32	18.69	342.40	6.60	19.28
Se.Ul.b.					**20.97**
Se.Dü.b.1	23.65	22.23	525.74	10.11	19.23
Se.Dü.b.2	23.91	23.09	552.08	5.00	9.06
Se.Dü.b.3	22.9	24.29	556.24	10.50	18.88
Se.Dü.b.4	24.49	25.21	617.39	7.10	11.50
Se.Dü.b.5	17.14	19.04	326.35	7.10	21.76
Se.Dü.b.					**16.08**

Table C.3 Tensile strength values of stone masonry mortars.

Sample	Diameter (mm)	Width (mm)	P (kN)	Tensile strength (MPa)
Se.Ul.s.1	25	12.5	0.59	1.20
Se.Ul.s.2	25	12.5	0.65	1.33
Se.Ul.s.3	25	12.5	0.76	1.55
Se.Ul.s.				**1.36**
Ur.He.s.	25	12.5	0.35	**0.81**
Ur.Ka.s.	25	12.5	0.36	**0.73**

Table C.4 Tensile strength values of brick masonry mortars.

Sample	Diameter (mm)	Width (mm)	P (kN)	Tensile strength (MPa)
Se.Dü.b.1	25	12.5	0.53	1.08
Se.Dü.b.2	25	12.5	0.58	1.18
Se.Dü.b.				**1.13**
Ur.He.b.1	25	12.5	0.44	0.90
Ur.He.b.2	25	12.5	0.61	1.24
Ur.He.b.				**1.07**
Ur.Ka.b.1	25	12.5	0.55	1.12
Ur.Ka.b.2	25	12.5	0.45	0.92
Ur.Ka.b.3	25	12.5	0.39	0.81
Ur.Ka.b.				**0.95**
Se.Ul.b.1	25	12.5	0.83	1.69
Se.Ul.b.2	25	12.5	0.60	1.22
Se.Ul.b.3	25	12.5	0.75	1.53
Se.Ul.b.				**1.48**

Table C.5 Modulus of elasticity values of stone masonry mortars.

Sample	Stroke (mm)	Load (kN)	ΔStroke (mm)	ΔLoad (kN)	ΔLoad/ΔStroke (kN/ mm)	Modulus of elasticity (MPa)
Ur.He.s.1	0.012	0.00392	0.007	0.0019	0.271	
	0.005	0.00202				
Ur.He.s.2	0.012	0.00668	0.008	0.00464	0.580	
	0.004	0.00204				
Ur.He.s.					**0.426**	**425.81**
Ur.Ka.s.1	0.009	0.000887	0.004	0.000537	0.134	
	0.005	0.00035				**134.30**
Ur.Ka.s.2	0.029	0.00214	0.01	0.00087	0.087	
	0.019	0.00127				
Ur.Ka.s.					**0.111**	**110.50**
Se.Ul.s.1	0.0201	0.00954	0.0077	0.00886	1.151	
	0.0124	0.00068				
Se.Ul.s.2	0.0239	0.00973	0.0105	0.00672	0.640	
	0.0134	0.00301				
Se.Ul.s.3	0.0375	0.01190	0.0058	0.01071	1.847	
	0.0317	0.00119				
Se.Ul.s.4	0.0305	0.01700	0.0086	0.0116	1.349	
	0.0219	0.00540				
Se.Ul.s.					**1.247**	**1246.51**
Se.Dü.s.1	0.0114	0.00138	0.004	0.000746	0.186	
	0.0074	0.000634				
Se.Dü.s.						**186.50**

Table C.6 Modulus of elasticity values of brick masonry mortars.

Sample	Stroke (mm)	Load (kN)	ΔStroke (mm)	ΔLoad (kN)	ΔLoad/ΔStroke (kN/ mm)	Modulus of elasticity (MPa)
Ur.He.b.1	0.013	0.00499	0.008	0.004732	0.592	
	0.005	0.000258				
Ur.He.b.2	0.023	0.00767	0.017	0.00671	0.395	
	0.006	0.00096				
Ur.He.b.					**0.493**	**493.12**
Se.Ul.b.1	0.0101	0.0089	0.0056	0.00699	1.248	
	0.0045	0.00191				
Se.Ul.b.2	0.0275	0.00855	0.0043	0.00565	1.314	
	0.0232	0.0029				
Se.Ul.b.3	0.0071	0.00991	0.0046	0.00784	1.704	
	0.0025	0.00207				
Se.Ul.b.4	0.00484	0.00849	0.00327	0.00721	2.2	
	0.00157	0.00128				
Se.Ul.b.					**1.618**	**1617.63**
Se.Dü.b.1	0.0141	0.0059	0.0039	0.00375	0.962	
	0.0102	0.00215				
Se.Dü.b.2	0.0399	0.0281	0.0143	0.0171	1.196	
	0.0256	0.011				
Se.Dü.b.3	0.0271	0.00875	0.0064	0.00539	0.842	
	0.0207	0.00336				
Se.Dü.b.4	0.022	0.0196	0.009	0.0078	0.867	
	0.013	0.0118				
Se.Dü.b.					**0.967**	**966.67**
Ur.Ka.b.1	0.0757	0.00815	0.0306	0.00603	0.197	
	0.0451	0.00212				
Ur.Ka.b.2	0.0689	0.00457	0.009	0.00264	0.293	
	0.0599	0.00193				
Ur.Ka.b.3	0.0206	0.0049	0.0128	0.004444	0.347	
	0.0078	0.000456				
Ur.Ka.b.4	0.0085	0.00119	0.003	0.00066	0.220	
	0.0055	0.00053				
Ur.Ka.b.					**0.264**	**264.39**

APPENDIX D

LIME/AGGREGATE RATIOS OF MORTARS AND PARTICLE SIZE DISTRIBUTIONS OF AGGREGATES

Table D.1 Lime/aggregate ratios and particle size distributions of aggregates used in stone masonry mortars.

Sample	Lime (%)	Aggregate (%)	Aggregate size distribution (%)					
			≥1180µm	500µm	250µm	125µm	53µm	<53µm
Se.s.1	42.41	57.59	34.26	13.54	6,43	2.46	0.57	0.40
Se.s.2	43.73	56.27	36.70	11.65	5.45	1.86	0.35	0.35
Se.s.	**43.07**	**56.93**	**35.48**	**12.59**	**5.94**	**2.16**	**0.46**	**0.38**
Se.Dü.s.1	39.03	60.97	39.61	14.77	4.34	1.24	0.51	0.39
Se.Dü.s.2	36.09	63.91	40.18	16.98	4.57	1.27	0.57	0.45
Se.Dü.s.	**37.56**	**62.44**	**39.89**	**15.88**	**4.46**	**1.26**	**0.54**	**0.42**
Se.Ul.s.1	22.32	77.68	50.15	15.94	5.55	4.16	1.30	0.43
Se.Ul.s.2	22.13	77.87	48.90	17.25	6.39	2.62	1.74	0.79
Se.Ul.s.	**22.23**	**77.77**	**49.52**	**16.60**	**5.97**	**3.39**	**1.52**	**0.61**
Ur.He.s.1	35.65	64.35	35.30	21.49	6.38	2.60	1.99	1.15
Ur.He.s.2	29.00	71.00	40.68	17.49	7.53	3.21	1.79	0.53
Ur.He.s.	**32.33**	**67.67**	**37.99**	**19.49**	**6.95**	**2.90**	**1.89**	**0.84**
Ur.Ka.s.1	42.17	57.83	24.07	15.37	10.41	6.90	0.76	0.46
Ur.Ka.s.2	42.76	57.24	26.39	14.31	9.50	6.11	0.63	0.18
Ur.Ka.s.	**42.47**	**57.53**	**25.23**	**14.84**	**9.96**	**6.50**	**0.70**	**0.32**

Table D.2 Lime/aggregate ratios and particle size distributions of aggregates used in brick masonry mortars.

Sample	Lime (%)	Aggregate (%)	Aggregate size distribution (%)					
			≥1180µm	500µm	250µm	125µm	53µm	<53µm
Se.Dü.b.1	26.34	73.66	42.42	17.70	5.92	3.35	3.00	1.58
Se.Dü.b.2	29.56	70.44	41.20	15.66	5.66	3.22	2.78	1.87
Se.Dü.b.	**27.95**	**72.05**	**41.81**	**16.68**	**5.79**	**3.29**	**2.89**	**1.72**
Se.Ul.b.1	28.82	71.18	46.41	11.33	4.98	3.67	4.10	0.79
Se.Ul.b.2	27.89	72.11	49.15	11.20	4.44	3.05	3.46	0.92
Se.Ul.b.	**28.35**	**71.65**	**47.78**	**11.27**	**4.71**	**3.36**	**3.78**	**0.86**
Ur.He.b.1	20.27	79.73	50.54	19.45	6.76	2.08	0.84	0.32
Ur.He.b.2	19.72	80.28	54.60	16.38	6.45	2.02	0.90	0.17
Ur.He.b.	**19.99**	**80.01**	**52.57**	**17.92**	**6.60**	**2.05**	**0.87**	**0.25**
Ur.Ka.b.1	40.66	59.34	19.04	19.54	9.61	5.30	4.57	2.03
Ur.Ka.b.2	41.00	59.00	25.72	17.40	8.59	4.22	2.35	0.96
Ur.Ka.b.	**40.83**	**59.17**	**22.38**	**18.47**	**9.10**	**4.76**	**3.46**	**1.49**

APPENDIX E

SOLUBLE SALTS IN MORTARS

Table E.1 Percent soluble salts in stone masonry mortars.

Sample	Conductivity (μS/cm)	Salinity (%)
Se.s.	145	0.46
Se.Dü.s.	97	0.31
Se.Ul.s.	245	0.78
Ur.He.s.	163	0.52
Ur.Ka.s.	115	0.37

Table E.2 Percent soluble salts in brick masonry mortars.

Sample	Conductivity (μS/cm)	Salinity (%)
Se.Dü.b.	124	0.40
Se.Ul.b.	113	0.36
Ur.He.b.	97	0.31
Ur.Ka.b.	118	0.38

Table E.3 Anion parts of soluble salts in stone masonry mortars.

Sample	Soluble salts				
	SO_4^{-2}	Cl^-	NO_3^-	CO_3^{-2}	PO_4^{-3}
Se.s.	-	+	-	-	-
Se.Dü.s.	-	-	-	-	-
Se.Ul.s.	-	-	-	-	-
Ur.He.s.	-	+	-	-	-
Ur.Ka.s.	-	-	-	-	-

Table E.4 Anion parts of soluble salts in brick masonry mortars.

Sample	Soluble salts				
	SO_4^{-2}	Cl^-	NO_3^-	CO_3^{-2}	PO_4^{-3}
Se.Dü.b.	-	-	-	-	-
Se.Ul.b.	-	-	-	-	-
Ur.He.b.	-	-	-	-	-
Ur.Ka.b.	-	-	-	-	-

APPENDIX F

POZZOLANIC ACTIVITY OF AGGREGATES AND BRICKS

Table F.1 Pozzolanic activity measurements of coarse aggregates used in stone and brick masonry mortars.

Sample	Electrical conductivity of $Ca(OH)_2$ (mS/cm)	Electrical conductivity of $Ca(OH)_2$ mixed with coarse aggregate (mS/cm)	Difference in conductivity (mS/cm)
Se.s.c-agg.	9.13	8.46	0.67
Se.Dü.s.c-agg.	9.06	8.39	0.67
Se.Ul.s.c-agg.	9.15	7.74	1.41
Ur.He.s.c-agg.	9.31	7.60	1.71
Ur.Ka.s.c-agg.	9.06	8.24	0.82
Se.Dü.b.c-agg.	9.20	7.31	1.89
Se.Ul.b.c-agg.	9.20	7.69	1.51
Ur.He.b.c-agg.	9.31	8.05	1.26
Ur.Ka.b.c-agg.	9.16	7.89	1.27

Table F.2 Pozzolanic activity measurements of fine aggregates used in stone and brick masonry mortars.

Sample	Electrical conductivity of $Ca(OH)_2$ (mS/cm)	Electrical conductivity of $Ca(OH)_2$ mixed with fine aggregate (mS/cm)	Difference in electrical conductivity (mS/cm)
Se.s.f-agg.	8.63	7.30	1.33
Se.Dü.s.f-agg.	6.62	5.28	1.34
Se.Ul.s.f-agg.	6.52	0.835	5.68
Ur.He.s.f-agg.	6.45	0.177	6.27
Ur.Ka.s.f-agg.	8.20	6.90	1.30
Se.Dü.b.f-agg.	6.50	0.320	6.18
Se.Ul.b.f-agg.	6.60	0.386	6.21
Ur.He.b.f-agg.	6.40	0.207	6.20
Ur.Ka.b.f-agg.	6.35	0.310	6.04

Table F.3 Pozzolanic activity measurements of bricks used in domes.

Sample	Electrical conductivity of Ca(OH)$_2$ (mS/cm)	Electrical conductivity of Ca(OH)$_2$ mixed with brick (mS/cm)	Difference in conductivity (mS/cm)
Se.Dü.brick	9.25	8.80	0.45
Se.Ul.brick	9.20	8.71	0.49
Ur.He.brick	9.22	8.79	0.43
Ur.Ka.brick	9.30	8.49	0.81

APPENDIX G

CHEMICAL COMPOSITIONS OF COARSE AND FINE AGGREGATES

Table G.1 Chemical compositions of coarse aggregates used in stone masonry mortars.

Coarse aggregate	Elemental Composition (%)					
	Na$_2$O	**MgO**	**Al$_2$O$_3$**	**SiO$_2$**	**K$_2$O**	**Fe$_2$O$_3$**
Se.s.c-agg-1	2.38	4.70	15.88	63.5	2.93	10.6
Se.s.c-agg-2	2.26	4.08	13.63	64.01	2.75	13.26
Se.s.c-agg-3	2.40	4.66	15.58	64.73	2.21	10.42
Se.s.c-agg.	**2.35**	**4.48**	**15.03**	**64.08**	**2.63**	**11.43**
Se.Dü.s.c-agg-1	2.34	5.08	18.93	54.28	3.01	16.36
Se.Dü.s.c-agg-2	3.19	5.7	19.32	52.18	2.65	16.96
Se.Dü.s.c-agg-3	2.55	5.18	19.01	54.33	2.7	16.23
Se.Dü.s.c-agg.	**2.69**	**5.32**	**19.09**	**53.60**	**2.79**	**16.52**
Se.Ul.s.c-agg-1	1.55	2.00	18.19	67.53	4.23	6.50
Se.Ul.s.c-agg-2	2.24	2.96	17.48	66.25	3.74	7.33
Se.Ul.s.c-agg-3	2.07	2.88	17.43	65.9	3.94	7.79
Se.Ul.s.c-agg.	**1.95**	**2.61**	**17.70**	**66.56**	**3.97**	**7.21**
Ur.He.s.c-agg-1	4.65	1.53	15.24	69.06	4.60	4.92
Ur.He.s.c-agg-2	4.49	1.77	15.08	67.25	5.51	5.9
Ur.He.s.c-agg-3	4.21	1.07	14.66	69.32	5.58	5.15
Ur.He.s.c-agg.	**4.45**	**1.46**	**14.99**	**68.54**	**5.23**	**5.32**
Ur.Ka.s.c-agg-1	1.00	1.34	9.07	79.31	1.86	7.42
Ur.Ka.s.c-agg-2	1.74	2.37	9.94	79.69	1.81	4.43
Ur.Ka.s.c-agg-3	1.79	2.21	10.19	76.98	2.06	6.78
Ur.Ka.s.c-agg.	**1.51**	**1.97**	**9.73**	**78.66**	**1.91**	**6.21**

Table G.2 Chemical compositions of coarse aggregates used in brick masonry mortars.

Coarse aggregate	Elemental Composition (%)					
	Na_2O	MgO	Al_2O_3	SiO_2	K_2O	Fe_2O_3
Se.Dü.b.c-agg-1	1.54	2.24	15.75	69.22	3.13	8.12
Se.Dü.b.c-agg-2	2.39	3.08	16.12	68.71	3.18	6.52
Se.Dü.b.c-agg-3	2.33	2.79	15.81	68.98	3.36	6.73
Se.Dü.b.c-agg.	**2.09**	**2.70**	**15.89**	**68.97**	**3.22**	**7.12**
Se.Ul.b.c-agg-1	1.63	1.59	17.51	69.24	3.95	6.09
Se.Ul.b.c-agg-2	2.33	2.13	17.16	69.96	3.79	4.62
Se.Ul.b.c-agg-3	2.38	2.2	17.46	68.36	3.81	5.79
Se.Ul.b.c-agg.	**2.11**	**1.97**	**17.38**	**69.19**	**3.85**	**5.50**
Ur.He.b.c-agg-1	4.65	1.22	14.82	70.86	5.04	3.41
Ur.He.b.c-agg-2	4.2	1.18	15.11	71.70	5.35	2.47
Ur.He.b.c-agg-3	4.17	0.99	14.75	74.24	5.85	-
Ur.He.b.c-agg.	**4.34**	**1.13**	**14.89**	**72.27**	**5.41**	**1.96**
Ur.Ka.b.c-agg-1	1.72	1.99	9.85	80.21	1.48	4.75
Ur.Ka.b.c-agg-2	1.54	1.63	9.73	80.99	1.84	4.27
Ur.Ka.b.c-agg-3	1.82	2.13	9.49	80.71	1.87	3.98
Ur.Ka.b.c-agg.	**1.69**	**1.92**	**9.69**	**80.64**	**1.73**	**4.33**

Table G.3 Chemical compositions of fine aggregates (less than 53µm) used in stone masonry mortars.

Fine aggregate	Elemental Composition (%)					
	Na_2O	MgO	Al_2O_3	SiO_2	K_2O	Fe_2O_3
Se.s.f-agg.1	2.37	4.02	15.11	60.67	1.82	16.01
Se.s.f-agg.2	2.24	4.00	16.43	59.89	2.23	15.22
Se.s.f-agg.	**2.31**	**4.01**	**15.77**	**60.28**	**2.03**	**15.62**
Se.Dü.s.f-agg.1	2.54	3.83	17.11	58.72	1.85	15.94
Se.Dü.s.f-agg.2	2.16	3.59	17.18	58.13	2.24	16.69
Se.Dü.s.f-agg.	**2.35**	**3.71**	**17.15**	**58.43**	**2.05**	**16.32**
Se.Ul.s.f-agg.1	0.81	*	9.66	87.72	1.81	*
Se.Ul.s.f-agg.2	1.08	*	10.47	86.45	2.00	*
Se.Ul.s.f-agg.	**0.95**	*	**10.07**	**87.09**	**1.91**	*
Ur.He.s.f-agg.1	1.63	1.16	7.25	88.39	1.56	*
Ur.He.s.f-agg.2	0.94	0.84	6.14	90.79	1.3	*
Ur.He.s.f-agg.	**1.29**	**1.00**	**6.70**	**89.59**	**1.43**	*
Ur.Ka.s.f-agg.1	1.82	2.72	13.6	66.53	2.09	13.24
Ur.Ka.s.f-agg.2	0.96	2.08	14.06	71.72	1.43	9.74
Ur.Ka.s.f-agg.	**1.39**	**2.40**	**13.83**	**69.125**	**1.76**	**11.49**
*: not detected						

Table G.4 Chemical compositions of fine aggregates (less than 53µm) used in brick masonry mortars.

Fine aggregate	Elemental Composition (%)					
	Na$_2$O	MgO	Al$_2$O$_3$	SiO$_2$	K$_2$O	Fe$_2$O$_3$
Se.Dü.b.f-agg.1	0.70	*	8.87	88.99	1.45	*
Se.Dü.b.f-agg.2	0.74	*	8.49	89.33	1.44	*
Se.Dü.b.f-agg.	**0.72**	*	**8.68**	**89.16**	**1.45**	*
Se.Ul.b.f-agg.1	0.71	1.26	12.97	83.05	2.01	*
Se.Ul.b.f-agg.2	0.87	1.37	12.88	82.03	2.85	*
Se.Ul.b.f-agg.	**0.79**	**1.32**	**12.93**	**82.54**	**2.43**	*
Ur.He.b.f-agg.1	1.17	*	6.17	91.87	0.78	*
Ur.He.b.f-agg.2	1.00	*	5.11	93.02	0.87	*
Ur.He.b.f-agg.	**1.09**	*	**5.64**	**92.45**	**0.83**	*
Ur.Ka.b.f-agg.1	0.99	*	8.16	89.75	1.1	*
Ur.Ka.b.f-agg.2	0.98	*	7.76	90.31	0.95	*
Ur.Ka.b.f-agg.	**0.99**	*	**7.96**	**90.03**	**1.03**	*
*: not detected						